Estimating the impacts of land use and land cover change on runoff and sediment yield using SWAT model: case study of Keleta watershed, Upper Awash Sub-basin

MSc. Thesis

By:

Teka Gemechu

January 2014

Arba Minch University

CERTIFICATION

I, the undersigned, certify that I read and here by recommend for the acceptance by the Arba Minch University a dissertation entitled: Estimating the impacts of land use and land cover change on runoff and sediment yield using SWAT model: case study of Keleta watershed, Upper Awash Sub-basin in partial fulfillment of a degree of Masters of Science in Water Resources and Irrigation Engineering.

Signature:_____________________ Date______________________

Dr. Mekonnen Ayana (AMU)

(Advisors)

Signature:_____________________ Date______________________

Dr.Ing. Kassa Tadele (AMU)

(Co-Advisors)

A Thesis submitted to School of Graduate studies, Arba Minch University in partial fulfillment requirements for the degree of masters of Science in Water Resources and Irrigation Engineering.

DECLARATION AND COPY RIGHT

I, Teka Gemechu, declare that this thesis is my own original and it has not presented and will not be presented to any other University for the similar or any other degree award.

Signature:______________________

Date:___________________________

teka.ie3504@gmail.com

DEDICATION

This thesis is dedicated to my mother Tsige Negesh

ACKNOWLEDGMENT

First of all I would like to thank my God, the almighty for providing me this opportunity and granting me the capability to proceed successfully.

I would like to express my deepest gratitude to my thesis advisors, Dr. Mekonnen Ayana and Dr. Ing. Kassa Tadele for their scientific guidance through constructive discussions, comments and corrections.

My special thanks also goes to Mr. Sisay Kebede, who initiated and taught SWAT model from the beginning and provided all the necessary data for the successful completion of my research. Special thanks go to Feyisa Lemi for his patient and competent support during all my life and others my friends in work area.

I would like to extend my sincere gratitude to Oromia Agriculture Bureau, Agriculture Sector Support Project(ASSP) who is financed by Africa Development Bank(ADB), for granting the scholar ship during the whole study period. I am also grateful to my employer Sire woreda for giving me leave of absence for study duration.

I would like to extend my special thanks to Ministry of water resource and Energy, Oromia Water Works Design and Supervision Enterprise, National Metreology Agency, Adama meteorological station and Awash Melkasa research centres since they were provided the necessary data for my work.

I would like to express my appreciation to all my friends and course mates for their support and wonderful social atmosphere.

Last but not least, I would like to thank my family, especially my father, Gemechu, my mother Tsige, my brother Tesfaye and Mitiku, my sister Beshedu and Feleku and my uncle Tefera and his family for their day-to-day encouragement and support.

Abstract

Impacts of land use land cover change on watershed runoff and sediment yield of the Keleta watershed (1150Km^2), Upper Awash sub-basin, were assessed using hydrological modeling. The study utilized different types of data including DEM, soil map, Landsat TM and ETM satellite data and the field observations. Two date Landsat image, 1986 and 2005, were used for generating the land use/land cover map of the study area and to detect the changes between these two time periods were simulated by the Soil and Water Assessment Tool (SWAT) model and were compared with measured values. The six main land use changes were identified as an increase of cultivation land from 52.5% to 68% and decrease of forest land 11.8% to 1.7 % of the watershed area during the two decade period. Using the two generated land cover maps, two SWAT models set up were run to evaluate the impacts the land use and cover changes on the stream flow of the study watershed. The performance of the SWAT model was evaluated through sensitivity analysis, calibration, and validation. The most sense parameters were identified to be sensitive for the runoff and sediment yield of the study area and used for model calibration and validation. This study presents the calibration and validation of SWAT for the runoff and sediment yield from 1995-2005 and 2006-2009 respectively. Based on this values for Coefficient of determination (R^2), Nash-Sutcliffe model efficiency (NSE), Root mean square error standard deviation ratio (RSR) and percent bias (PBIAS) are found to be 0.82, 0.81, 0.44 and -9.29% in calibration and 0.83, 0.76, 0.49 and -7.92% in validation for flow analysis respectively. Similarly, sediment model efficiency indicators R^2, NSE, RSR and PBIAS 0.73, 0.69, 0.55 and -10.65% for calibration and 0.74, 0.62, 0.61 and 2.81% for validation respectively. The average annual simulated runoff and sediment yield is 1424.24mm and 54.98t/ha in 1986 and for 2005 1557.33mm and 73.11t/ha respectively. Average annual variability of sediment yield in each sub-watershed range from 0.06 to 13.83tha^{-1}y^{-1} in 1986, whereas in 2005 the sub-watershed contribute from 0.26 to 17.86tha^{-1}y^{-1} of the sediment yield. The built SWAT model can be utilized to simulate different scenarios to examine the effect of different types of management practices and land use land cover.

Key words: Keleta watershed, Land cover change, Runoff, Sediment yield, GIS, Remote Sensing, SWAT model

List of Acronyms

AMC = Antecedent Moisture Condition

ArcSWAT =ArcGIS Interface for Soil and Water Assessment Tool

CN = Curve Number

DEM = Digital Elevation Model

DEW02= Dew Point Temperature Calculator

ERDAS=Earth Resources Data Analysis System

ETM+=Enhanced Thematic Mapper Plus

FAO =Food Agricultural Organization

GIS = Geography Information System

GPS=Global Position System

HRU =Hydrologic Response Unit

LH = Latin Hypercube

LULC=Land Use Land Cover

MoWR = Ministry of Water Resource

MUSLE=Modified Universal Soil Losses Equation

NMSA=National Metrological Service Agency

OAT = One- factor At a Time

OWWDSE= Oromia Water Works Design and Supervision Enterprise

SCS = Soil Conservation Service

SWAT= Soil and Water Assessment Tool

TM=Thematic Mapper

USDA = United State Department of Agriculture

WXGEN = Weather Generator

Table of Contents

List of Figure

List of Table

List of Appendix

CHAPTER ONE

1 INTRODUCTION

1.1 Background

Soil erosion is a complex land degradation process which leads to decline in soil quality and productivity, because resulting in a decrease in effective root depth, nutrient and water imbalance in the root zone, reduction in infiltration and increase in runoff (Lal, 2001) . This sediment yield can result in the acceleration of natural sedimentation in rivers and reservoirs reducing their storage capacity as well as life span (Pandey et al, 2007). Consequently, soil erosion is a serious environmental and economic problem and it is sensitive mainly to land use, through deforestation, agricultural intensification and improper practices, and due to climatic change (Zhang et al, 2009; Nearing et al, 2004).

Land use has been driven by the technology development and depends on social, political and economic development (Bakker et al, 2008). The relationship between land use and soil erosion has attracted the interest of a wide variety of researchers (Wang et al, 2003; Cantón et al, 2011). These investigations found that these changes in land use greatly affected runoff and soil erosion. In the Ethiopian highlands, land use change has led to severe soil erosion, which reduced the soil moisture holding capacity and challenged food production (Hurni, 1993; Tibebe and Dewket, 2010). In the Ethiopian highlands soil erosion rates measured on test plots amount to 130 to 170 metric tons $ha^{-1}yr^{-1}$on cultivated land (Hurni et al, 2008). There are many consequences to this loss of fertile soil in Ethiopia.

Land cover changes commonly are highly pronounced in the developing countries that are characterized by agriculture based economics and rapidly increasing human population. (Meyer and Turner, 1994) discussed that land cover changes are caused by a number of natural and human driving forces. Whereas natural effects such as climate change are only over a long period of time, the effects of human activities are immediate and often direct. From the human factors, population growth is the most important in Ethiopia (Hurni, 1993) as it is common in developing countries. Some 85% of the population of lives in rural areas and directly depend on the land for its livelihood. This means the demands of lands are increasing as population increases.

Land cover changes may have immediate and long-lasting impacts on terrestrial hydrology and, alter the long term balance between rainfall and evapotranspiration and the resultant runoff. In the short-term, destructive land use change may affect the hydrological cycle either through increasing the water yield or through diminishing, or even eliminating the low flow in some circumstances (Croke et al, 2004). (Saveniji, 1995) suggested that in the long-term the reduction in evapotranspiration and water recycling arising from land cover changes may initiate a feedback mechanism that results in reduction rainfall.

Study of stream flow patterns with respect to land cover dynamics enables assessment of sustainability of land use systems; because stream flows reflect on the hydrological state of the entire watershed. As stated by (Calder, 2002), the hydrological impact of land cover changes is a referencing issue and much research is necessary.

Given that impacts of land use/cover change on water resources are the result of complex interactions between diverse site-specific factors and offsite conditions, standardized types of responses will rarely be adequate. General statements about land–water interactions need to be continuously questioned to determine whether they represent the best available information and whose interests they support in decision-making processes (FAO, 2002).

Appropriate tools are needed for better assessment of long-term hydrology and soil erosion processes and as decision support for planning and implementing appropriate measures. The tools include various hydrological and soil erosion models, as well as geographical information system (GIS). Due to technological developments in recent years, distributed catchment models are increasingly being used to implement alternative management strategies in the area of water resource allocation and flood control (Setegn et al, 2009). Many hydrological and soil erosion models are designed to describe hydrology, erosion and sedimentation processes. Hydrological models describe the physical processes controlling the transformation of precipitation to runoff, while soil erosion modeling is based on understanding the physical laws of processes that occur in the natural landscape (Setegn et al, 2009).

From the point view of planning, designing and management of water resource, application of hydrological models becoming paramount importance. Hence, study of hydrological processes of the basin under different scenarios would generate information that could be used for development planning so as to enable better utilization and management of water resources.

Therefore, a comprehensive understanding of hydrological process in the watershed is the prerequisite for successful water management and environmental restoration. Due to the spatial and temporal heterogeneity in soil properties, vegetation and land use practices, a hydrologic cycle is a complex system. As a result mathematical model and geospatial analysis tool are required for studying hydrological process and hydrological responses to land use and climatic changes.

Hydrological models are generally used as utility in various areas of water resources development, in assessing the available resources, in studying the impact of human interference in an area such as land use change, deforestation and other hydraulic structure such as dam and reservoirs.

The purpose of this research is therefore applying the integration of geographical information system (GIS) and remote sensing and physically based semi distributed model i.e. Soil and water assessment tool (SWAT), to understand the impacts of land use and land cover change on runoff and sediment yield of the watershed.

1.2 Statement of the problem

As in many parts of the world, the population in Ethiopia increased rapidly in the last century. This eventually resulted in large-scale land use changes, deforestation, overgrazing, expansion of crop land to marginal and steep sloping areas, poor soil management practices and unsustainable use of natural resources (Tesfahunegn et al., 2012). These practices reduce rainwater infiltration resulting in more surface runoff and water erosion. This leads to exhaustion of the soil, decreasing soil quality and eventually a decline in soil productivity (Bewket, 2003) .

Understanding the hydrological processes is crucial towards better water and land resource management, as the hydrology largely influences soil erosion and is highly important to agricultural productivity (Easton et al., 2010). Widespread land use changes have often been associated with changes in the local hydrology as hydrologic responses of a catchment are influenced by land cover. Changes in land cover may lead to significant changes in evapo-transpiration, leaf area index, soil moisture content, infiltration rates, (sub-) surface flow regimes, surface roughness, surface runoff, and soil erosion through interactions with vegetation, topography, soils, geology and climate processes (Nejadhashemi et al., 2011).

Although the impact of land use change on hydrologic responses is widely studied, only a few studies were conducted in Ethiopia (e.g. Legessa et al, 2003; Bewket and Sterk, (2005); Kassa, (2009)). Legessa et al, (2003) modeled the impact of the change of arable land into forested land on river discharge, which showed a decrease in discharge, mainly caused by changes in evapo-transpiration rates. Bewket and Sterk, (2005) studied the effect of expansion of agricultural land on flow regimes in the Chemoga river, which resulted in decreased dry season flow and no changes in peak flows. Kassa, (2009) modeled the impact of the replacement of natural forest in to farmland and settlements, the mean monthly discharge for wet months had increased while in the dry season decreased in Hare watershed.

Soil type, land use/cover and slope gradient appeared to be the major influences on the amount of soil loss and runoff generation was the highest in the Keleta watershed (Tibebe and Bewket, 2010). Deforestation is a day to day activity of the people living in the watershed. The watershed is also facing high erosion by the effects of intense rainfall of the watershed which aggravates the land cover change of the watershed. This continuous change in land cover has impacted the runoff and sediment yield of the watershed by changing the magnitude and pattern of the components of stream flow which are surface runoff and sediment transport, which results increasing the extent of the water management problem. The rapid land use/cover changes caused by clearing of the forest for agricultural production and settlement are presumed to adversely affect the runoff and sediment of the Keleta watershed. This is shown by reduced stream flow during dry periods and increased flash floods in wet seasons. In addition spatial variability in soil erosion and siltation has also occurred in the catchment. Therefore, a strong need is identified for the hydrological techniques and tools that can assess the effects of land cover changes on the runoff and sediment yield of a watershed. Such techniques and tools can provide information that can be used for water resources management at a watershed.

1.3 Objectives of the study

1.3.1 General objective

The overall objective of this study was to estimate the impacts of land use and land cover change on runoff and sediment in Keleta watershed using Remote Sensing and GIS Techniques, and Soil and Water Assessment (SWAT model) Tool for a period of two decades.

1.3.2 Specific objective

- Identify and map the extent of LULC changes over a period of two decades
- To identify the flow and sediment sensitive parameters of the watershed
- Calibrate and validate SWAT model and quantify the effects of LULC change on the runoff and sediment yield.
- To characterize the spatial variability of sediment yields in the watershed

1.4 Significant of the study

Effective watershed planning requires understanding of the types and impacts of land use and land cover change. This is essential indicator for resource base analysis and development of effective and appropriate response strategies for sustainable management of natural resources in the country in general and at the study area in particular. Once the extent and effect of land use/land cover change on hydrology and sediment loss of the catchment is known, this may help policymakers to design proper land management strategies. Therefore, the study presents a method to quantify land use and land cover change and their impact on runoff and sediment yield.

CHAPTER TWO

2 DESCRIPTION OF STUDY AREA

2.1 Location

The Keleta watershed is found in South Eastern part highland Plateau and Great Rift Valley of Ethiopia in Oromia Regional State, Arsi Zone. The watershed area comprises of 8 districts/woredas' namely: Tiyo, Degeluna Tijo, Tena, Diksis, Sire, Lode Hetosa, Hetosa and Dodota. The geographical extent of the study area falls in Upper Awash Sub-basin which ranges from 8.42° and 7.90° North and 39.54° and39.22° East (Figure 2.1). It covers a total drainage area of 1,150km^2. Keleta river is one of the major tributaries of the Awash river which its headwaters originate from the afroalpine area of the Chilalo Mountain among many other rivers flow to northeast direction.

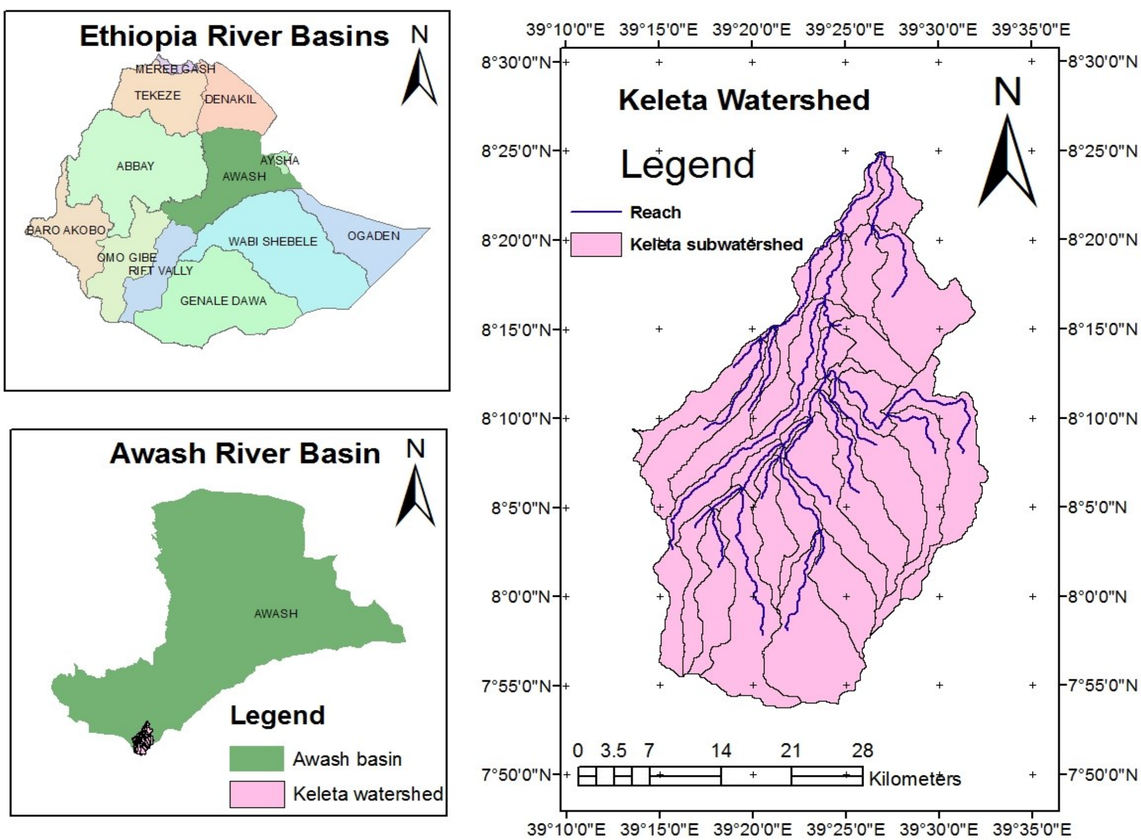

Figure 2.1:-The study watershed is located in Awash river basin, Ethiopia

2.2 Climate

Basically, climate of Ethiopia is classified into five climate zones based on the altitude and temperature. Namely which are called Wurch (cold climate and the altitude is more than 3000m), Dega (temperate like climate of high land and the altitude is between 2500-3000m), Woina-Dega (warm climate the altitude is between 1500-2500m), Kola (hot and arid type of climate and the altitude is less than 1500m) and Bereha (hot and hyper arid type of climate) (NMSA, 2001). Since the elevation of the study area lays between 1341 to 4189 m above the mean sea level the study area is characterized by all kinds of the above mentioned climate zones expect bereha.

There are two seasons, viz. rainy and dry. The rainy season has two periods, the little rains, during March to May, and the big rains, which last from June to September. The rainfall distribution in the watershed is bi-modal pattern. The main rainy season often extends from June through September and the short rainy season occurs in March until May while the rest of the months are generally drier. Due to large topographic contrast of the study area and unevently distribution of rain gauges, annual average aerial precipitation of the study area was assessed by Thiessen methods. Thiessen method attempts to adjust for non-uniform gauge distribution by weighing the record of each gauge in proportion to the area which is closer to that gauge than to any other gauge by calculating weighted area of influence by equation 2.1. The mean monthly rainfall of the watershed varies from 13.73mm to 177.81mm (Figure 2.2 & 2.3). Similarly mean annual rainfall is varied from 757.35mm to 1058.88mm (Figure 2.4). As recorded at different stations, temperature of the study area varies from place to place. As the analysis result showed the maximum and minimum temperature of each station is varying with the altitude of the area (Figure 2.5). The monthly average maximum temperature of the watershed varies between 31.19°C and 20.49°C and similarly average monthly minimum temperature of the watershed varies between 16.25°C and 5.47°C.

$$P = \frac{\sum_{i=1}^{n} A_i P_i}{A_t} \qquad 2.1$$

where, P is effective aerial precipitation (mm), A_i is the ith polygon area, P_i is the precipitation recorded at the ith rain gauge, A_t total area.

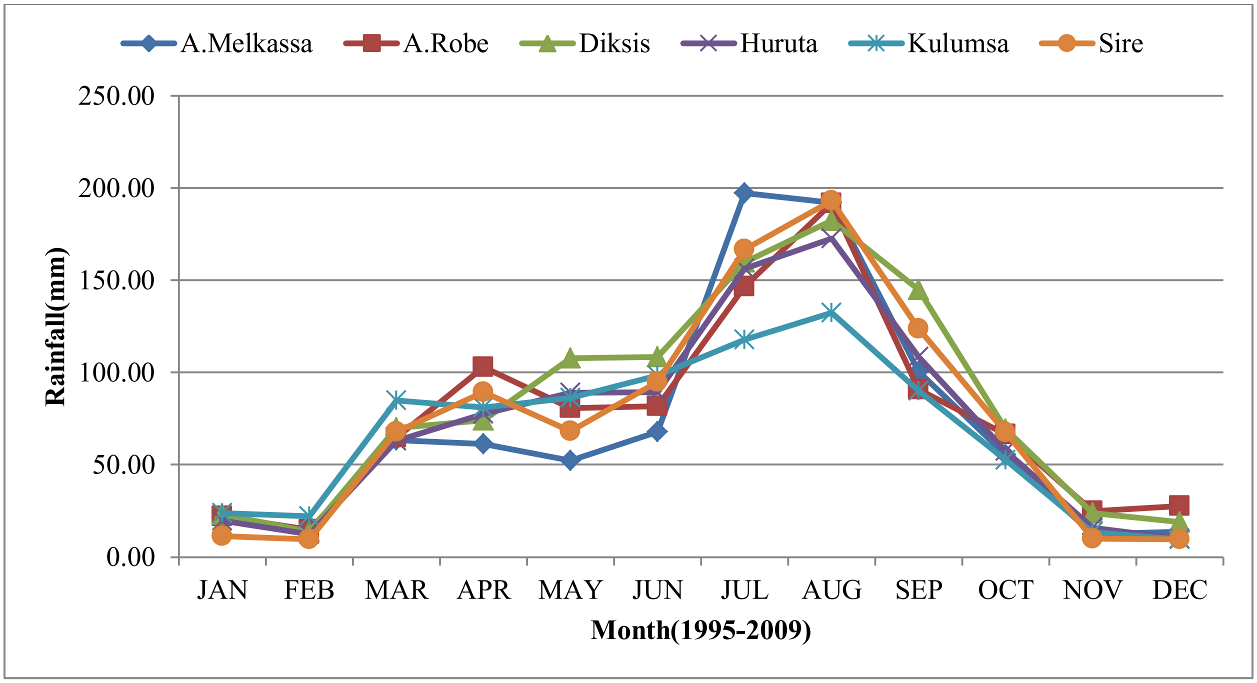

Figure 2.2:-Monthly Average Rainfall

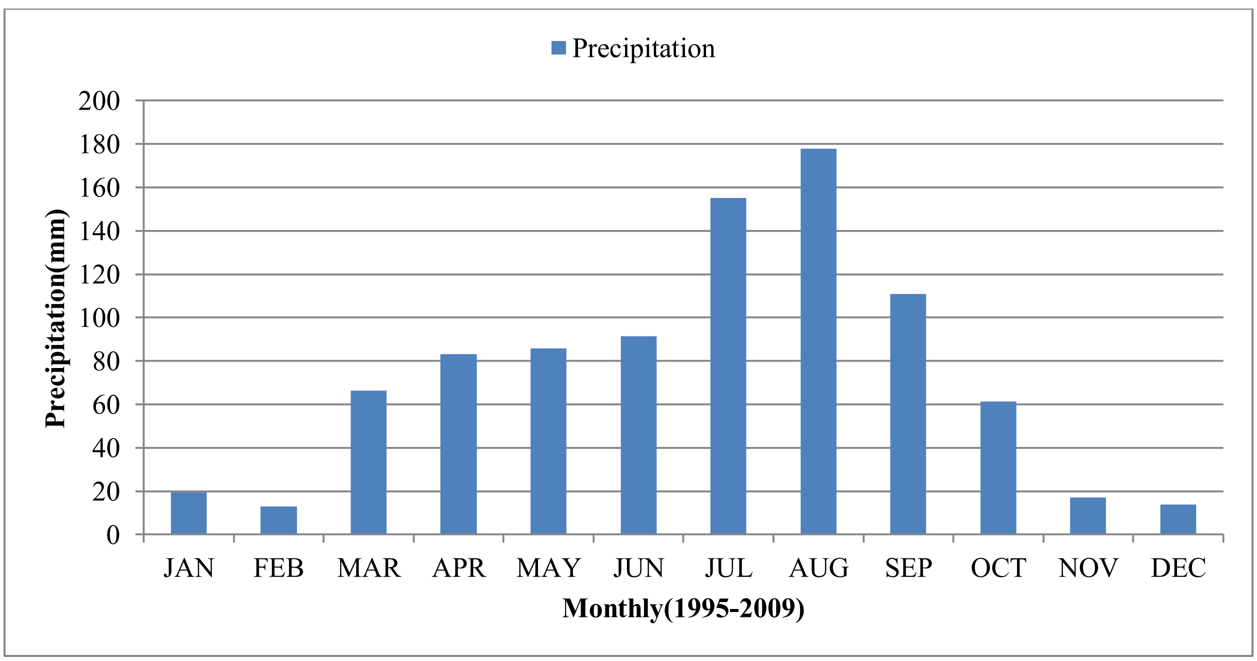

Figure 2.3:-Monthly areal precipitation

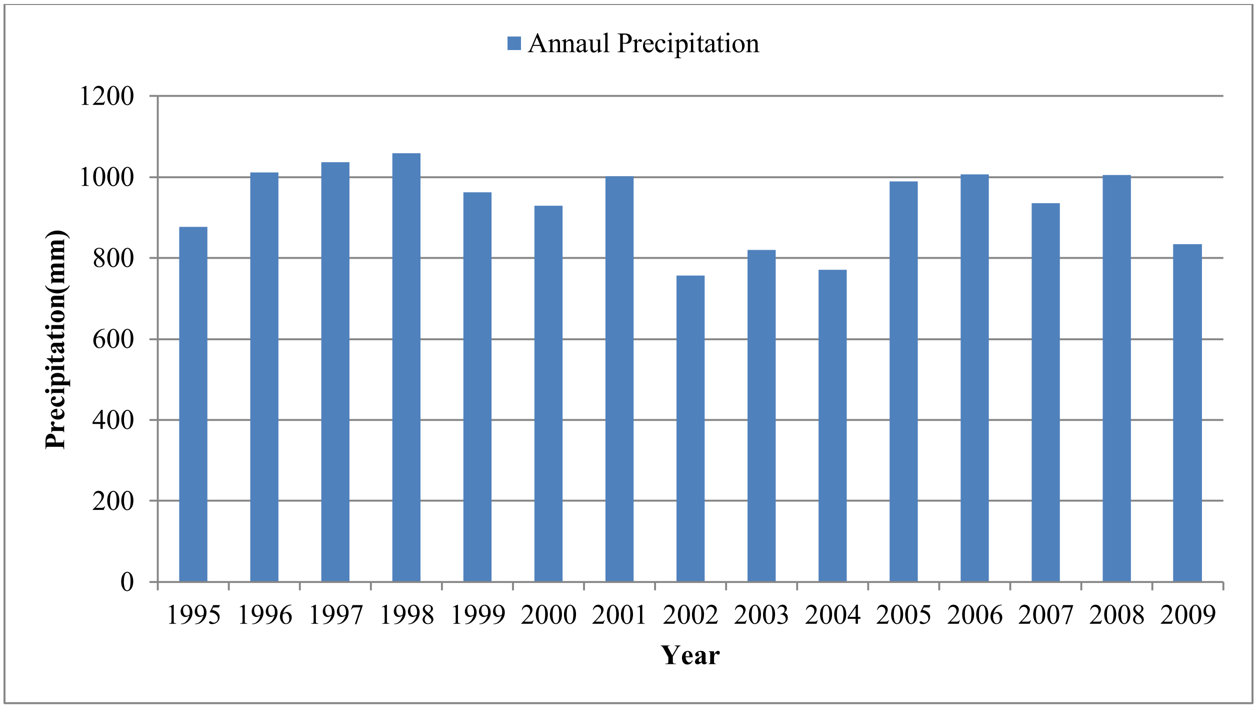

Figure 2.4:-Annual areal precipitation

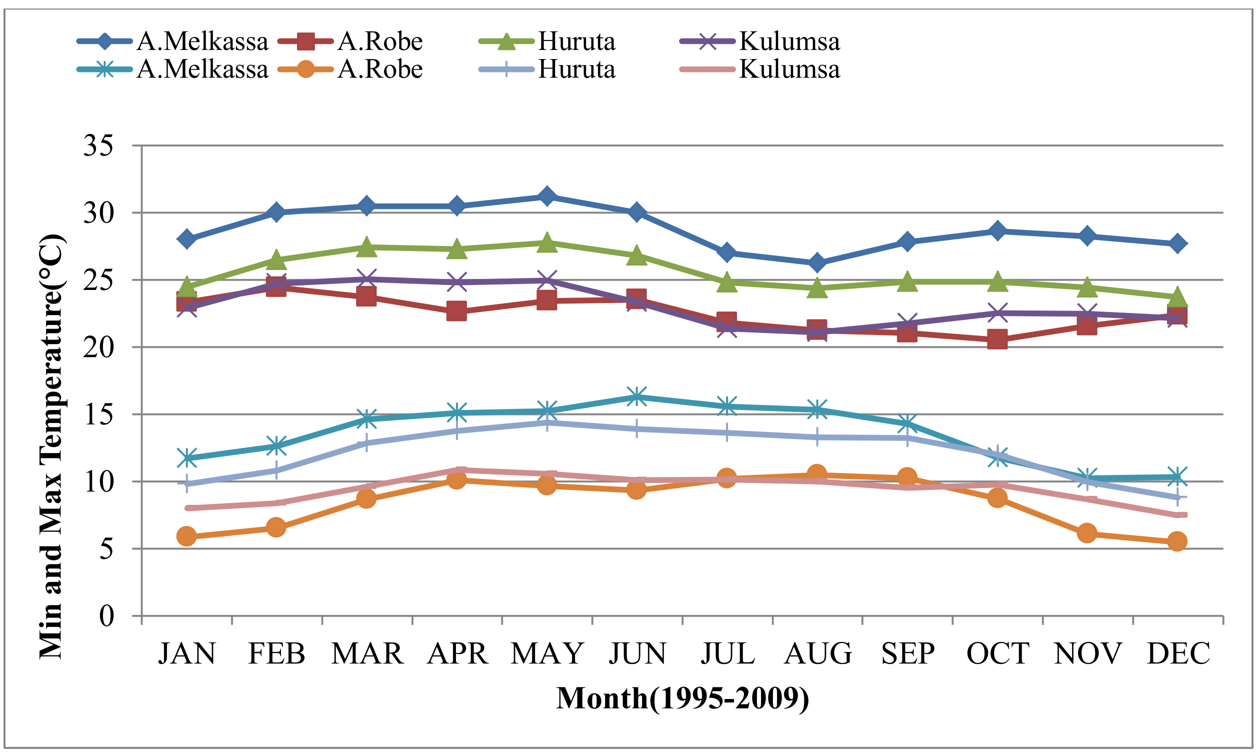

Figure 2.5:-Monthly Average Minimum and Maximum Temperature

2.3 Physiographic and Geology

The Keleta watershed is made up of two main physiographic components: the flat to undulating high plateau and mountains and the rift valleys. The upper part of the Watershed is an expression of the underlying geology with the Ethiopian plateau underlain by tertiary volcanic (basalt tuffs, agglomerates, and younger royalties, tuffs) and the lower part of the watershed under the Rift valley floor Comprising basalts and ignimbrites near active volcanic such as Fantale, Dofan and Afrera in between thick, Quaternary-aged lacustrine, Fluvial and beach sediments.

2.4 Soil

The major soil groups in the study area are: Vertisols, Cambisols, Luvisols, Andosols, Nitisols and Leptosols (OWWDSE, 2013). Vertislos are the most dominant and important soils which cover 57% of the watershed, have high clay contents. Vertisols are, very deep and uniformly thick consisting of dark grey or very dark greyish brown colour. During the dry season these soils develop cracks (i.e., 4-8cm wide and as deep as 60 to 80 cm). Vertisols are imperfectly to poorly drained, clay soils. Cambisols are well, to somewhat excessively drained, deep, light to medium textured, with variable colors. The soils are formed on a wide range of parent materials. The soils have a moderately developed subsoil horizon, which is only in an initial stage of development. Structure is weak to strongly developed angular blocky, occasionally prismatic in the topsoil over moderate angular blocky to massive in the subsoil. Consistence is hard when dry, friable to firm when moist and slightly sticky and slightly plastic when wet. And cover 19.9% of the watershed. Luvisols are generally well to moderately well drained, predominantly with clay loam to clay texture. These soils are developed in the sub-basin only in well drained areas. They have Medium to high base saturation with argellic horizons and deep to very deep depth. Andosols are formed from volcanic ash materials and occur mainly in volcanic areas. They are very porous and hence can absorb much water. These soils are moderately deep over soft weathering parent rock, light brown to dark brown, fine to coarse grained sandy loams with weak granular to massive structure. They are loose (dry), friable (moist), slightly sticky and plastic (wet) and are well drained. Nitisols are developed only in well drained areas at higher altitude receiving sufficient rainfall. They correspond to the red to reddish brown or yellowish brown. They are characterized by their very thick profile and their sub angular and angular blocky structure throughout their profile. The soils are developed on variable parent materials, basaltic and colluvial deposits. Occurrence is mainly in the central highland part of the basin, on undulating to rolling plateaus, hill side slopes, and mountain foot slopes. Leptosols are occurring mainly, on undulating & rolling volcanic plains and steep hill and mountain side slopes. The soils are generally young, which are limited by their topsoil horizon over an initial development of subsoil horizon or directly over an altered parent rock from which they have developed. They are shallow with limited profile development. They are well to somewhat excessively drained, reddish brown to dark reddish brown to very dark reddish brown. The structure is mainly weak to moderately developed, fine to medium sub-angular blocky. Consistence is friable (moist), slightly sticky and slightly plastic (wet) (OWWDSE, 2013).

2.5 Hydrology

Keleta river is originated from the afro alpine area of highland Plateau of the Chilalo Mountain and are perennial stream and major tributaries of Awash river from southwest direction. Keleta stream has different flow pattern from the other two characterized by two seasons of flow in March to May and June to September which is related to the bi-modal pattern of rainfall in the study area. During the rainy season, flows increase to peak in all streams in response to high rainfall and subsides rapidly following rainfall cessation.

CHAPTER THREE

3 LITERATURE REVIEW

3.1 Concept of Land Use and Land Cover

Land cover refers to the vegetation (natural and planted), water, bare rock, sand and similar surface and also man-made construction occur on the earth's surface. While land use refers to a series of operations on land, carried out by humans, with the intention to obtain products and/or benefit through using land resources including soil resources and vegetation resources which is part of land cover (DeBie et al, 1996). Thus, land use often influences land cover. In this context, change is defined as an alteration in the surface component of the landscape and is only considered to occur if the surface has a different appearance when viewed on at least two successive occasions (Lemlem, 2007).

Land cover is defined by the attributes of the earth's land surface captured in the distribution of vegetation, water, desert and ice and the immediate subsurface, including biota, soil, topography, surface and groundwater, and it also includes those structures created solely by human activities such as mine exposures and settlement (Lambin et al, 2003).

The growing population and increasing and improvement in socio-economic creates a pressure on land use/land cover. This pressure results in unplanned and uncontrolled changes in LULC (Seto et al, 2002). The LULC alterations are generally caused by mismanagement of agricultural, urban, range and forest lands which lead to severe environmental problems such as landslides, floods etc.

Every parcel of land on the Earth's surface is unique in the cover it possesses. Land use and land cover are distinct yet closely linked characteristics of the Earth's surface. The use to which we put land could be grazing, agriculture, urban development, logging, and mining among many others. While land cover categories could be cropland, forest, wetland, pasture, roads, urban areas among others. According to (Meyer, 1995), the term land cover originally referred to the kind and state of vegetation, such as forest or grass cover but it has broadened in subsequent usage to include other things such as manmade structures like building, soil type, biodiversity, surface and ground water.

According to (Morgan, 2005), ground cover exerts a strong moderating impact on dissipating the energy supplied by agents of soil erosion especially rain drop. Soil erosion potential is increased if the soil has no or very little vegetative cover of plants and/or crop residues. Plant and residue cover protects the soil from raindrop impact and splash, tends to slow down the movement of surface runoff and allows excess surface water to infiltrate. The erosion reducing effectiveness of plant and/or residue covers depends on the type, extent and quantity of cover. Vegetation and residue combinations that completely cover the soil, and which intercept all falling raindrops at and close to the surface are the most efficient in controlling soil erosion (e.g. forests, shrubs and permanent grasses).

Increase of crop lands and decrease of forest, results increase of stream flow because of the crop soil moisture demand. Crops need less soil moisture than forests; therefore, the rainfall satisfies the shortage of soil moisture in agricultural lands more quickly than in forests there by generating more runoff when the area under agricultural land is extensive. Hence, this leads to an increases stream flow. In addition, deforestation also has its own impact on hydrological processes, leading to declines in rainfall, and more rapid runoff after precipitation (Legessa et al, 2003).

3.2 Application of Remote Sensing to Assess LULCC

In most part of the world, land cover is dynamic, especially in rural and semi-rural areas. Under such condition, accurate, meaningful and availability of data on land is highly essential for planning and decision making. Among the various sources of land cover data, satellite remote sensing is particularly attractive. The importance of remote sensing was emphasized as a “unique view” of the spatial and temporal dynamics of the processes in land cover changes (Herold, 2003). Stefanov (2001) described that satellite remote sensing techniques have started to be used in 1970’s as a modern tools to detect and monitor land cover change at various scales with useful results.

The change in land cover from rural to urban conditions and mapping of land cover establishes the baseline to predict to plan water resources, to monitor adjacent environmentally sensitive areas, and to evaluate development, resource management, industrial activity, and/or reclamation efforts. The vital component of mapping is to show the land cover changes in the watershed area and to divide land use in the various classes of land use. At this stage, remotely sensed imagery is of great help for obtaining information on temporal trends and spatial distribution of watershed areas and possible changes over the time dimension for projecting land cover changes but also to support changes impact assessment (Atasoy et al, 2006). Furthermore, multitemporal remotely sensed images are widely considered effective data sources that can be use to monitor the rapid changes of land cover, to classify types of land cover, and to obtain a timely regional overview of land cover information in a practical and economical manner over large areas.

In general, change evaluation in land cover can be obtained by using the analysis of multitemporal images to extract more classes or sub-classes besides the broad land cover types which used in the change detection limited by the historical map (Goetz et al, 1999; Prol-Ledesma et al, 2002). The acquisition of series of appropriate satellite images is often not possible for some change applications due to low spectral resolution.

In cases when large areas are to be analyzed for the study of times series historical land cover change, it is necessary to use LANDSAT Enhanced Thematic mapper (ETM+), LANDSAT Thematic Mapper according to their spatial and spectral capabilities and then reduced or combined for later comparison purpose. The images belonging to various time intervals have different sensor performances investigating the change in the Land Use/Cover(LULC). In this case, the classification results will be different, because resolutions of vary. Thus, the change analysis is preferred (Hashiba et al, 2000). The MSS sensor mounted on the Landsat satellite collected data between 1972 and 1994, while the TM and ETM+ sensor have been in use and have been in use and have acquired the image of the earth since 1982 and 1999 respectively.

3.3 Land Use and Land Cover Change Studies in Ethiopia

In Ethiopia most of the land in the country is being used by smallholders who farm for subsistence. With the rapid population growth and in the absence of agricultural intensification, smallholders require more land to grow crops and earn a living; it results in deforestation and land use conversions from other types of land cover to cropland.

The researches that have been conducted in different parts of Ethiopia have shown that there were considerable land use and land cover changes in the country. Most of these studies indicated that croplands have expanded at the expanse of natural vegetation including forests and shrublands; for example (Belay, 2002); (Bewket, 2003) ; (Kidanu, 2004); (Abebe, 2005) in northern part of Ethiopia, (Zeleke and Hurni, 2001) in north western part of Ethiopia, (Kassa, 2003) in north eastern part of Ethiopia; and (Denboba, 2005) in south western part of Ethiopia.

Kassa (2003) in his study, in southern Wello, reported the decline of natural forests and grazing lands due to conversions to croplands. Bewket (2003) have reported an increase in wood lots (eucalyptus tree plantations) and cultivated land at the expense of grazing land in both Chemoga watershed in north-western Ethiopia, and Sebat-bet Gurage land in south-central Ethiopian. The changes of land use and land cover that occurred from 1971/72 to 2000 in Yerer Mountain and its surrounding results an expansion of cultivated land at the expense of the grasslands (Gebrehiwet, 2004).

(Hadgu, 2008) identified that decrease of natural vegetation and expansion of agricultural land over a period of 41 years in Tigray, northern part of Ethiopia. He concluded that population pressure was an important deriver for expansion and intensification of agricultural land in recent periods. (Garedew, 2010) in the semiarid areas of the central Rift Valley of Ethiopia, during the period 1973-2000 cropland coverage has increased and woodland cover lost. Similarly, (Feoli et al, 2002) also reported the expansion of evergreen vegetation with increase of population. Study on a Hare watershed, in Rift Valley of Ethiopia, Kassa, (2009) reported that due to the replacement of natural forest in to farmland and settlements, the mean monthly discharge for wet months had increased while in the dry season decreased.

According to many literatures, population growth has a paramount impact on the environment. For instance, population pressure has been found to have negative effect on Riverine vegetation, scrublands and forests in Kalu district (Tekle and Hedlund, 2000), Riverine trees in Chemoga watershed (Bewket, 2003), and natural forest cover in Dembecha Woreda north-western Ethiopia (Zeleke and Hurni, 2001). Similarly, (Pender et al, 2001) report that the population growth has significant effect on land degradation, poverty and food insecurity in the northern Ethiopian highlands.

3.4 Impacts of Land Use on Stream Flow Regimes

3.4.1 Effect on mean flow

Afforestation and deforestation are two of the most important land use changes influencing the hydrological response of catchments. Catchment experiments worldwide have demonstrated that substantially altering the type and extent of vegetative cover on a catchments can significantly affect the interception and evapotranspiration (ET) processes, consequently cause a change in the runoff volume. Generally, land use changes that reduce ET increase annual runoff from catchments, whereas land use changes that increase ET decrease annual runoff. Coniferous forest, deciduous hardwood, brush and grass cover (in that order) have been found to have a decreasing influence on annual runoff of the source areas in which the land covers are manipulated (Brooks et al, 1991).

Peak flows can increase as a result of a change in land use if the infiltration capacity of the soil is reduced, for example through soil compaction or erosion, or if drainage capacity is increased. Peak flow may increase after trees are cut down (Bruijnzeel, 1990) . Relative increases in storm flow after tree removal is smallest for large events and largest for small events. As the amount of precipitation increases, influence on storm flow of soil and plant cover diminishes (Bruijnzeel, 1990).

According to Brooks et al. (1991) the degree of change in annual runoff from catchments depends on the intensity and extent of land development. The generalized relationship based on catchments experiments worldwide is that a 10% reduction in coniferous forest (deciduous forest, shrub), being converted to grassland, causes an average increase of 40 mm (25 mm for deciduous forest, 10 mm for shrub) in annual runoff.

3.4.2 Effects on flood and low flows

Land use activities may affect storm flow response and in turn flood peaks through changes in vegetation cover, soil infiltration capacity, conveyance system, increased erosion and sedimentation (Brooks et al, 1991).

The potential impacts of land use changes on surface and near surface hydrological processes (fluxes or storages) under "normal" conditions in humid temperature zones. Forests and forest soils have popularly been thought to influence the timing of stream flow by storing water during wet periods and releasing water during dry periods because of their high infiltration and soil moisture storage capacities, and hence reduce flood peaks. Conversely, deforestation is generally accepted to be a cause of increased flooding downstream (Bronstert et al, 2002).

3.5 Impact of Land Use on Erosion and Sediment Load

Forests are checkers of soil erosion. Protection is largely because of under storey vegetation and litter, and the stabilizing effect of the root network. On steep slopes, the net stabilizing effect of trees is usually positive. Vegetation cover can prevent the occurrence of shallow landslides (Bruijnzeel, 1990). However, large landslides on steep terrain are not influenced appreciably by vegetation cover. These large slides may contribute the bulk of the sediment, as for example in the middle hills of the Himalayas (Bruijnzeel and Bremmer, 1989).

Afforestation does not necessarily decrease soil erosion. Splash erosion may increase substantially when litter is cleared from the forest floor (Bruijnzeel, 1990). The spectrum for the size of the drops that are formed by the canopy varies widely among different species, resulting in large differences in the potential of splash erosion (Calder, 1998).

Deforestation may increase erosion. The actual soil loss, however, depends largely on the use to which the land is put after the trees have been cleared. Surface erosion from well-kept grassland, moderately grazed forests and soil-conserving agriculture are low to moderate (Bruijnzeel, 1990). Road construction may be a major cause for erosion during timber harvesting operations.

In the USA, forest roads are estimated to account for 90 percent of the erosion caused by logging activities.

Effects of erosion control measures on sediment yield will be most readily felt on-site. There is an inverse relation between basin size and sediment delivery ratio. In basins of several hundred km^2 improvements may only be noticeable after a considerable time lag (Decades), due to storage effects (Bruijnzeel, 1990).

3.6 Hydrological Model

Hydrological models are characterizations of the real world system. Modeling of the rainfall-runoff processes of hydrology is needed for many different reasons. The main reasons being limited range of hydrological measurement techniques and limited range of measurements in space and time (Beven, 2000). Therefore, it is necessary to develop a means of extrapolating from those available measurements in space and time to ungauged catchments and into the future to assess the likely impact of future hydrological changes. A wide range of hydrological models are used by the researchers, however, the applications of those models are highly dependent on the purposes for which the modeling is made. (Beven, 2000) stated that many rainfall-runoff models are carried out purely for research purposes as a means of enhancing knowledge about hydrological systems. He also added that other types of models are developed and employed as tools for simulation and prediction aiming ultimately to allow decision makers to improve decision making about hydrological problems. Before developing the hydrological models, it is very important to understand how the catchment responds to rainfall under different conditions.

3.6.1 Types of Hydrological Model

Lumped models: Parameters of lumped hydrologic models do not vary spatially within the basin and thus, basin response is evaluated only at the outlet, without explicitly accounting for the response of individual sub basins. Parameters of lumped models often do not represent physical features of hydrologic processes and usually involve certain degree of empiricism. The impact of spatial variability of model parameters is evaluated by using certain procedures for calculating effective values for the entire basin. The most commonly employed procedure is an area-weighted average (Haan et al, 1994). Lumped models are not usually applicable to eventscale processes. If the interest is primarily in the discharge prediction only, then these models can provide just as good simulations as complex physically based models (Beven, 2000).

Semi-distributed models: Parameters of semi-distributed (simplified distributed) models are partially allowed to vary in space by dividing the basin into a number of smaller subbasins. There are two main types of semi-distributed models: 1) kinematic wave theory models (KW models, such as HEC-HMS), and 2) probability distributed models (PD models, such as TOPMODEL). The KW models are simplified versions of the surface and/or subsurface flow equations of physically based hydrologic models (Beven, 2000). In the PD models spatial resolution is accounted for by using probability distributions of input parameters across the basin. SWAT (Arnold et al, 1993), HEC-HMS (US-ACE, 2001), HBV (Bergström, 1995), are considered as semi-distributed models.

Distributed models: Parameters of distributed models are fully allowed to vary in space at a resolution usually chosen by the user. Distributed modeling approach attempts to incorporate data concerning the spatial distribution of parameter variations together with computational algorithms to evaluate the influence of this distribution on simulated precipitation-runoff behaviour. Distributed models generally require large amounts of (often unavailable) data for parameterization in each grid cell. However, the governing physical processes are modeled in detail, and if properly applied, they can provide the highest degree of accuracy.

3.7 SWAT Development and Interface

SWAT (Arnold et al, 1998) is a semi-distributed, time continuous watershed simulator operating on a daily time step. It is developed for assessing the impact of management and climate on water supplies, sediment, and agricultural chemical yields in watersheds and larger river basins. The model is semi-physically based, and allows simulation of a high level of spatial detail by dividing the watershed into a large number of sub-watersheds. The major components of SWAT include hydrology, weather, erosion, plant growth, nutrients, pesticides, land management, and stream routing. The program is provided with an interface in Arc GIS (Arc SWAT 2005, (Winchell et al, 2008) for the definition of watershed hydrologic features and storage, as well as the organization and manipulation of the related spatial and tabular data.

3.7.1 Theoretical Description of SWAT

The large scale spatial heterogeneity of the study area is represented by dividing the watershed into sub basins. Each sub basin is further discredited into a series of hydrologic response units (HRUs), which are unique soil-land use combinations. Soil water content, surface runoff, nutrient cycles, sediment yield, crop growth and management practices are simulated at each HRU and then aggregated for the sub basin by a weighted average. Physical characteristics, such as slope, reach dimensions, and climatic data are considered for each sub basin. For climate, SWAT uses the data from the station nearest to the centric of each sub basin. Calculated flow, sediment yield, and nutrient loading obtained for each sub basins are then routed through the river system. Channel routing is simulated using the variable storage or Muskingum method. The water in each HRU in SWAT is stored in four storage volumes: shallow soil profile (0-2m), snow shallow aquifer (typically 2-20m), and deep aquifer. Surface runoff from daily rainfall is estimated using a modified SCS curve number method, which estimates the amount of runoff based on local land use, soil type, and antecedent moisture condition. Peak runoff predictions are based on a modification of the Rational Formula (Chow et al, 1988). The watershed concentration time is estimated using Manning.s formula, considering both overland and channel flow. The soil profile is subdivided into multiple layers that support soil water processes including infiltration, evaporation, plant uptake, lateral flow, and percolation to lower layers. The soil percolation component of SWAT uses a water storage capacity technique to predict flow through each soil layer in the root zone. Down ward flow occurs when field capacity of a soil layer is exceeded and the layer below is not saturated. Percolation from the bottom of the soil profile recharges the shallow aquifer. Daily average soil temperature is simulated as a function of the maximum and minimum air temperature. If the temperature in a particular layer reaches less than or equal to 0°C, no percolation is allowed from that layer. Lateral sub-surface flow in the soil profile is calculated simultaneously with percolation.

The model computes evaporation from soils and plants separately. Potential evapotranspiration can be modeled with the Penman-Monteith (Monteith, 1965), Priestly-Taylor (Priestley and Taylor, 1972), or Hargreves methods (Hargreves et al, 1985), depending on data availability. Potential soil water evaporation is estimated as a function of potential ET and leaf area index (area of plant leaves relative to the soil surface area). Actual soil evaporation is estimated by using exponential functions of soil depth and water content. Plant water evaporation is simulated as a linear function of potential ET, leaf area index, and root depth, and can be limited by soil water content.

Sediment yield in SWAT is estimated with the modified soil loss equation (MUSLE) developed by (Wischmeier and Smith , 1978). The sediment routing model consists of two components operating simultaneously: deposition and degradation. The deposition in the channel and flood plain from the sub-watershed to the watershed outlet is based on the sediment particle settling velocity. The settling velocity is determined using Stoke.s law (Chow et al, 1988) and is calculated as a function of particle diameter squared. The depth of fall through a r each is the product of settling velocity and the reach travel time. The delivery ratio is estimated for each particle size as a linear function of fall velocity, travel time, and flow depth. Degradation in the channel is based on Bagnold.s stream power concept (Bagnold, 1977; Williams, 1980).

3.7.2 SWAT Model Application

The SWAT Model is one of the most widely used and scientifically accepted tool for assessing water quality, sediment transport and streamflow in a watershed; as evidenced by worldwide conferences and publications of SWAT related reports and articles. The use of the model is primary driven by the demand of various environmental agencies for direct and exploratory assessments of the impact of anthropogenic activities, climate change, and other wide range of land management issues on water and soil resources (Gassman et al, 2007). Since many watersheds globally are already experiencing degradation and calls for sound management of resources, SWAT has been increasingly used even outside of the United States of America. According to (Arnold et al, 2011), the SWAT model has also been used in countries such as China, Iran, Japan, Korea, Philippines, as well as countries in Europe and in Africa.

In the Upper Nile Basin in Africa, SWAT has been used for hydrology/water balance, erosion, water quality, and climate change assessments, calibration uncertainty, land use change studies, and SWAT development (vanGriensven et al, 2012). Additionally, (Gassman et al, 2007) showed that the global application of SWAT included calibration and/or sensitivity analysis, climate change impacts, GIS interface descriptions, hydrologic assessments, variation in configuration or data input effects, comparison with other models or techniques, interfaces with other models, and pollutant assessments. The SWAT model application was calibrated and validated in some parts of Ethiopia (e.g., Chekol, 2006; Setegn et al, 2009; Tibebe and Bewket, 2010; vanGriensven et al, 2012; Tesfahunegn et al., 2012) have already shown that SWAT model was evaluated with adequate level of accuracy in gauged catchments in some parts of Ethiopia.

CHAPTER FOUR

4 MATERIALS AND METHODS

4.1 General

The general methodology for this study is shown in figure 4.1. The historical climate data, sediment and flow data have been collected from National metrological agency and ministry of water resources respectively. The DEM data were obtained from the NASA website. Soil data is obtained from Oromia water work design and supervision enterprises and land use land cover data of two Landsat images were downloaded from the Global Land Cover Facility's Earth Science Data Interface website. The watershed is automatically delineated via the SWAT2005 model interface with ArcGIS 9.3 (ArcSWAT) using the input DEM while sub-basins and finer subdivisions in the watershed called the hydrologic response units (HRU) are defined by setting threshold limits for land use/land cover, soil type and slope class. Writing the input parameter file and running the SWAT model. Available flow and sediment data were used to sensitivity analysis, calibrate and validate the model. Calibrate the model for two LULC, the results of which are compared and final analysis.

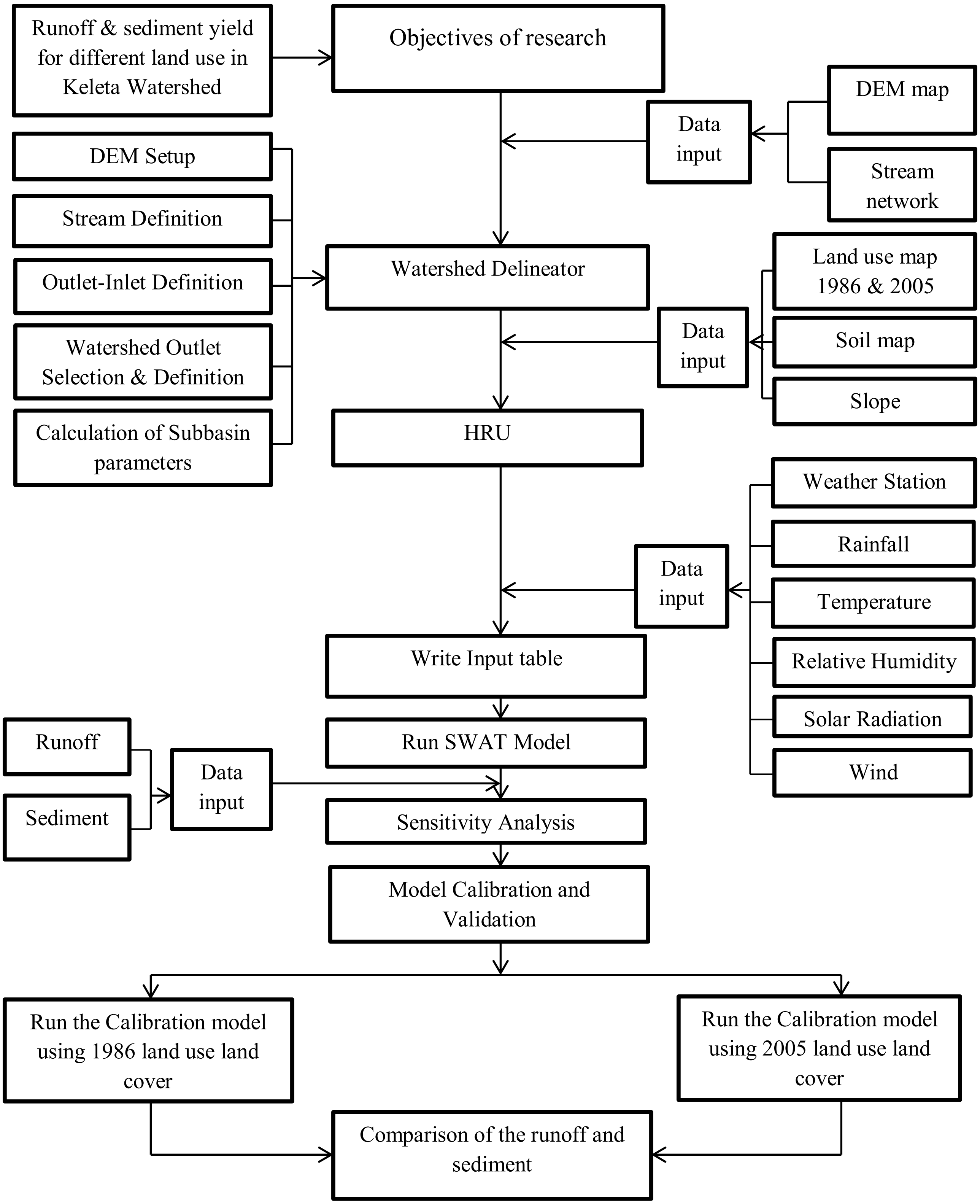

Figure 4.1:-Flow chart of SWAT model application in Keleta watershed

As shown in figure 4.2 the prepare land use/ land cover map for Keleta watershed, the downloaded two satellite images Landsat TM and Landsat ETM+ imagery acquired on 21 January 1986 and 03 December 2005 respectively. The Landsat images once downloaded were unzipped and they consisted of the constituent spectral bands that made up the satellite image. These constituent bands are stored in a Tagged Image File Format (TIFF) format which are not as useful individually as when stacked together to form a single image. The subsetted areas were then geometrically rectified with reference to the topographic map coordinates marked on the tracing paper in the ERDAS Imagine software. As training samples were collected during field visit using hand held GPS and Google earth supervised classification method using Maximum Likelihood classification algorithm was used for preparing the land use/ land cover map of the study area for both the years and analysis the change.

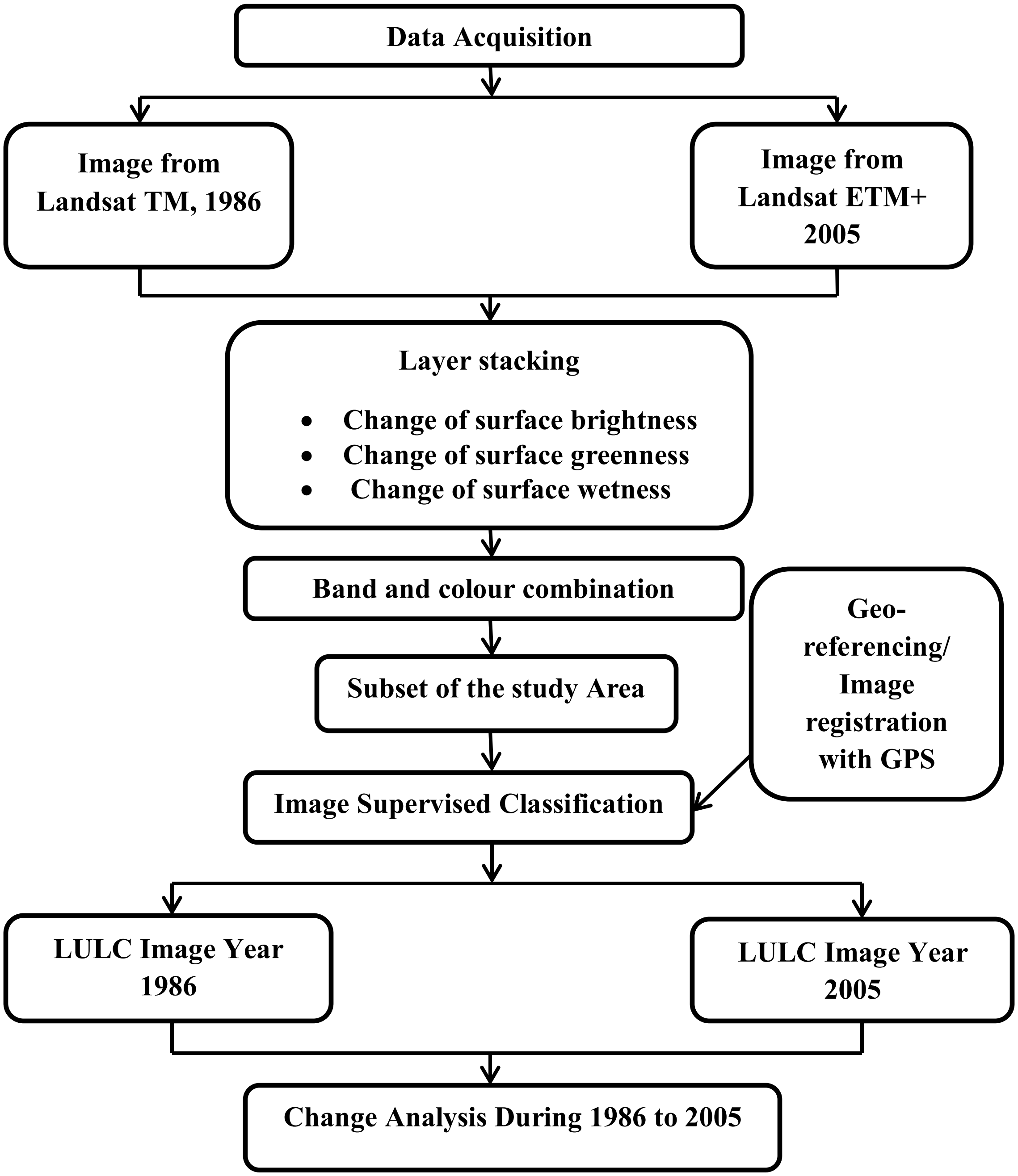

Figure 4.2:-Flow chart for land use land cover mapping

4.2 Land Use/Land Cover Change Analysis

Change analysis was conducted using post-classification image comparison technique (Singh, 1989). Post-classification change analysis was selected in order to minimize possible effects of atmospheric variations and sensor differences (Lu et al , 2004). Classification with high accuracy is a prerequisite for effective change detection using post-classification technique (Foody, 2001). Images of different reference years were first independently classified. Classified images with highest accuracy were used in the change detection process.

The classified images were compared from land use land cover 1986 to 2005. Change statistics were computed by comparing image values of one data set with the corresponding value of the second data set in each period. This results in a summary table of the overall changes per class. The values were presented in terms of kilometer square and percentages. The percentage LULC changes were calculated using the following equation:

$$Percentage\ LULC\ change = \left(\frac{Area_{final\ year} - Area_{initial\ year}}{Area_{initial\ year}}\right) * 100 \qquad 4.1$$

where Area is extent of each LULC type. Positive values suggest an increase whereas negative values imply a decrease in extent.

4.3 Description of Soil and Water Assessment tool (SWAT) Model

SWAT is a public domain model actively supported by the USDA (United State Department of Agriculture) – ARS (Agricultural Research Service) at the Grassland, Soil and Water Research Laboratory in Temple, Texas, USA. SWAT is a river basin scale, a continuous time, a spatially distributed model developed to predict the impact of land management practices on water, sediment and agricultural chemical yields in large complex watersheds with varying soils, land use and management conditions over long periods of time (Arnold et al, 1998; Neitsch et al, 2005). SWAT can analyze both small and large watersheds by subdividing the area into homogenous parts. As a physically-based model, SWAT uses hydrologic response units (HRUs) to describe spatial heterogeneity in terms of land cover, soil type and slope within a watershed. The SWAT system embedded with-in geographic information system (GIS) that can integrate various spatial environmental data including soil, land cover, climate and topographic features.

Currently SWAT is imbedded in an ArcGIS interface called ArcSWAT. It is computationally efficient, uses readily available inputs and enables users to study long-term impacts.

4.3.1 Hydrological Component of SWAT

The Simulation of the hydrology of a watershed is done in two separate divisions. One is the land phase of the hydrological cycle that controls the amount of water, sediment, nutrient and pesticide loadings to the main channel in each subbasin. Hydrological components simulated in land phase of the Hydrological cycle are canopy storage, infiltration, redistribution, evapotranspiration, lateral subsurface flow, surface runoff, ponds, tributary channels and return flow. The second division is routing phase of the hydrologic cycle that can be defined as the movement of water, sediments, nutrients and organic chemicals through the channel network of the watershed to the outlet. In the land phase of hydrological cycle, SWAT simulates the hydrological cycle (Figure 4.3) based on the water balance equation applied to water movement through soil and it is expressed by equation 4.2.

$$SW_t = SW_o + \sum_{i=1}^{t} \left(R_{day} - Q_{surf} - E_a - W_{seep} - Q_{qw}\right) \quad 4.2$$

In which SW_t is the final soil water content (mm), SW_o is the initial soil water content on day i (mm), t is the time (days), R_{day} is the amount of precipitation on day i (mm), Q_{surf} is the amount of surface runoff on day i (mm), E_a is the amount of evapotranspiration on day i (mm), W_{seep} is the amount of water entering the vadose zone from the soil profile on day i (mm), and Q_{qw} is the amount of return flow on day i (mm). Brief description of some of the key model components are provided in this thesis. More detailed descriptions of the different model components are listed in (Arnold et al, 1998; Neitsch et al, 2005).

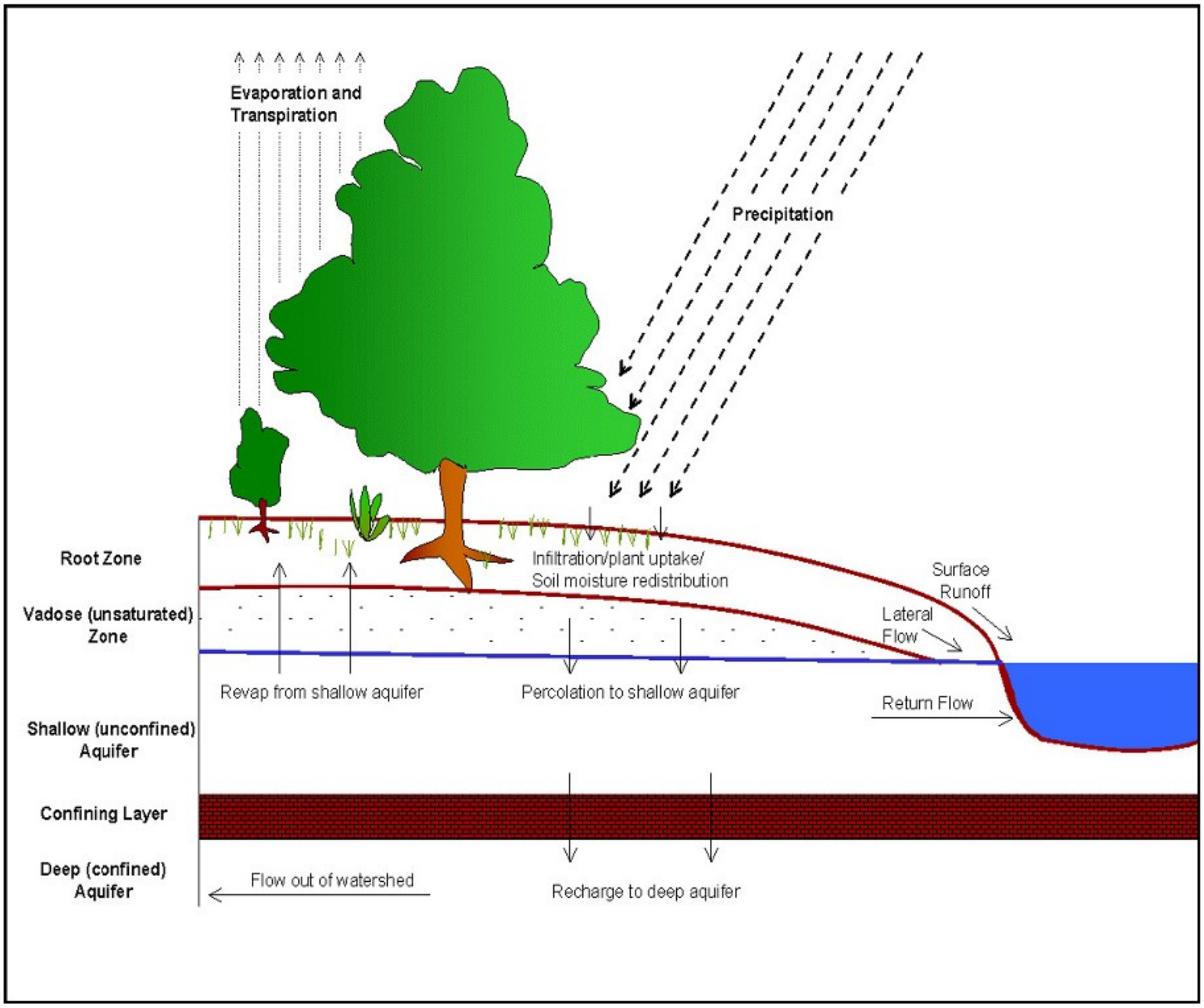

Figure 4.3:-Hydrologic cycle considered by SWAT model from (Neitsch et al, 2005)

Surface Runoff

Surface runoff occurs whenever the rate of precipitation exceeds the rate of infiltration. SWAT offers two methods for estimating surface runoff: the SCS curve number procedure (USDA-SCS, 1972) and the Green and Ampt infiltration method (Green and Ampt, 1911). Using daily or sub daily rainfall, SWAT simulates surface runoff volumes and peak runoff rates for each HRU. In this study, the SCS curve number method was used to estimate surface runoff because of the unavailability of sub daily data for Green and Ampt method.

The SCS curve number equation (USDA-SCS, 1972) is described by equation 4.3.

$$Q_{surf} = \frac{(R_{day} - 0.2S)^2}{(R_{day} + 0.8S)} \qquad 4.3$$

In which, Q_{surf} is the accumulated runoff or rainfall excess (mm), R_{day} is the rainfall depth for the day (mm), S is the retention parameter (mm).

The retention parameter is defined by equation 4.4

$$S = 25.4\left(\frac{100}{CN} - 10\right) \qquad 4.4$$

SWAT2005 version includes two methods for calculating the retention parameter; the first one is retention parameter varies with soil profile water content and the second method is the retention parameter varies with accumulated plant evapotranspiration. The soil moisture method (equation 4.6) over-estimates runoff in shallow soils. But calculating daily CN as a function of plant evapotranspiration, the value is less dependent on soil storage and more dependent on antecedent climate.

$$S = S_{max}\left(1 - \frac{SW}{[SW + exp(w_1 - w_2.SW)]}\right) \qquad 4.5$$

In which S is the retention parameter for a given day (mm), S_{max} is the maximum value that the retention parameter can have on any given day (mm), SW is the soil water content of the entire profile excluding the amount of water held in the profile at wilting point (mm), and w_1 and w_2 are shape coefficients. The maximum retention parameter value, S_{max}, is calculated by solving equation 4.4.using CN1.

$$S_{max} = 25.4\left(\frac{100}{CN_1} - 10\right) \qquad 4.6$$

When the retention parameter varies with plant evapotranspiration, the following equation is used to update the retention parameter at the end of every day:

$$S = S_{prev} + E_o * exp\left(\frac{-cncoef - S_{prev}}{S_{max}}\right) - R_{day} - Q_{surf} \qquad 4.7$$

In which S_{prev} is the retention parameter for the previous day (mm), E_o is the potential evapotranspiration for the day (mm/day), $cncoef$ is the weighting coefficient used to calculate the retention coefficient for daily curve number calculations dependent on plant evapotranspiration, S_{max} is the maximum value the retention parameter can achieve on any given day (mm), R_{day} is the rainfall depth for the day (mm), and Q_{surf} is the surface runoff (mm). The initial value of the retention parameter is defined as S=0.9S_{max}.

The SCS curve number is a function of the soil's permeability, land use and antecedent soil water conditions. SCS defines three antecedent moisture conditions: I – dry (wilting point), II – average moisture, and III – wet (field capacity). The moisture condition I curve number is the lowest value the daily curve number can assume in dry conditions. The curve numbers for moisture conditions I and III are calculated with equations 4.8 and 4.9.

$$CN_1 = CN_2 - \frac{20.(100 - CN_2)}{(100 - CN_2 exp[2.533 - 0.0636.(100 - CN_2)])} \quad 4.8$$

$$CN_3 = CN_2.exp[0.00673.(100 - CN_2)] \quad 4.9$$

Where CN_1 is curve number for moisture condition I, CN_2 is curve number for moisture condition II and CN_3 is curve number for moisture condition III.
Typical curve numbers for moisture condition II are listed in various tables (Neitsch et al, 2005). The values are appropriate for a 5 % slope. (Williams, 1995) developed an equation to adjust the curve number to a different slope:

$$CN_{2S} = \frac{(CN_3 - CN_2)}{3}.[1 - 2.exp(-13.86.slp)] + CN_2 \quad 4.10$$

In which CN_1 is the moisture condition I curve number, CN_2 is the moisture condition II curve number for the default 5 % slope, CN_3 is the moisture condition III curve number for the default 5 % slope, CN_{2S} is the moisture condition II curve number adjusted for slope and slp is the average percent slope of the sub basin.

Surface runoff lag

In large subbasin with a time of concentration greater than one day, only a portion of the runoff will reach the main channel on the day it is generated. SWAT model incorporates a surface runoff storage feature to lag a portion of the surface runoff to the main channel. Once the surface runoff is calculated with curve number method the amount of surface runoff released to the main channel is calculated by:

$$Q_{surf} = \left(Q'_{surf} + Q_{stor,i-1}\right).\left(1 - exp\left[\frac{-surlag}{t_{conc}}\right]\right) \quad 4.11$$

Where Q_{surf} is the amount of surface runoff discharged to the main channel on a given day (mm), Q'_{surf} is the amount surface runoff generated in the subbasin on the given day(mm), $Q_{stor,i-1}$ is surface runoff stored or lagged from the previous day (mm), $surlag$ is surface runoff lag coefficient and t_{conc} it time of concentration for the basin (hrs).

Routing method

This is the second division of the hydrologic cycle that can be defined as the movement of water, sediments, nutrients and organic chemicals through the channel network of the watershed to the outlet (Figure 4.4). There are two options available to rout water through the channel network, that are the Muskingum storage routing or river routing method and Variable storage routing method. The variable storage routing method was developed by (Williams, 1969) based on the principle continuity equation in routing the storage volume and used in the HYMO (Williams and Hann, 1973) and ROTO (Arnold et al, 1995) models. For a given segment, storage routing is based on the continuity equation. Therefore this routing method was adopted in this study and it is expressed as:

$$\Delta V_{stored} = V_{in} - V_{out} \quad 4.12$$

Where V_{in} the volume of inflow during the time step (m^3 H_2O), V_{out} is the volume of outflow during the time step (m^3 H_2O) and V_{stored} is the change in volume of storage during the time step (m^3 H_2O). Hence this method is used in this study and detail of this method is given in the SWAT model 2005 Manual.

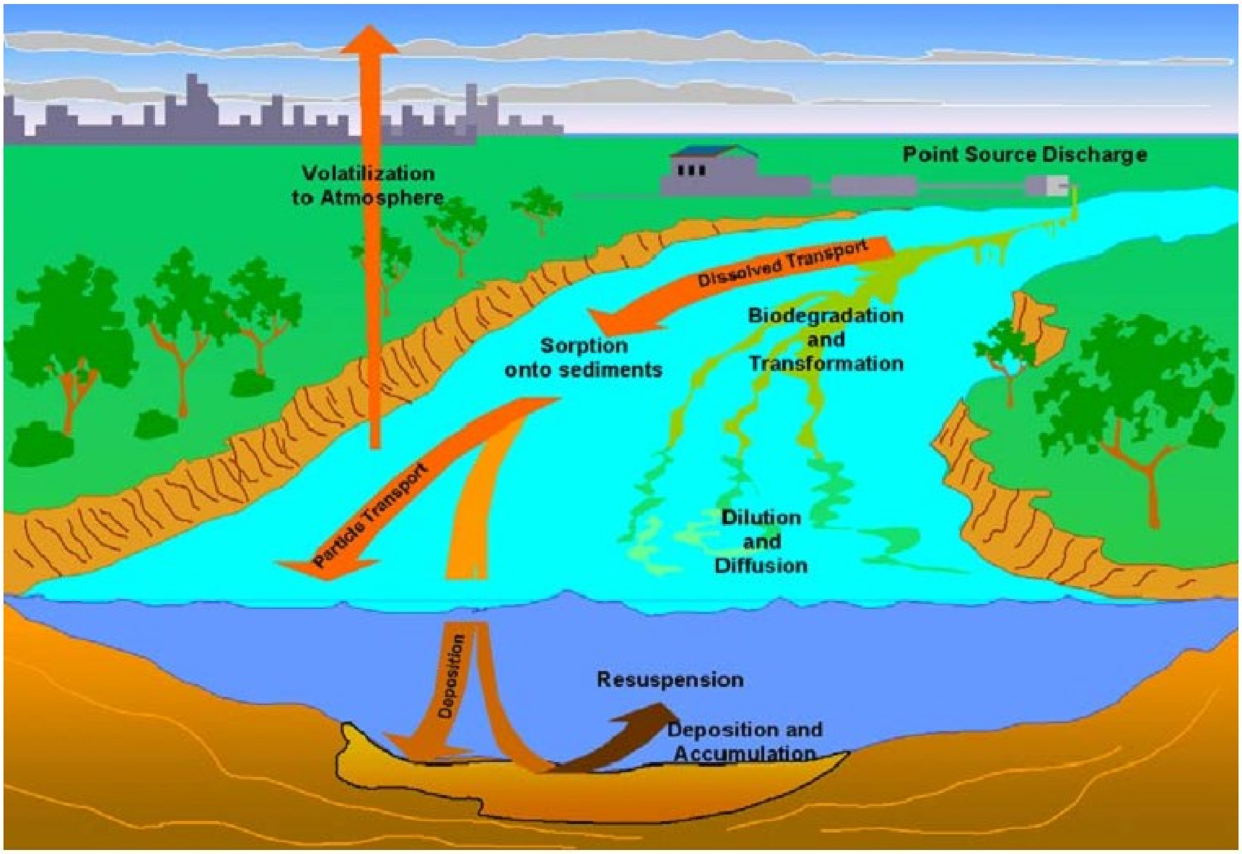

Figure 4.4:-In stream processes considered by the SWAT model (Neitsch et al, 2005)

Potential Evapotranspiration (PET)

SWAT calculates the peak runoff rate with a modified rational method. There are many methods that are developed to estimate potential evapotranspiration (PET). Three methods are incorporated into SWAT: the Penman-Monteith method (Monteith, 1965), the Priestley-Taylor method (Priestley and Taylor, 1972) and the Hargreaves method (Hargreves et al, 1985). The three PET methods included in SWAT vary in the amount of required inputs. The Penman-Monteith method requires solar radiation, air temperature, relative humidity and wind speed. The Priestley-Taylor method requires solar radiation, air temperature and relative humidity. Hargreaves method requires air temperature only. For this study Hargreaves method was used due to limitation of weather data such as wind speed, humidity and sunshine hours.

Ground water system

In the SWAT model; the simulation of groundwater is partitioned into two aquifer systems. Such that unconfined aquifer (shallow) and a deep-confined aquifer in each sub basin. The unconfined aquifer contributes to flow in the main channel or reach of the sub basin and water that enters the deep aquifer is assumed to contribute to stream flow outside the watershed (Arnold et al, 1993). In SWAT2005 the water balance for a shallow aquifer is calculated with equation 4.13.

$$aq_{sh,i} = aq_{sh,i-1} + w_{rchrg,sh} - Q_{gw} - w_{revap} - w_{pump,sh} \qquad 4.13$$

In which $aq_{sh,i}$ is the amount of water stored in the shallow aquifer on day i (mm), $aq_{sh,i-1}$ is the amount of water stored in the shallow aquifer on day i-1 (mm), $w_{rchrg,sh}$ is the amount of recharge entering the aquifer on day i (mm), Q_{gw} is the groundwater flow, or base flow, into the main channel on day i (mm), w_{revap} is the amount of water moving into the soil zone in response to water deficiencies on day i (mm), and $w_{pump,sh}$ is the amount of water removed from the shallow aquifer by pumping on day i (mm).

The shallow aquifer may contribute base flow to the main channel or reach within the subbasin and the steady state response of groundwater flow to recharge is estimated by (Hooghoudt, 1940) equation:

$$Q_{gw} = \frac{800 * K_{sat}}{L_{gw}} h_{wtbl} \qquad 4.14$$

In which K_{sat} is the hydraulic conductivity of the aquifer (mm/day), L_{gw} is the distance from the ridge or subbasin divide for the groundwater system to the main channel (m), and h_{wtbl} is the water table height (m).

Similarly the groundwater system for deep aquifer estimated by:

$$aq_{dp,i} = aq_{dp,i-1} + W_{deep} - W_{pump,dp} \qquad 4.15$$

Where $aq_{dp,i}$is amount of water stored in the deep aquifer on day I (mm H2O), $aq_{dp,i-1}$ is amount of water stored in the deep aquifer on day i-1 (mm H2O), W_{deep} is the amount of water percolating from the shallow aquifer into the deep aquifer on day I (mm H2O) and $W_{pump,dp}$ is the amount of water removed from the deep aquifer by pumping on day I (mm H2O).

Base flow separation

The first step in hydrograph analysis entails separation of stream flow in to the two major components: surface runoff and base flow. However the exact separation of each component is often arbitrary and based on either the use of standard methodologies cited in the literature (McCune, 1989) or in a few instances, the use of chemical or isotopic tracers and mass balance approaches (Pinder and Jones, 1968).

The automated base flow separation and recession analysis techniques (Arnold et al, 1995), (http://pasture.ecn.purdue.edu/~what/) are among the several methods available to separate base flows. Due its simplicity, this technique was applied. As indicated by (Nathan and McMahon, 1990) by comparing with different methods, the recursive digital filter was found to be a fast and objective method of continuous base flow separation.

The recursive digital filter technique as described by (Nathan and McMahon, 1990) was originally used in signal analysis and processing (Lyne and Hollick, 1979). Filtering surface runoff (high frequency signals) from base flow (low frequency signals) is analogous to the filtering of high frequency signals in signal analysis and processing. The equation of the filter is

$$q_t = \beta * q_{t-1} + \frac{(1+\beta)}{2} * (Q_t - Q_{t-1}) \qquad 4.16$$

Where q_t is the filtered surface runoff (quick response) at the t time step, Q_t is the original stream flow, β is the filter parameter, base flow b_t is calculated with the equation

$$b_t = Q_t - q_t \qquad 4.17$$

The filter can be passed over the stream flow data three times, depending on users selected estimates of base flow. In general, each pass will result in less base flow as a percentage of total flow. Output parameters of this program are the time series of base flow and surface runoff, base flow recession constant (alpha factor) and Base flow days i.e. number of days for the base flow recession to decline through one log cycle. The result of base flow, such as alpha factor directly used in to the SWAT simulation.

4.3.2 Sediment component

Sediment yield is estimated for each HRU using the Modified Universal Soil Loss Equation (MUSLE) (Williams , 1975). Sediment routing in the channel is controlled by two processes, degradation and deposition, with deposition occurring when the upland sediment load is larger than the transport capacity of the channel and degradation occurring when it is smaller. The transport capacity of a channel segment is calculated as a function of the peak channel velocity (Arnold et al, 1995).

SWAT calculates the soil erosion and sediment yield with the Modified Universal Soil Loss Equation (MUSLE) 4.18, (Williams , 1975).

$$sed = 11.8.\left(Q_{surf}.q_{peak}.area_{hru}\right)^{0.56}.K_{USLE}.C_{USLE}.P_{USLE}.LS_{USLE}.CFRG \qquad 4.18$$

In which sed is the sediment yield on a given day (metric tons), Q_{surf} is the surface runoff volume (mm /ha), q_{peak} is the peak runoff rate (m^3/s), $area_{hru}$ is the area of the HRU (ha), K_{USLE} is the soil erodibility factor (0.013 metric ton m^2 hr/(m^3-metric ton cm)), C_{USLE} is the cover and management factor, P_{USLE} is the support practice factor, LS_{USLE} is the topographic factor and $CFRG$ is the coarse fragment factor. The details of the USLE factors and the descriptions of the different model components can be found in (Neitsch et al, 2005).

The peak runoff rate is calculated as:

$$q_{peak} = \frac{C.i.Area}{3.6} \qquad 4.19$$

where q_{peak} is the peak runoff rate (m^3/s), C is the runoff coefficient, i is the rainfall intensity (mm hr-1), $Area$ is the HRU area (km^2) and 3.6 is a unit conversion factor. The calculation of the runoff coefficient and the rainfall intensity is explained by (Neitsch et al, 2005).

In SWAT, sediment routing model consists of two components that operate simultaneously to simulate the sediment transport in the channel network. These are the deposition and degradation processes (Neitsch et al, 2005). To decide such processes, the maximum sediment concentration in the reach is compared with that of sediment in the reach at the beginning of the time step. The maximum amount of sediment that can be transported from a reach segment is calculated as (Neitsch et al, 2005):

$$Conc_{sed,ch,mx} = C_{sp} . v_{ch,pk}^{spexp} \qquad 4.20$$

Where $Conc_{sed,ch,mx}$ is the maximum concentration of sediment that can be transported by the water (ton m^{-3} or kg/L), C_{sp} is a coefficient defined by the user, $v_{ch,pk}$ is the peak channel velocity (m/s), and $spexp$ is exponent parameter for calculating sediment reentrained in channel sediment routing that is defined by the use and normally varies between 1.0 and 2.0.

The maximum concentration of sediment calculated in equation 4.20 is compared with the concentration of sediment in the reach at the beginning of the time step, $conc_{sed,ch,i}$. If $conc_{sed,ch,i} > conc_{sed,ch,mx}$, deposition is the dominant process in the reach segment and the net amount of sediment deposited (Neitsch et al, 2005) is:

$$sed_{dep} = \left(conc_{sed,ch,i} - conc_{sed,ch,mx}\right) . V_{ch} \qquad 4.21$$

where sed_{dep} is the amount of sediment deposited in the reach segment (metric tons), $conc_{sed,ch,i}$is the initial sediment concentration in the reach (tons m^{-3}), $conc_{sed,ch,mx}$ is the maximum concentration of sediment that can be transported by the water (ton m-3), and $V_{ch}$is the volume of water in the reach segment (m^3). Conversely, if $conc_{sed,ch,i} < conc_{sed,ch,mx}$, degradation is the dominat process in the reach segment and the net amount of sediment reentrained is calculated as (Neitsch et al, 2005):

$$sed_{deg} = \left(conc_{sed,ch,mx} - conc_{sed,ch,i}\right) . V_{ch} . K_{CH.} C_{CH} \qquad 4.22$$

where sed_{deg} is the amount of sediment reentrained in the reach segment (metric tons), $conc_{sed,ch,mx}$ is the maximum concentration of sediment that can be transported by the water (tons m-3), $conc_{sed,ch,i}$ is the initial sediment concentration in the reach (tons m3), K_{CH} is the channel erodibility factor (cm h^{-1} Pa^{-1}), and C_{CH} is the channel cover factor.

Once the amount of degradation and deposition has been calculated, the final amount of sediment in the reach (basin´s outlet) is determined as:

$$sed_{ch} = sed_{ch,i} - sed_{dep} + sed_{deg} \quad 4.23$$

Where sed_{ch} is the amount of suspended sediment in the reach (metric tons), $sed_{ch,i}$ is the amount of suspended sediment in the reach at the beginning of the time period (metric tons), sed_{dep}, is the amount of sediment deposited (metric tons) and sed_{deg} is the amount of sediment reentrained in the reach segment (metric tons).

The amount of sediment transported out of the reach is calculated by equation

$$sed_{out} = sed_{ch} \frac{V_{out}}{V_{ch}} \quad 4.24$$

In which sed_{out} is the amount of sediment transported out of the reach (metric tons), V_{out} is the volume of outflow during the time step (m^3).

4.4 Sensitivity, Calibration and Validation Analysis

A computer based watershed models can save time and money because of their ability to perform long term simulation of the effect of watershed processes and management activities on water quality and quantity and soil quality (Moriasi et al, 2007). But, obviously these hydrological models under estimate or overestimate the long term simulation of the hydrological processes activities within the watersheds. To increase the applicability of the any hydrological model, it need to check there performance before to use for simulation of the hydrological processes using graphical or statistical methods.

4.4.1 Sensitivity

Model users are often faced with the difficulty task of determining which parameters to calibrate so that the model response mimics the actual field, subsurface, and channel conditions as closely as possible. When the number of parameters in the model is substantial as a result of either a large number of sub- processes becomes complex and computationally extensive. Especially for big hydrological models like SWAT, which involves a wide range of data and parameters in the simulation process and calibration is quite a cumbersome task (Kassa, 2009).

In such case sensitivity analysis helps as tools to identify and rank the parameters that have a significant impact on specific model outputs of interest (Saltelli et al, 2000; Sorroshian and

Gupta, 1995; and Rosso, 1994). Parameters that are identified in the sensitivity analysis influences the predicted outputs often used to calibrate the model.

Actually, sensitivity analysis is the process of determining the rate of change in model output with respect to changes in model inputs (parameters). It is a necessary process to identify key parameters and parameter precision required for calibration (Moriasi et al, 2007). As proposed by (Van Griensven et al, 2005), in SWAT model the sensitivity is implemented in two ways. That are called One- factor -At- a time (OAT) design and the Latin Hypercube (LH) sampling technique. The detail of this method is given in (Huisman et al, 2004).
During sensitivity analysis, SWAT runs (p+1)*m times, where p is the number of parameters being evaluated and m is the number of LH loops. For each loop, a set of parameter values is selected such that a unique area of the parameter space is sampled. That set of parameter values is used to run a baseline simulation for that unique area. Then, using one-at-a-time (OAT), a parameter is randomly selected, and its value is changed from the previous simulation by a user defined percentage. Based on this SWAT is running on the new parameter set and then a different parameter is randomly selected and varied. After all the parameters have been varied, the LH algorithm locates a new sampling area by changing all the parameters (Veith and Ghebremichael, 2009).

Basically, the Arc-SWAT sensitivity analysis tool has the capability of performing two types of sensitivity analysis. The first type of analysis uses only modeled data to identify the impact of adjusting a parameter value on some measure of simulated output, such as average stream flow. The second type of analysis uses measured data to provide overall "goodness of fit" estimation between the modeled and the measured time series. The first analysis may help to identify parameters that improve a particular process or characteristic of the model, while the second analysis identifies the parameters that are affected by the characteristics of the study watershed and those to which the given project is most sensitive (Veith and Ghebremichael, 2009).

Therefore after model run, the **s**ensitivity analyses were conducted for the Keleta watershed runoff and sediment yield to determine the parameters needed to improve simulation results and thus to better understand the behavior of the hydrologic system and to evaluate the applicability of the model. The sensitivity for the watershed carried-out with the observed data and ranks the mean value of the parameters and selects the most sensitive parameters based on the classification of (Lenhart et al, 2002). He classified the sensitivity in to four classes see table 4.1 and also he indicated the value 0.20 is to be significant variation of hydrological processes between individual watersheds. In this study also used this sensitivity index as a guideline to select the most sensitive parameter for the watershed.

Table 4.1:-Sensitivity classification (Lenhart et al, 2002)

Class	Index	Sensitivity
I	$0 \le MRS < 0.05$	Small to negotiable
II	$0.05 \le MRS < 0.2$	Medium
III	$0.2 \le MRS < 1$	High
IV	$MRS \ge 1$	Very high

MRS=Mean Relative Sensitivity

Sensitivity analysis has been done on the built in extension program embedded in SWAT. Sensitivity analysis has been carried out for flow 26 and sediment 6 parameters list in Appendix 2 and Appendix 3 respectively.

4.4.2 Calibration

Model calibration is the processes of estimating model parameters by comparing model prediction (output) for a given set of assumed conditions with observed data for the same conditions. The calibration of the model has been done based on the assumption of there is a linear relation between the observed and the simulated one. That mean all of the error variance is contained in the simulated values and the measured data are free of error. But in reality the measured data are not free of error (Moriasi et al, 2007). The goal of calibration is to find those set of parameter values for the model that gives a simulated hydrological series adequately matches with the observed series.

Generally there are two broad approaches to hydrological model calibration: manual and automatic. Manual calibration is mostly common and recommended in cases where a good graphical representation is strongly demanded for the application of more complicated models. However, it is very cumbersome, time consuming, and requires personal experience. Automatic calibration makes use of a numerical algorithm in the optimization of numerical objective functions. The method undertakes a large number of iterations until it find the best parameters. And the success of automatic calibration depends on model structure, quality of calibration data, calibration criteria and optimization method. Therefore for this study, the calibration was done manually based on physical catchment understanding and sensitive parameters from published literature e.g (Barlund et al, 2007; Xu et al, 2009) and calibration techniques from the SWAT user manual. After calibration of flow, calibration of sediment was carried out.

The calibration was carried out at monthly time steps using flow and sediment data series of 15 years length, from 1995 to 2009, was used in this study. Out of this data the first two year, i.e 1995 and 1996, is used as warming up period. While the 2/3rd of the remaining data series (the next 9 years), 1997-2005, is used for flow calibration. And the last 1/3rd (4 years), 2006-2009, is used for validation of the model.

4.4.3 Validation

After achieving the objective function by calibration validation of the model is followed. The validation procedures are similar to calibration procedure in that predicted and measured values are compared to determine if the objective function is met. However a data set of measured watershed response selected for validation preferably should be different than the one calibration and the model parameters are not adjusted during validation. Validation provides a test whether the model was calibrated to a particular dataset or system it is to represent. If the objective function is not achieved for the validation dataset, calibration and/or model assumptions may be revisited (Kati and Indrajeet, 2005).

4.5 Model performance evaluation

There are different types of statistical method of model performance evaluation techniques. Among this the, most commonly used for this study are:- coefficient of determination (R^2) and Nash-sutcliffe efficiency (NSE), percent bias (PBIAS) and root mean square error standard deviation ratio (RSR) are the most widely used to evaluate the performance of the hydrological model. Table 4.2.shows the performance ratings for three performance statistics, RSR, NSE and PBIAS, as suggested by (Moriasi et al, 2007).

The coefficient of determination (R^2) describes the proportion of the variance in measured data explained by the model. The value ranges from 0 to 1 with higher values indicating less error variance and typically values greater than 0.5 are considered as acceptable. The R^2 value is calculated using the following equation:

$$R^2 = \frac{\left[\sum_{i=1}^{n}\left(Q_i^{obs} - Q_{mean}^{obs}\right)\left(Q_i^{sim} - Q_{mean}^{sim}\right)\right]^2}{\sum_{i=1}^{n}\left(Q_i^{obs} - Q_{mean}^{obs}\right)^2 \sum_{i=1}^{n}\left(Q_i^{sim} - Q_{mean}^{sim}\right)^2} \qquad 4.25$$

Where Q_i^{sim} is the simulated data at time i, Q_i^{obs} is the observed data at time i, Q_{mean}^{sim} is mean of simulated data, Q_{mean}^{obs} mean of observed data and n is the number of registered data points.

The NSE value indicates how well the plot of observed versus simulated values fits the 1:1 line (Nash and Sutcliffe, 1970). NSE values range from -∞ to one, with values less than or very close to zero indicating unacceptable or poor model performance and values equal to one indicating perfect performance. The NSE value is calculated using the following equation:

$$NSE = 1 - \left(\frac{\sum_{i=1}^{n}\left(Q_i^{obs} - Q_i^{sim}\right)^2}{\sum_{i=1}^{n}\left(Q_i^{obs} - Q_{mean}^{obs}\right)^2}\right) \qquad 4.26$$

Where Q_i^{sim} is the simulated data at time i, Q_i^{obs} is the observed data at time i, Q_{mean}^{obs} mean of observed data, and n is the number of registered data points

The RSR value is calculated as a ratio of the RMSE and standard deviation of the measured data (Moriasi et al, 2007). RSR incorporates the benefits of error index statistics and indicates a scaling/normalization factor. The RSR value varies from the optimal value of zero, which indicates zero RMSE or residual variation, to a large positive value (Moriasi et al, 2007). The RSR value is calculated using the following equation:

$$RSR = \frac{RMSE}{STDEV_{obs}} = \frac{\left[\sqrt{\sum_{i=1}^{n}\left(Q_i^{obs} - Q_i^{sim}\right)^2}\right]}{\left[\sqrt{\sum_{i=1}^{n}\left(Q_i^{obs} - Q_{mean}^{obs}\right)^2}\right]} \qquad 4.27$$

Where Q_i^{sim} is the simulated data at time i, Q_i^{obs} is the observed data at time i, Q_{mean}^{obs} mean of observed data, and n is the number of registered data points

The PBIAS is used to determine if the average tendency of simulated data is larger or smaller than its observed counterparts (Gupta et al, 1999). The optimal value of PBIAS is zero, with low-magnitude values indicating accurate model simulation. Positive values indicate model underestimation bias, while negative values indicate model overestimation bias (Gupta et al, 1999). PBIAS is calculated using the following equation:

$$PBIAS = \left[\frac{\sum_{i=1}^{n}\left(Q_i^{obs} - Q_i^{sim}\right) * 100}{\sum_{i=1}^{n}\left(Q_i^{obs}\right)}\right] \qquad 4.28$$

Where Q_i^{sim} is the simulated data at time i, Q_i^{obs} is the observed data at time i and n is the number of registered data points

Table 4.2:-General Performance ratings for recommended statistics for a monthly time step. (Moriasi et al, 2007).

Performance Rating	RSR	NSE	PBIAS (%)	
			Stream flow	Sediment
Very good	0.00≤RSR≤0.50	0.75<NSE≤1.00	PBIAS<±10	PBIAS<±15
Good	0.50<RSR≤0.60	0.65<NSE≤0.75	±10≤PBIAS<±15	±15≤PBIAS<±30
Satisfactory	0.60<RSR≤0.70	0.50<NSE≤0.65	±15≤PBIAS<±25	±30≤PBIAS<±55
Unsatisfactory	RSR>0.70	NSE≤0.50	PBIAS≥±25	PBIAS≤±55

4.6 Estimating of land use land cover change on runoff and sediment yield

The two scenarios were used for the estimating of impact of land use land cover change on runoff and sediment yield. In the first scenario the land use land cover for year 1986 was used for calibration and validation of the model. In the second scenarios land use maps for the year 2005 were used to simulate the impact of land use change on runoff and sediment yield.

CHAPTER FIVE

5 DATA AND MODEL INPUTS ANALYSIS

5.1 Image processing

A land-use and land-cover map of the study area was prepared from two satellite images Landsat TM and Landsat ETM+ imagery acquired on 21 January 1986 and 03 December 2005 respectively download from Global Land Cover Facility (GLCF) Earth Science Data Interface website: www.glovis.USGS.gov (Figure 5.1). Supervised digital image classification technique was employed, using ERDAS EMAGINE 9.1 software which was complemented with field surveys that provided on the-ground information about the types of land use and land-cover classes. Six land-use and land-cover classes were recognized. These include built up areas, cultivated land, Afro-alpine, grassland, forest and shrubs land. The acquisition dates, sensor, path/row, resolution and the producers of the satellite images used in this study are summarized in the Table 5.1.

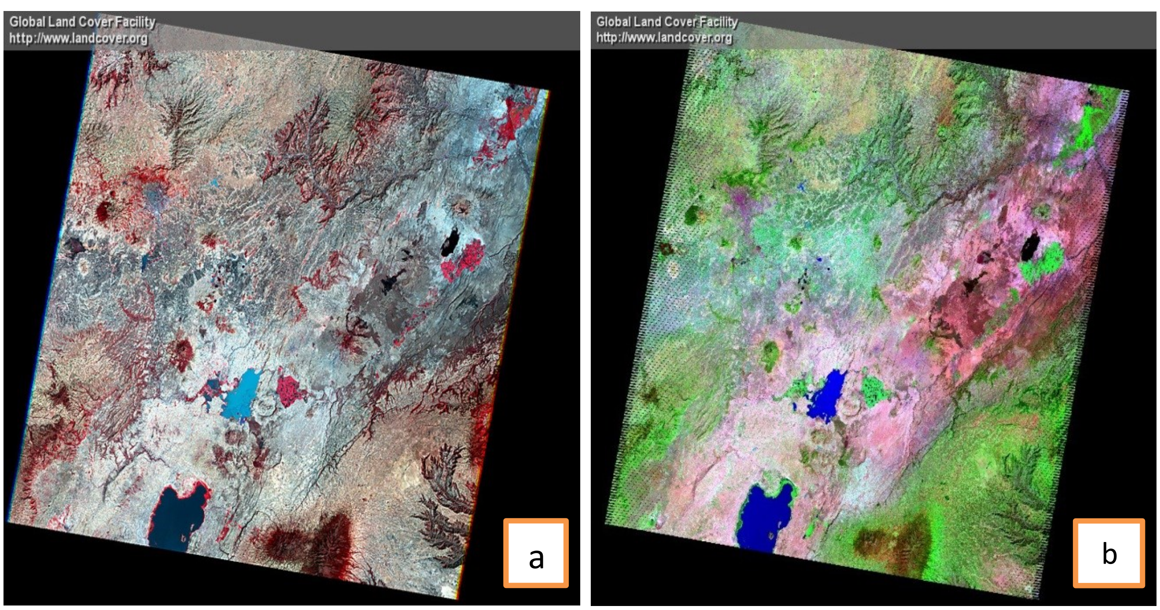

Figure 5.1:-Satellite images a) 21 January 1986 and b) 03 December 2005

Table 5.1:-The acquisition dates, sensor, path, row, resolution and the producers of the two Landsat images.

Path	Row	Acquisition data	Sensor	Resolution(m)	Producers
168	054	21-Jan-86	TM	30	USGS
168	054	3-Dec-05	ETM+	30	USGS

5.2 Land use land cover class

The satellite imagery from the previous local knowledge, visual and digital interpretations the different land use land cover categories were identified. Global Positioning System (GPS) and Google earth was used during training site collection and ground verification of image interpretations. Based on the satellite images, Google earth and ground truth for the recent image, the six land use land cover classes analyzed for changes were: built up, cultivated land, Afro-alpine, grassland, forest and shrubs land described table 5.2.

Table 5.2:-Description of land use/land covers classes used for change study from 1986 to 2005

Land use land changes types	General description
Afro-alpine Vegetation	High altitude herbaceous and Erica/Hypericum forest
Built up	Built-ups (houses) in both urban and rural parts.
Forest	Areas dominated by natural high forests, which are coniferous and few man-made trees
Grassland	All areas covered with natural grass and small shrubs dominated by grass.
Shrubs land	Areas covered with mainly shrubs and other small sized plant species (less than 3m).
Cultivation land	Areas of land ploughed/prepared for growing various crops. This category includes areas currently under crop, fallow and land under preparation.

5.3 Hydro-metrological and Hydrological data

SWAT model largely depends on hydro-meteorological data such as precipitation, temperature, relative humidity, wind speed and solar radiation and hydrological data such as river discharge and sediment.

5.3.1 Hydro-metrological data

The weather input data required by SWAT consists of daily precipitation, maximum/minimum air temperature, solar radiation, wind speed and relative humidity. The model allows values for daily precipitation, maximum/ minimum air temperatures, solar radiation, wind speed and relative humidity to be input from records of observed data or generated during the simulation. These data were obtained from the Ethiopian National Meteorological Agency, Adama National Meteorology Agency branch and Awash Melkassa Research Institution. The weather data used were represented from six stations in and around watershed: Awash Melkassa, Sire, Huruta, Kulumsa, Diksis and Arsi Robe. For this research work the weather information considered was for the period of 1995-2009. Meteorological stations used in and around Keleta watershed list in Table 5.3 and Figure 5.2

Table 5.3:-Meteorological station names, locations and variables

No	Station name	Latitude	Longitude	Elevation	Elements					
					RF	Tmax	Tmin	RH	Ss	WS
1	A.Melkassa	8.4	39.33	1540	✓	✓	✓	✓	✓	✓
2	A.Robe	7.86	39.63	2420	✓	✓	✓	IN	IN	IN
3	Diksis	8.06	39.56	2761	✓					
4	Huruta	8.14	39.36	2043	✓	✓	✓			
5	Kulumsa	8.01	39.16	2209	✓	✓	✓	IN	✓	✓
6	Sire	8.28	39.49	2042	✓					

Note: RF= Rainfall, Tmax= Maximum Temperature, Tmin= Minimum Temperature, RH= Relative Humidity, Ss= Sunshine, WS= Wind Speed, ✓= available data and IN= Incomplete data.

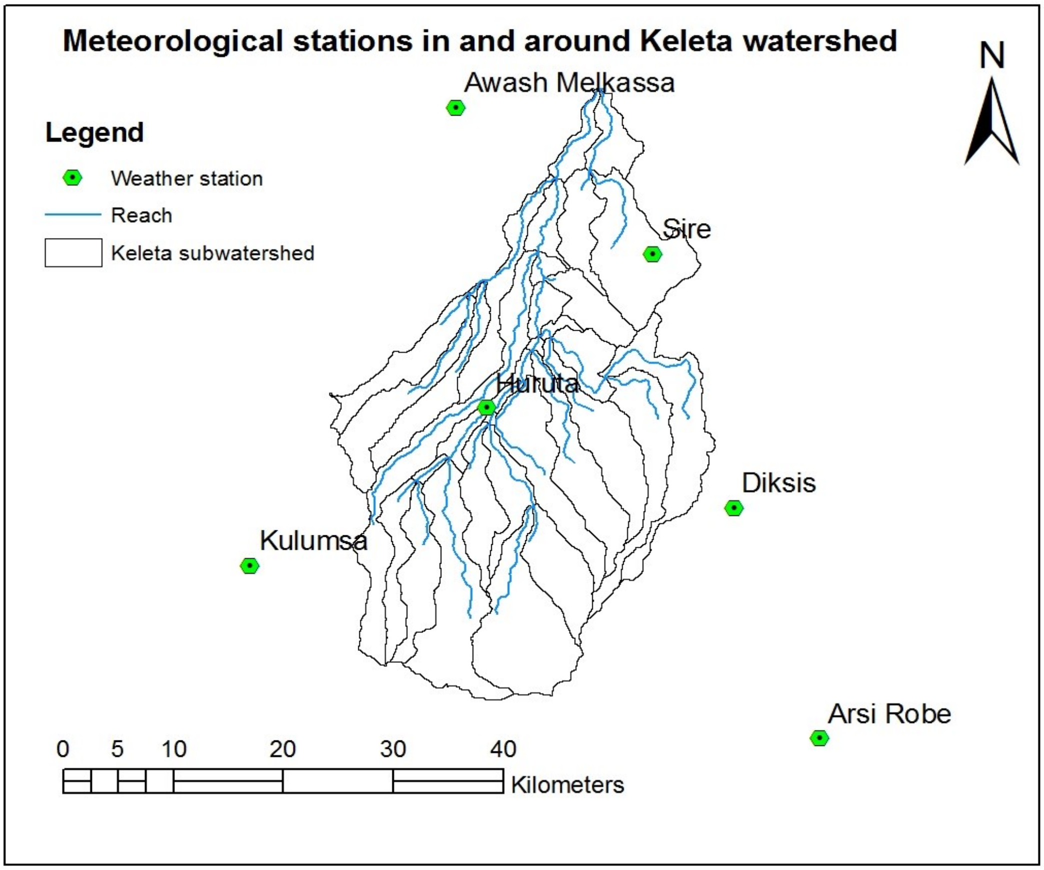

Figure 5.2:-Location of meteorological stations used in and around Keleta watershed

In any water resource development and management activities, the hydro-metrological data screening and analysis come first before design and construction. Checking the data its consistency, Stationerity and homogeneity is the techniques that are used to check the quality of the hydro-metrological data. Therefore in this study the following techniques are used to check the quality of available data. In this study Inverse Distance Interpolation method (equation 5.1) was used to estimate the missing data.

$$P_o = \frac{\sum_{i=1}^{n}(P_i/d_i)}{\sum_{i=1}^{n}(1/d_i)} \qquad 5.1$$

Where P_o is the estimated value of the missing data, P_i is the value of the i^{th} nearest weather station, and d_i is the distance between the station of missing data and the i^{th} nearest weather station.

The method is easy to use for fill in missing precipitation data (Hubbard, 1994). It is reliable if only the weather stations are situated inside of 100 Km radius (Tronci et al, 1986).

Homogeneity and consistency test

A time serious observed data are relatively consistent and homogeneous if the periodic data are proportional to an appropriate simulation period (Chang and Lee, 1974). Most of the time this proportionality is tested by different techniques before the data is used. Among the common technique used to check the consistency and homogeneity of the data are Non-Dimensional Homogeneity test(Figure 5.3) and Double Mass Curve Method (DMCM) (Figure 5.4). In this study both method are applied to check the quality of data for selected metrological station and mathematically the non-dimensional homogeneity test is calculated by:

$$P_i = \frac{P_i^*}{P_l^\#} . 100 \qquad 5.2$$

Where P_i is non-dimensional value of rainfall for month i, P_i^* is over year-averaged monthly rainfall at the station i and $P_l^\#$ is the over year average yearly rainfall of the station.

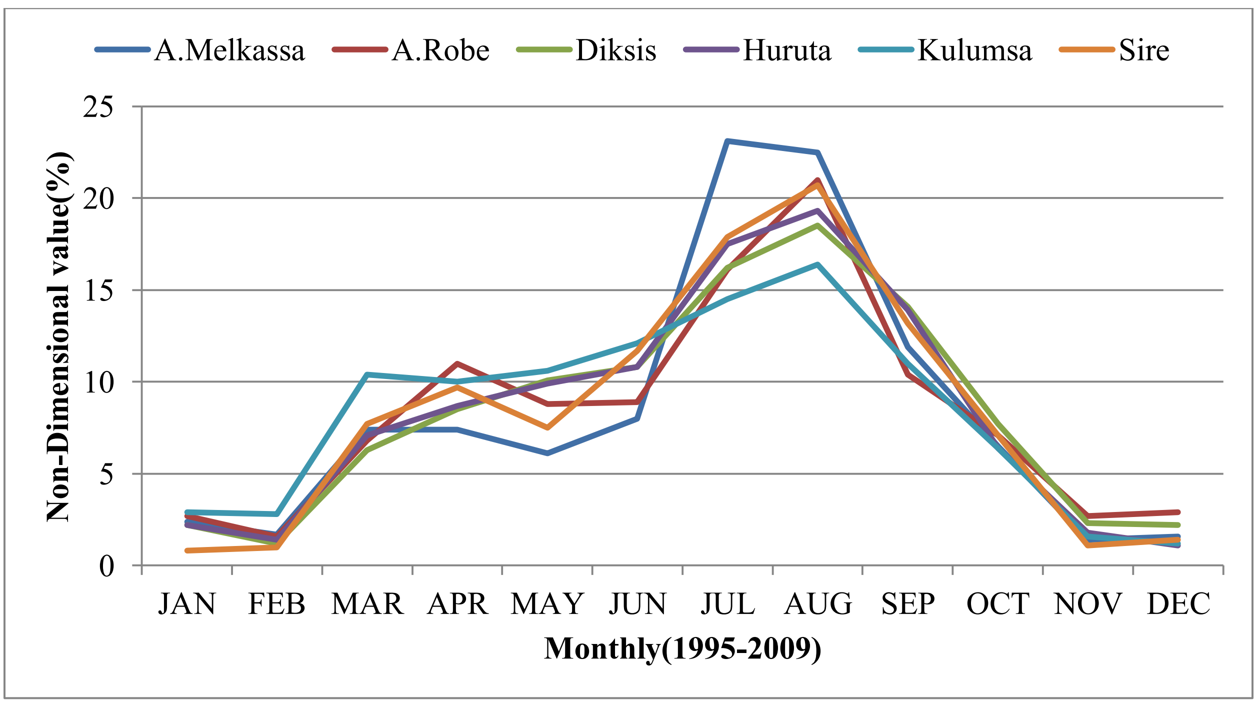

Figure 5.3:-Non Dimensional Homogeneity test

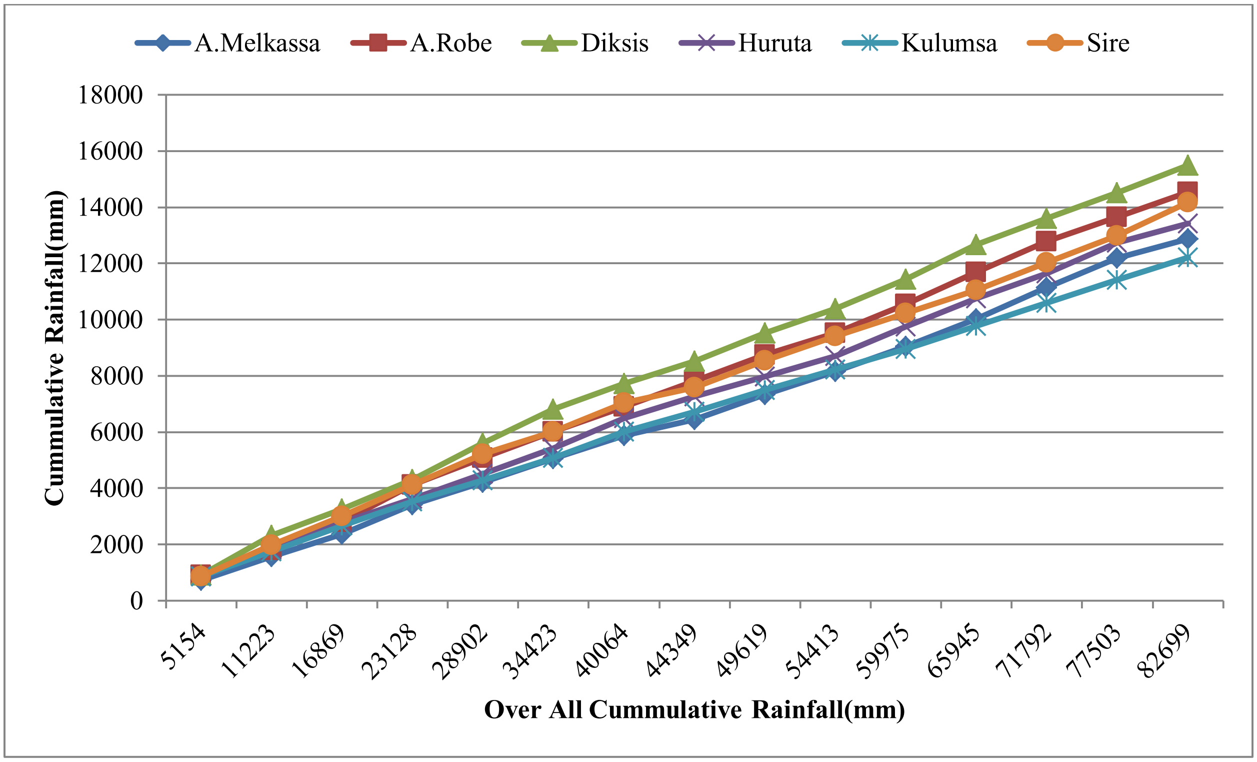

Figure 5.4:-Double Mass Curve Method

Weather input data preparation

An important component of the SWAT model is the weather generator (WXGEN). SWAT requires daily values of precipitation, maximum and minimum temperature, solar radiation, relative humidity, and wind speed. Missing weather data are left as it was in name.dbf format and a negative (-99.0) inserted for missing data. This value tells SWAT to generate weather data for that day. Daily values for weather are generated from average monthly values.

The user may read these inputs from a file or generate the values using SWAT's weather generator model based on monthly average data summarized over a number of years (Neitsch et al, 2005). The weather generator model (Sharpley and Williams, 1990) can be used to generate climatic data or to fill in gaps in weather data. The weather generator first independently generates precipitation for the day. Maximum temperature, minimum temperature, solar radiation, and relative humidity are then generated based on the presence or absence of rain for the day. Finally, wind speed is generated independently.

To do these the weather generator (WXGEN) model and Dew point calculator (Dew02) was included in SWAT model and used to calculate the statistical parameters that required in filling the missed data. This weather generator was developed for USA. Since the watershed is located outside the USA, all necessary statistical parameters are calculated using WGNmaker4.1 program and integrated with the result in to SWAT weather generator. This Excel macro program is designed to calculate the monthly averages and standard deviations of all variables as well as probability of wet and dry days, skew coefficient, and average number of precipitation days in the month. The results of WGNmaker4.1 are used by SWAT's weather generator to fill in missing information or simulation.

Average Daily Dew Point Temperature was calculated using the Dew point calculator (Dew02) from daily maximum temperature, daily minimum temperature and average relative humidity. Moreover, daily solar radiation was calculated from the daily available sunshine hour's data. The weather generator parameters used and their values are shown in Appendix 1.

5.3.2 Hydrological data

The hydrological data was required for performing sensitivity analysis, calibration and validation of the model. Daily stream flow data of Keleta river were collected from the Ministry of Water Resource and Energy of Ethiopia.

For calibration of simulated flows, the total gauged stream flow data should be separated into surface and base flow components. The automated base flow separation and recession analysis techniques (Arnold et al. 1999), (http://pasture.ecn.purdue.edu/~what/) are among the several methods available to separate base flows. Due its simplicity, this technique was applied. Figure 5.5 shows mean monthly stream flow of the Keleta river.

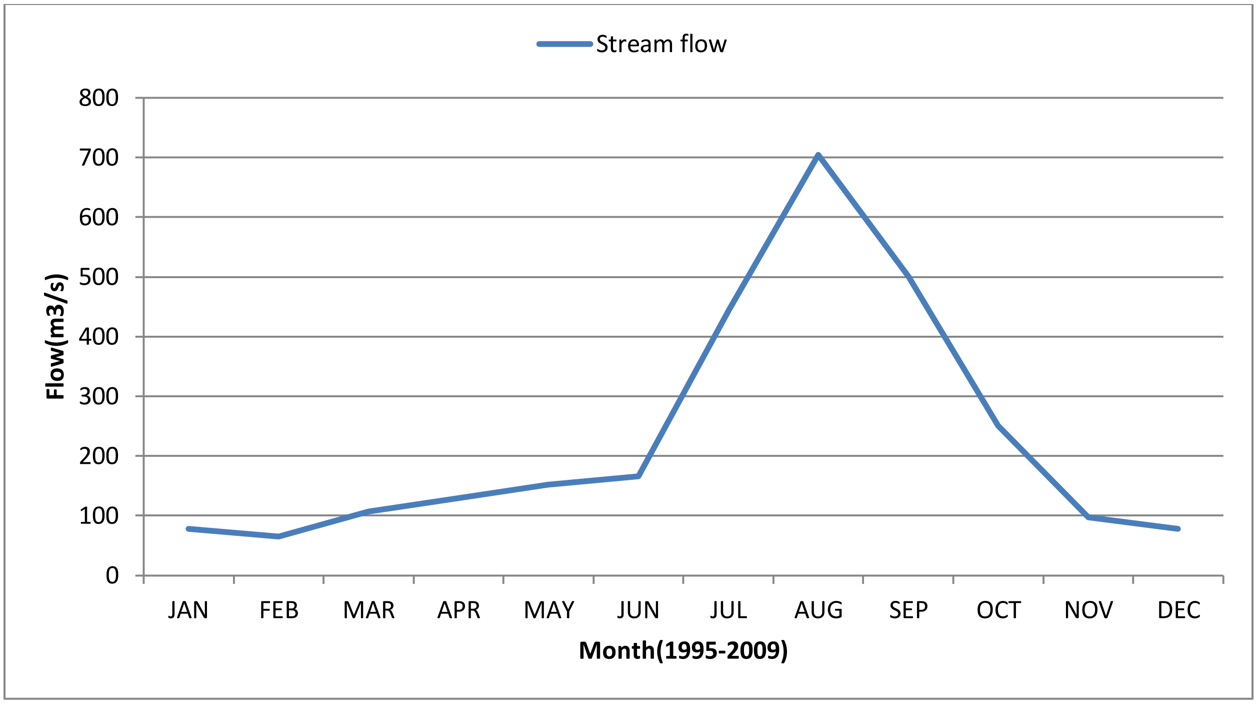

Figure 5.5:-Mean monthly stream flow of Keleta river.

5.3.3 Sediment data

There are few sites which has measured suspended sediment data in Keleta river at different time collected from Ministry of Water Resource and Energy of Ethiopia. The rating curve equation developed shows stream and sediment flows are correlated at an R^2 value of 0.84(Figure 5.6). In this study used equation given below:

$$Q_s = 19.366Q^{1.7381} \quad 5.2$$

where, Q_s is daily sediment load in (t/day) and Q is daily stream flow in (m^3/s).

Depending on the rating curve equation developed generate the sediment data for sensitivity analysis, calibration and validation.

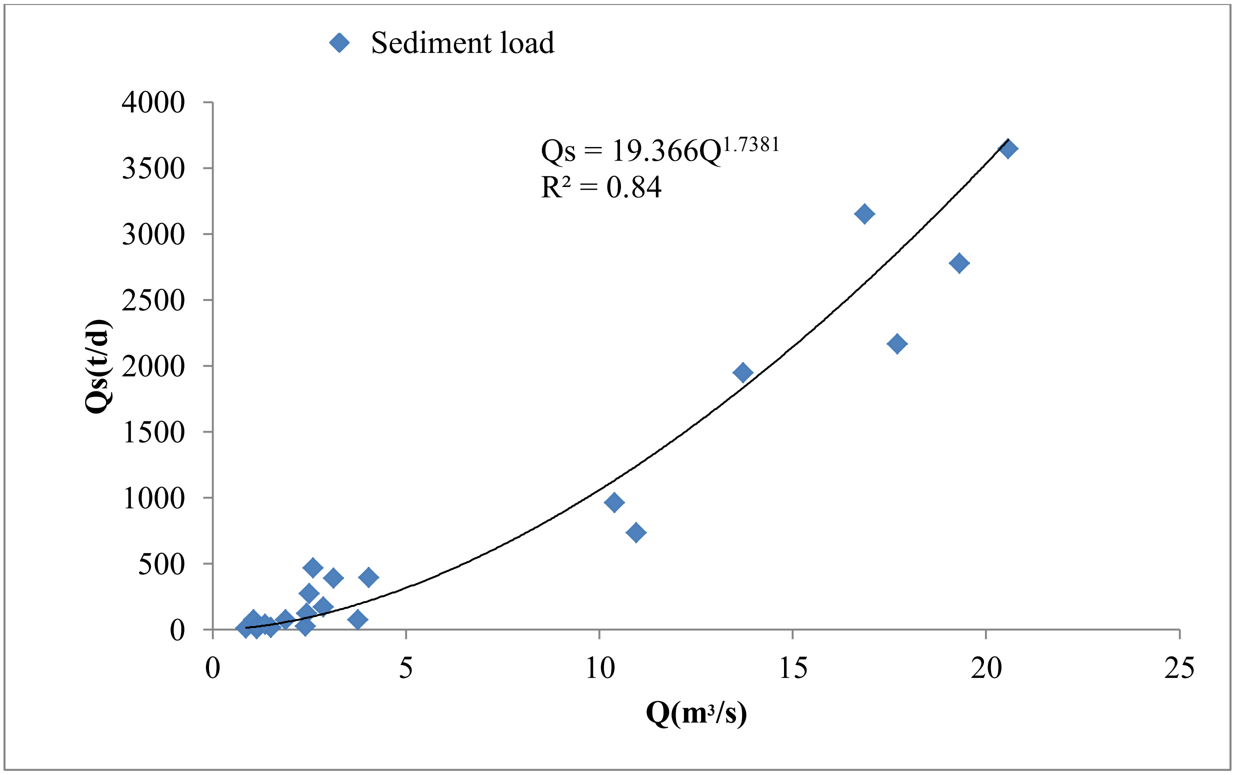

Figure 5.6:-Stream flow and sediment rating curve for Keleta gauging station

5.4 Spatial input data

5.4.1 Digital Elevation Model (DEM)

The Digital Elevation Model (DEM) is an elevation matrix which is used to delineate the watershed using the Arc-GIS software. Also it was used for automatic derivation of stream networks and the quantitative description of geomorphologic characteristics of the catchments. Such as slope, aspect, altitude and etc. used for runoff estimation in SWAT model. The digital elevation model used in this study was obtained from the NASA Shuttle Radar Topographic Mission (SRTM) with a resolution of 90m*90m. DEM for the study area was extracted from the Ethio-DEM using the GIS software by masking the shape file of the Keleta watershed. The extracted DEM was used in SWAT model for watershed delineation and for further analysis. The DEM of the watershed presented in Figure 5.7.

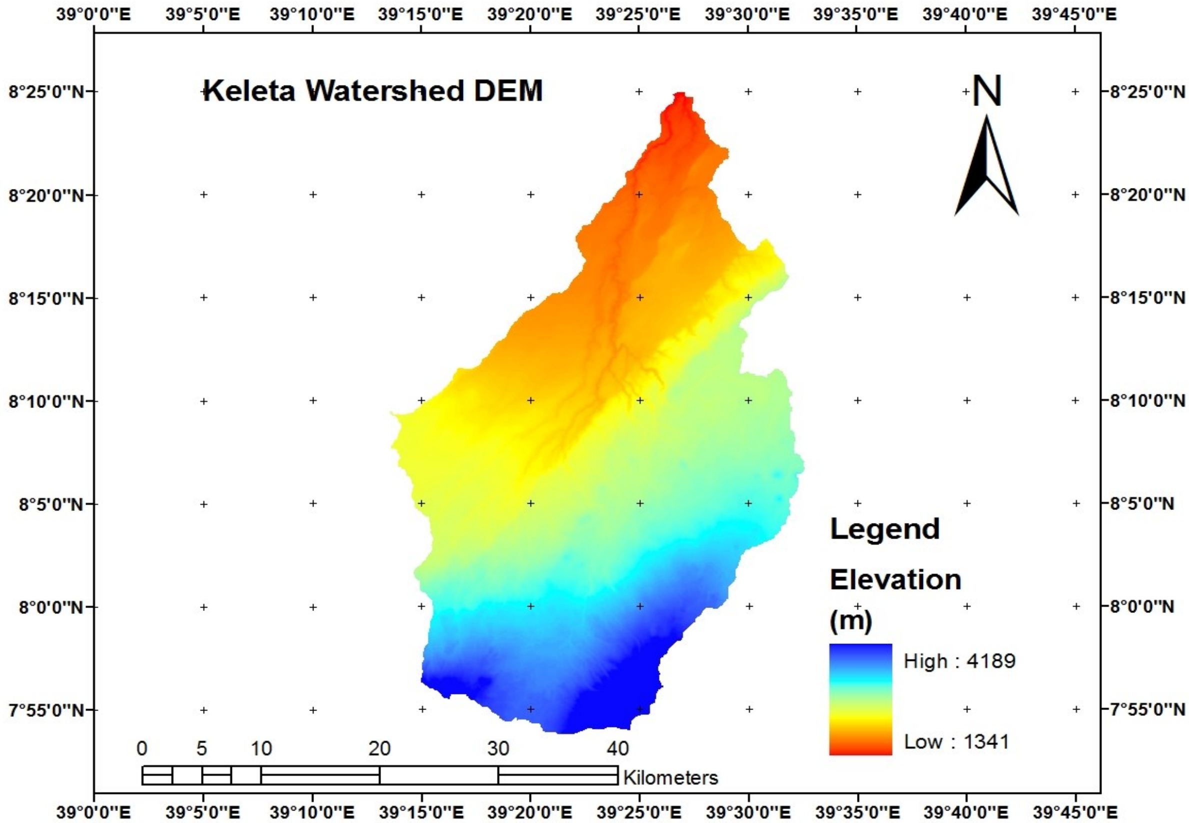

Figure 5.7:-Keleta watershed DEM

5.4.2 Soil data

The response of a river basin to rainfall events depends on the nature and conditions of underlying soils (Shrestha et al, 2008). The SWAT model requires soil property data such as the texture, chemical composition, physical properties, available moisture content, hydraulic conductivity, bulk density and organic carbon content for the different layers of each soil type (Setegn et al, 2009). Soil data is one of the inputs data for the SWAT model and it has a great influence on amount of runoff generations. The SWAT model requires physical and chemical properties of the soil. Soil texture, hydraulic conductivities available moisture content and bulk density are the main physical properties which govern the movement of water and air through the profile and have a major impact on the cycling of water within each HRU. The chemical properties of the soil which are used in SWAT model are organic carbon and electrical conductivities to set initial of the different chemicals in the soil.

The soil map and soil data is obtained from the Oromia Water Work Design and Supervision Enterprises (OWWDSE). The information regarding soil physical and chemical properties were taken from soil survey of the upper Awash sub-basin which was prepared on the scale of 1:50000. To integrate the soil map with SWAT model, a user soil database which contains textural and chemical properties of soils was prepared for each soil layers and added to the SWAT user soil databases. The summery of soil type is given in Table 5.4 and Figure 5.8. The details of chemical and physical properties of soil are available in Appendix 4

Table 5.4:-Soil unit name of Keleta watershed with their symbols and areal coverage

Soil unit name	Symbol	Area	
		Km^2	%
Vitric Andosols	ANvi	89.7	7.8
Pellic Vertisols	VRpe	266.11	23.14
Umbric Leptosols	LPum	21.62	1.88
Eutric Cambisols	CMeu	108.79	9.46
Chromic Vertisols	VRcm	390.31	33.94
Haplic Nitisols	NTha	64.74	5.63
Vertic Cambisols	CMvr	120.06	10.44
Chromic Luvisols	LVcm	88.67	7.71

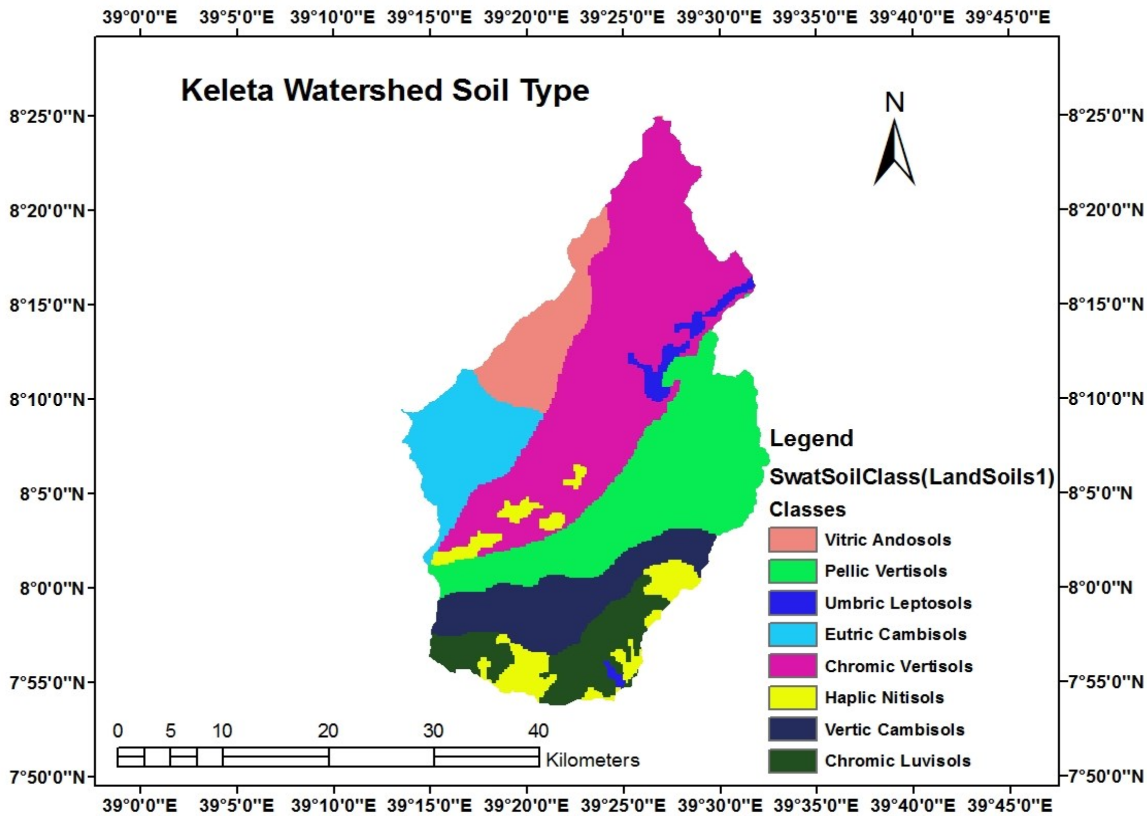

Figure 5.8:-Soil map of Keleta watershed

5.4.3 Land use and Land cover

The land use of an area is one of the most important factors that affect surface erosion, runoff, and evapotranspiration in a watershed during simulation (Neitsch et al, 2005). The reclassification of the land use map was done to represent the land use according to the specific land cover types. There are six major types of land use and land cover for the study area has been identified. The land cover/use mainly built up areas, cultivated land, Afro-alpine, grassland, and shrubs land. Since the model already has a predefined SWAT four letter codes for each land cover classification in such a way that the land use/Land covers classification used in the study area were assigned in SWAT database. Hence, while preparing the lookup-table, the land use types were made compatible with the input needs of the model.

Table 5.5:-Land use land cover of Keleta watershed

Land use land cover	Land use according to SWAT database	SWAT code
Afro-alpine Vegetation	Forest-Deciduous	FRSD
Built up	Residential-Medium/Low Density	URML
Forest	Forest-Evergreen	FRSE
Grassland	Range-Grasses	RNGE
Shrubs land	Range-Brush	RNGB
Cultivation land	Agricultural Land-Generic	AGRL

5.4.4 Slope

Slope is another important input parameter to develop the Hydrologic Response Unit (HRU) in SWAT model. A slope for the study area where generated from DEM using Arc-GIS spatial analysis tool. Arc-SWAT allows the integration of land slope up to five classes when defining the hydrologic response unit. And in SWAT model there is an option to select a single or multiple slope classes. For this study the (OWWDSE, 2013) slope suitability for soil survey were adopted for slope classification and the second assumptions of SWAT multiple slope class was applied. Therefore the slope classes adopted for this study were given in the Table 5.6 and Figure 5.9 for the definition of the Hydrologic Response Unit (HRU).

Table 5.6:-The slope classes of the Keleta watershed

Classes	Slope range (%)	Area	
		Km^2	%
1	0-2	72.68	6.32
2	2-8	542.22	47.15
3	8-16	355.58	30.92
4	16-30	138.46	12.04
5	>30	41.06	3.57

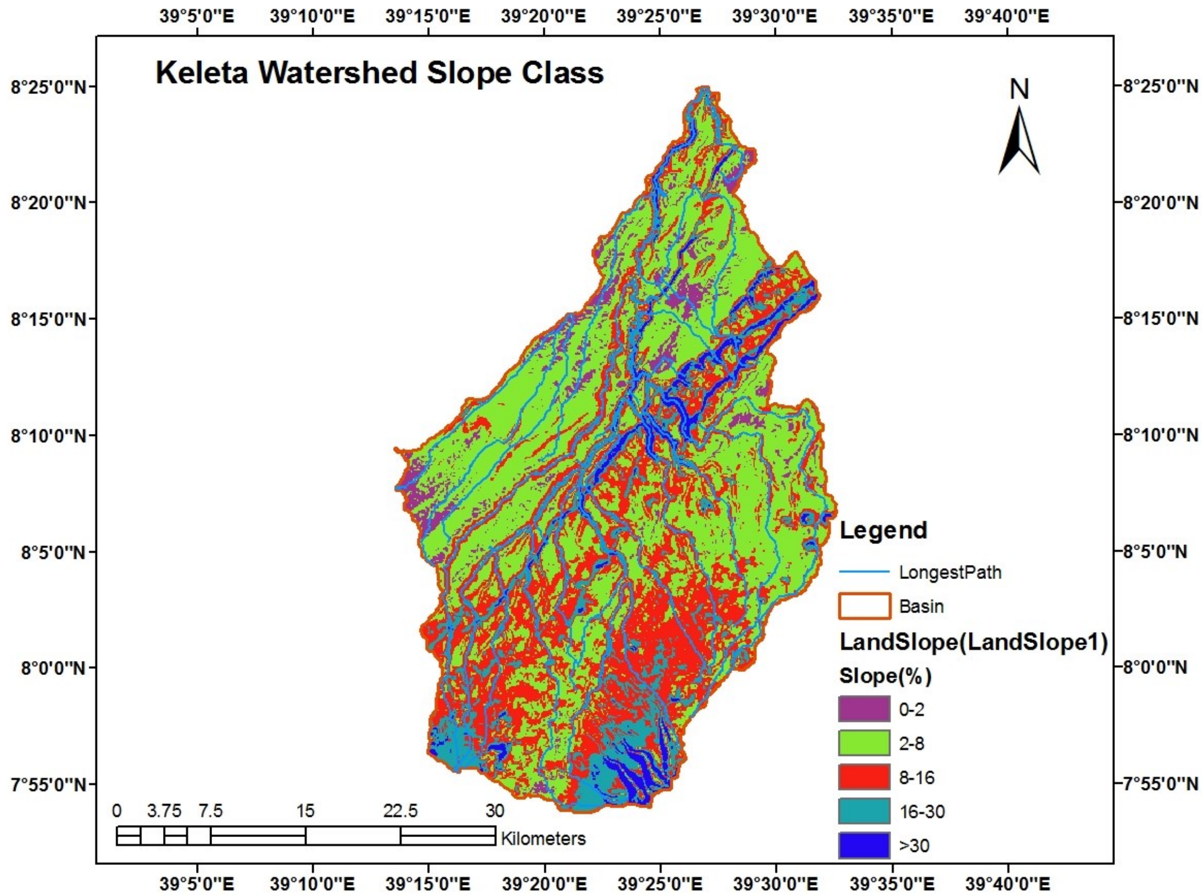

Figure 5.9:-Slope class map of Keleta Watershed

5.5 SWAT Model setup

5.5.1 Watershed Delineation

SWAT models allow the user to delineate the watershed and sub watershed using Digital Elevation Model (DEM) by expanding the Arc-GIS and spatial analyst extension function to perform the watershed delineation. Watershed and sub-watershed delineation was carried out using various steps including: DEM setup, stream definition, inlet outlet definition, watershed outlet selection and definition and finally calculation of sub-basin parameters.

By default, the Arc SWAT model interface proposes the minimum and maximum watershed area and it also suggested the size of the sub basin in hectare to define the minimum drainage area required to form the origin of the stream. Actually the smaller the threshold area, gives more detail of the drainage network, large numbers of the sub basin and HRU. But this needs more processing time and large computer space. As the result of this, the optimum size of the threshold area was taken the threshold that proposed by the model and 35 sub-basin were obtained (Figure 5.10).

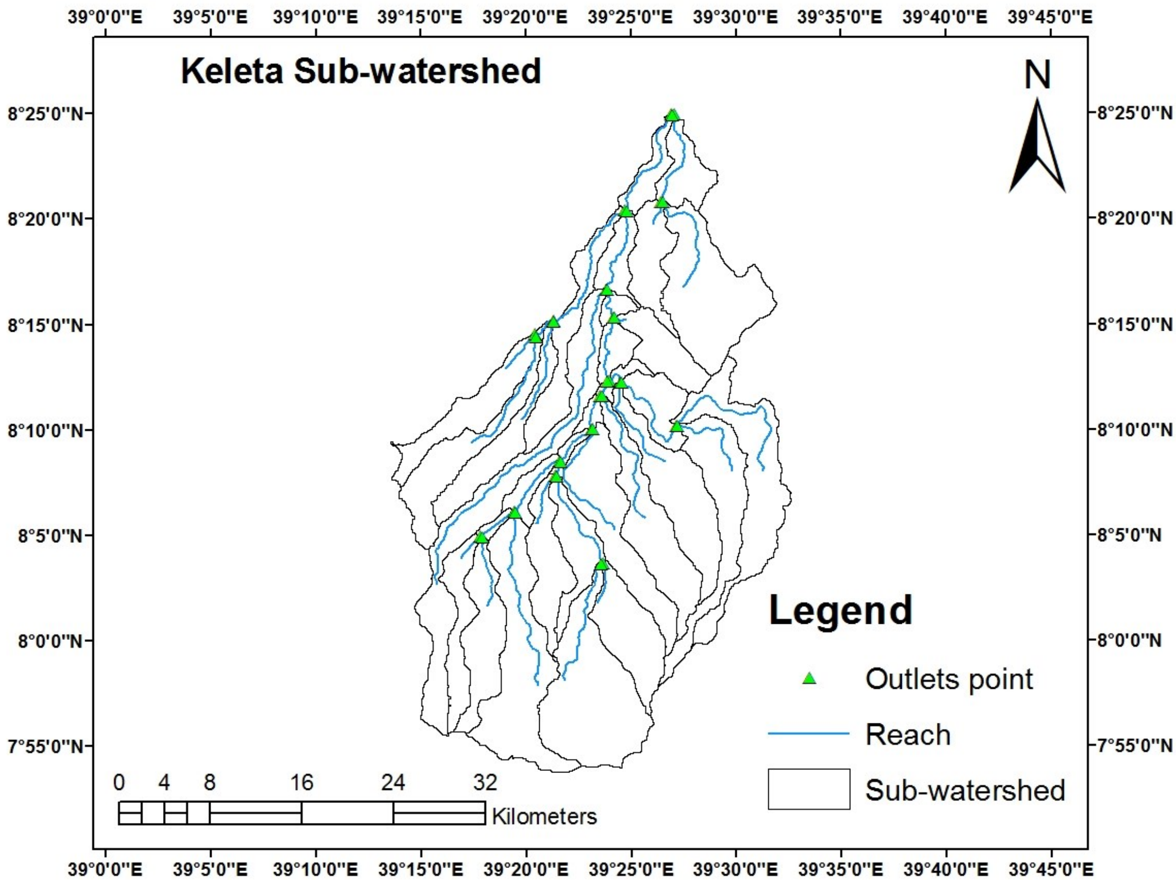

Figure 5.10:-Sub-watersheds map of the Keleta watershed

5.5.2 Hydrologic Response Unit (HRU) Definition

The land area in a sub-basin was divided into HRUs. The HRU analysis tool in ArcSWAT helped to load land use, soil layers and slope map for the project. The delineated watershed by ArcSWAT and the prepared land use and soil layers were overlapped 100 %. HRU analysis in SWAT includes divisions of HRUs by slope classes in addition to land use and soils. The multiple slope option (an option which considers different slope classes for HRU definition) was selected. The land use land cover, soil and slope map was reclassified in order to correspond with the parameters in the SWAT database. After reclassifying the land use, soil and slope in SWAT database, all these physical properties were made to be overlaid for HRU definition. For this specific study a 5 % threshold value for land use, 10 % for soil and 10 % for slope were used to define the HRU and a total number of 453 HRU were obtained for further analysis. Because of these thresholds, minor land use, soil, and slope classes within a sub-basin were eliminated during HRU definition.

CHAPTER SIX

6 RESULT AND DISCUSSION

6.1 Land use land cover changes and map

The classification of the satellite imagery for the two study periods provided the spatial distribution of land use/ land cover categories.

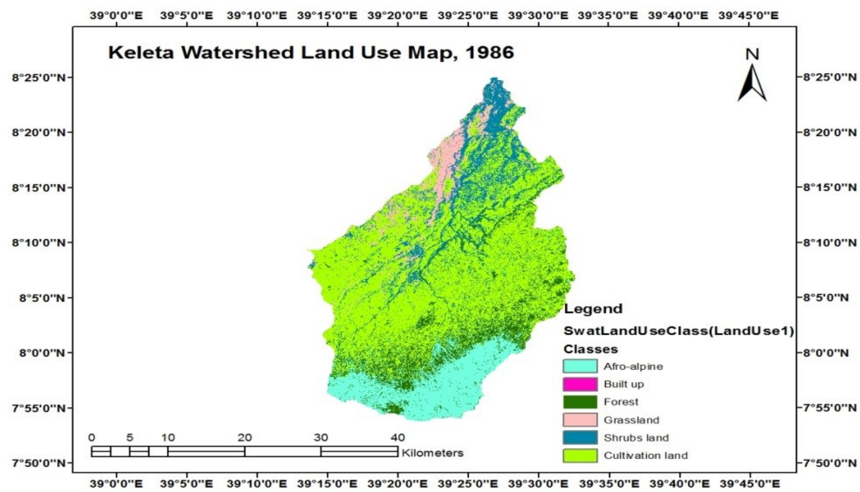

Figure 6.1:-Land use map of Keleta watershed in 1986

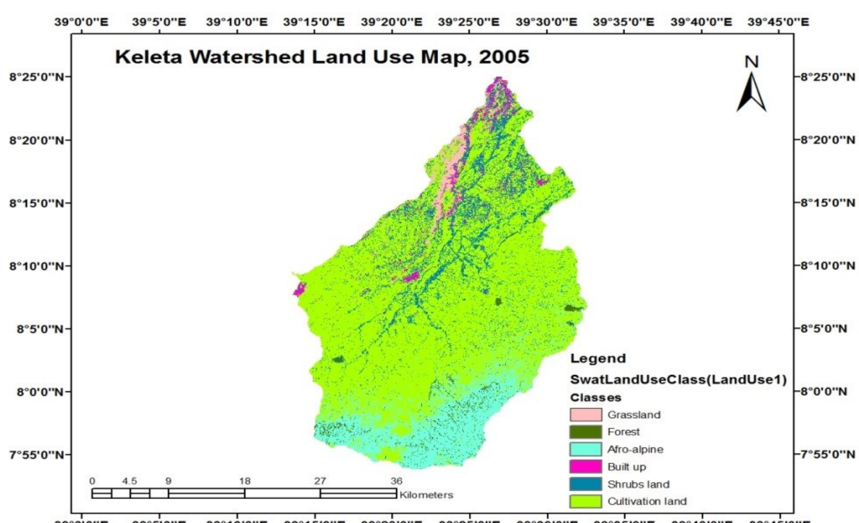

Figure 6.2:-Land use map of Keleta watershed in 2005

Figure 6.1 and Figure 6.2 show the spatial distribution of land use/ land cover in 1986 and 2005 respectively, with the statistics and change in area given in Table 6.1. Both the years were classified into six land use/ land cover classes namely afro-alpine, forest, cultivation land, shrub land, grassland and built up. As it can be observed from Table 6.1, cultivation was the most dominant land use type in 1986 in the study area covering 603.75Km^2(52.5%) followed by afro-alpine 171.005Km^2(14.87%), shrub land 156.4Km^2(13.6%), forest 135.7Km^2(11.8%), grassland 65.5Km^2(5.7%) and built up 17.595Km^2(1.53%) were the least dominant classes. The situation in 2005 revealed that the cultivation land again is the dominant land use type covering an area of 782Km^2(68%) followed by afro-alpine 164.45Km^2, shrub land 131.1Km^2(11.4%), grassland 27.6Km^2(11.4%), built up 25.3Km^2(2.2%) and forest 19.55Km^2(1.7%).

The results revealed that a considerable reduction of forests, grasslands, afro-alpine and shrubs land and increase cultivation land and built up over the two decade period (Table 6.1 and Figure 6.3). The forests, grasslands, afro-alpine and shrubs land areas were reduced by about 85.59%, 57.89%, 3.83% and 16.18% respectively. The cultivation land and built up areas have increased by 29.52% and 43.79% respectively. During this period the increase in agricultural land has made possible through, deforestation and clearing of shrubs on upper and lower portions of the watershed respectively.

In general, during the two periods considered the cultivated land and built-up have increased and other land use land cover types decreased.

Table 6.1:-Land use land cover change in Keleta watershed during the period from 1986 to 2005

Land cover types	1986		2005		Change from 1986 to 2005	
	Km^2	%	Km^2	%	Km^2	%
CL	603.75	52.5	782	68	178.25	29.52
F	135.7	11.8	19.55	1.7	-116.15	-85.59
AP	171.01	14.87	164.45	14.3	-6.555	-3.83
SL	156.4	13.6	131.1	11.4	-25.3	-16.18
GL	65.55	5.7	27.6	2.4	-37.95	-57.89
BU	17.595	1.53	25.3	2.2	7.705	43.79
Total	1150	100	1150	100	0	

Note: CL= Cultivation land, F= Forest, AP= Afro-alpine, SL= Shrub land, GL= Grassland and BU= Built-up

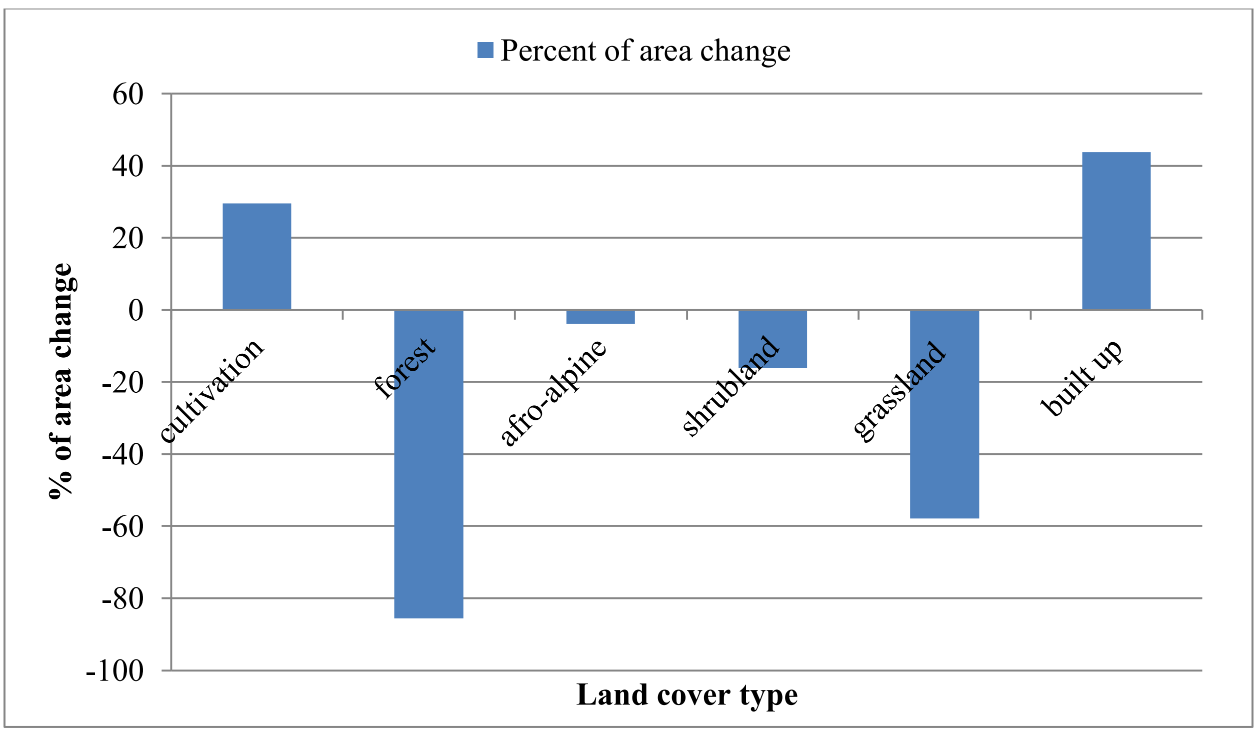

Figure 6.3:-Percentage of land use/cover change between 1986 and 2005.

6.2 Sensitivity analysis

As already explained in section 4.4.1, the Sensitivity analysis helps to select model parameters that change to an individual input parameter in the model response and can be performed using a number of different methods.

The sensitivity analysis window in Arc-SWAT model allows to select the simulation that will be used to perform the sensitivity analysis and the location of the sub basin where observed data to compare against the simulated output. To do this, sub-basin 35 was selected where gauge is located and the sensitivity analysis was carried out. Therefore into considering this, the sensitivity analysis has been done for this study with observed data for nine years (i.e. from 1997-2005) and ranked the parameter based on the mean value of the sensitivity output.

Hence after the sensitivity analysis has been carried out and based on (Lenhart et al, 2002) sensitivity parameter index (i.e. for mean value are >0.2) that was already explained in section 4.4.1. The eight flow parameters and two sediment parameter were selected for calibration of the model (Table 6.2) and presents parameters that resulting greater relative mean sensitivity values for monthly flow and sediment.

As shown in Table 6.2, the eight parameters showed a relatively high sensitivity, being the curve number (CN2) the most sensitive of all. The three most sensitive parameters controlling the surface runoff in the sub watershed are the curve number (CN2), the soil available water capacity (SOL_AWC), and the soil evaporation compensation factor (ESCO).

With respect to the base flow, the threshold water depth in the shallow aquifer for flow (Gwqmn), and the groundwater revap coefficient (REVAPMN) have the highest influence in controlling the flow.

The most sensitive parameters for predictions of sediment yield in Keleta watershed are USLE equation support practice factor (USLE_P) and minimum value of USLE C factor for land cover/plant (USLE_C).

Table 6.2:-Result of the sensitivity analysis of flow and sediment in gauged watershed.

Variable	Sensitivity analysis rank	Parameter code	Parameter description`	Range	MRS index	Category
Flow	1	CN2	Initial SCS CN II value	35-98	2.58	Very high
	2	Esco	Soil evaporation compensation factor	0-1	0.805	High
	3	Revapmn	Threshold water depth in the shallow aquifer for "revap"(mm)	0-500	0.584	High
	4	Blai	Leave area index for crops	0-1	0.506	High
	5	Sol_Z	Soil depth (mm)	0-3000	0.46	High
	6	Sol_Awc	Available water capacity capacity (mmH_2O/mm soil)	0-1	0.386	High
	7	Canmx	Maximum potential leaf area index	0-10	0.339	High
	8	Gwqmn	Threshold water depth in the shallow aquifer for flow (mm)	0-5000	0.207	High
Sediment	1	Usle_P	Universal soil loss equation management factor	0-1	2.94	Very high
	2	Usle_C	Universal soil loss equation cover factor	0-1	0.571	High

6.3 Calibration and Validation

6.3.1 Flow calibration and validation

After the sensitivity analysis, model calibration was followed and the flow calibration for the Keleta watershed was conducted. The simulation of the model with the default value of parameters in the watershed showed relatively weak matching between the simulated and observed. Sensitive parameters found from the sensitivity analysis were varied within their ranges till the volume is adjusted to the required quantity. The parameters varied were taken according to their relative sensitivity. The curve number (CN), available water capacity (SOL_AWC) and the soil evaporation compensation factor (ESCO) are the most sensitive among the parameters used in the surface runoff calibration. The surface runoff adjustment was then followed by that of the base flow. The same approach was followed as above being the adjustment made to the most sensitive parameters affecting the base flow: the threshold water depth in the shallow aquifer for flow (GWQMN) and the groundwater revap coefficient (REVAPMN). During the calibration processes the CN was adjusted by +9% which are incorporated in SWAT model database. The available soil water capacity (SOL_AWC) was also adjusted by +9%. The soil evaporation compensation factor (ESCO) was adjusted to 0.05. This parameter allows us to modify the depth distribution used to meet the soil evaporative demand to account for the effect of capillary action, crusting, and cracks. The REVAPMN was adjusted to 100. Movement of water from the shallow aquifer to the unsaturated zone is allowed to only if the volume of water in the shallow aquifer is equal to or greater than REVAPMN. Groundwater flow to the reach is allowed only if the depth of water in the shallow aquifer is equal to or greater than GWQMN and adjusted by default value. The final values of most sensitive flow parameters are shown in Table 6.3. The calibration of runoff resulted in a good agreement of simulated and observed data as indicated by the model evaluation statistics given in Figure 6.4. The performance of the model for simulating the monthly runoff is NSE=0.81, RSR=0.44, PBIAS=-9.29% and R^2=0.82 as shown in Table 6.4.

During the validation process, the model was run with input parameters set during the calibration process without any change. Means that all input data including land use and soil was considered unchanged except the meteorological inputs. The performance rating NSE=0.76, RSR=0.49, PBIAS=-7.92% and R^2=0.83 as shown in Table 6.4 the monthly runoff simulation can be rated as very good for the validation periods. As Figure 6.5 showed that a time-series plot of the measured and simulated monthly runoff for model validation period.

Table 6.3:-Default and final values of SWAT calibration parameters for flow and sediment.

Variable	Parameter	File	IMET	Range	Default value	Final value
Flow	CN2	.mgt	3	35-98	55-87	60-95
	Esco	.hru	1	0-1	0	0.05
	Revapmn	.gw	2	0-500	1	100
	Blai	crop.dat	1	0-1	0.5	0.8
	Sol-Z	.sol	3	0-3000	1225	1335.25
	Sol-Awc	.sol	3	0-1	0.10-0.15	0.11-0.16
	Canmx	.hru	1	0-10	0	0.025
	Gwqmn	.gw	2	0-5000	0	0
Sediment	Usle_P	.mgt	1	0-1	1	0.875
	Usle_C	crop.dat	3	0-1	0.41	0.035

Table 6.4:-The model performance statistics for runoff calibration and validation

Variable	Period	R2	NSE	RSR	PBIAS (%)
Runoff	Calibration(1997-2005)	0.82	0.81	0.44	-9.29
	Validation(2006-2009)	0.83	0.76	0.49	-7.92

According to performance evaluation ratings proposed by Moriasi et al. (2007) the result show that, based on NSE, RSR and PBIAS the monthly runoff simulation can be rated as very good for both the calibration and the validation periods.

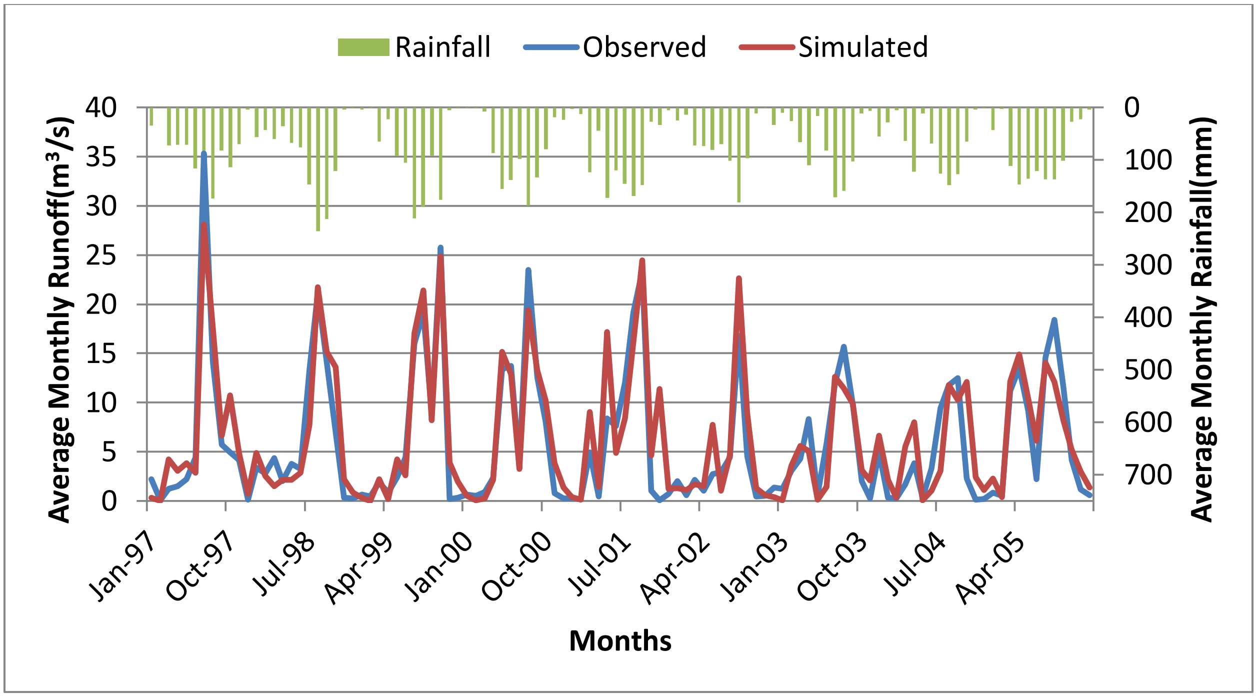

Figure 6.4:-Monthly average simulated and observed runoff for the calibration periods.

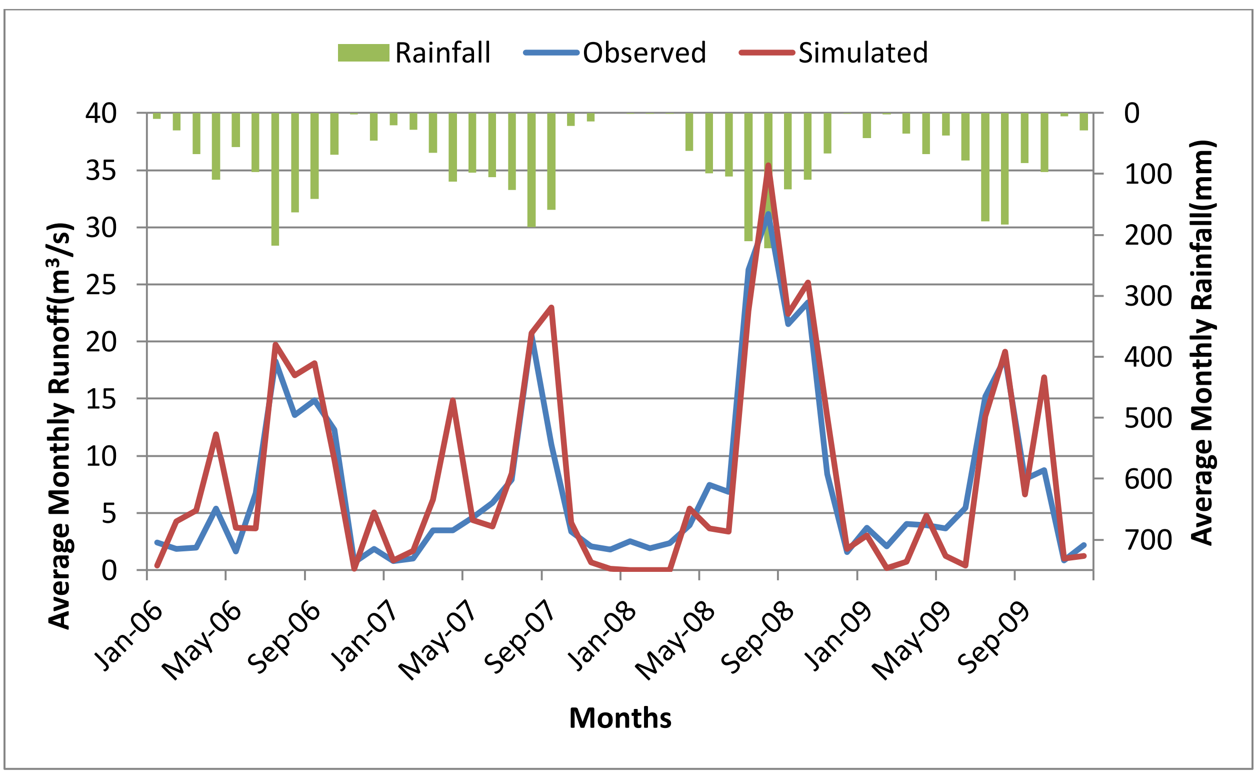

Figure 6.5:-Monthly average simulated and observed runoff for the validation periods.

6.3.2 Sediment Calibration and Validation

The SWAT calibration of the sediment load was conducted after the model was calibrated and validated for the flow. During the calibration process, model parameters were subjected to adjustments, in order to obtain model results that correspond better to the measured datasets. Sediment parameters considered during the calibration process were USLE C-factor for water erosion applicable to land cover and USLE equation support practice factor. These parameters were adjusted to the level where they could represent the characteristics of the existing land use and topographic condition of the watershed. The final fitted values are listed in Table 6.3

The SWAT model was found to simulate well on a monthly basis of the sediment load. The performance rating R^2=0.73, NSE=0.69, RSR=0.55 and PBIAS=-10.65% statistic computed between the simulated and observed monthly sediment loads for the calibration periods (Table 6.5). As Figure 6.6 showed that a time-series plot of the measured and simulated monthly sediment yield for model calibration period.

After calibration then the SWAT model was validated to sediment load using the same parameters, which were adjusted during calibration processes. Monthly model simulated sediment load against monthly measured sediment load were compared graphically (Figure 6.7) and statistically (Table 6.5).

The performance of the model for simulating the monthly sediment load is R^2=0.74, NSE=0.62, RSR=0.61 and PBIAS=2.81% statistic computed between the simulated and observed monthly sediment yields for the validation periods. Figure 6.7 show that a time-series plot of the measured and simulated monthly sediment yield for model validation period.

Table 6.5:-The model performance statistics for sediment yield calibration and validation

Variable	Period	R^2	NSE	RSR	PBIAS (%)
Sediment	Calibration(1997-2005)	0.73	0.69	0.55	-10.65
	Validation(2006-2009)	0.74	0.62	0.61	2.81

The results of the performance evaluation with regard to sediment yield show that RSR and NSE indicate good performance and satisfactory, for the calibration and validation period, respectively. During the calibration and validation period, model performance is very good according to PBIAS.

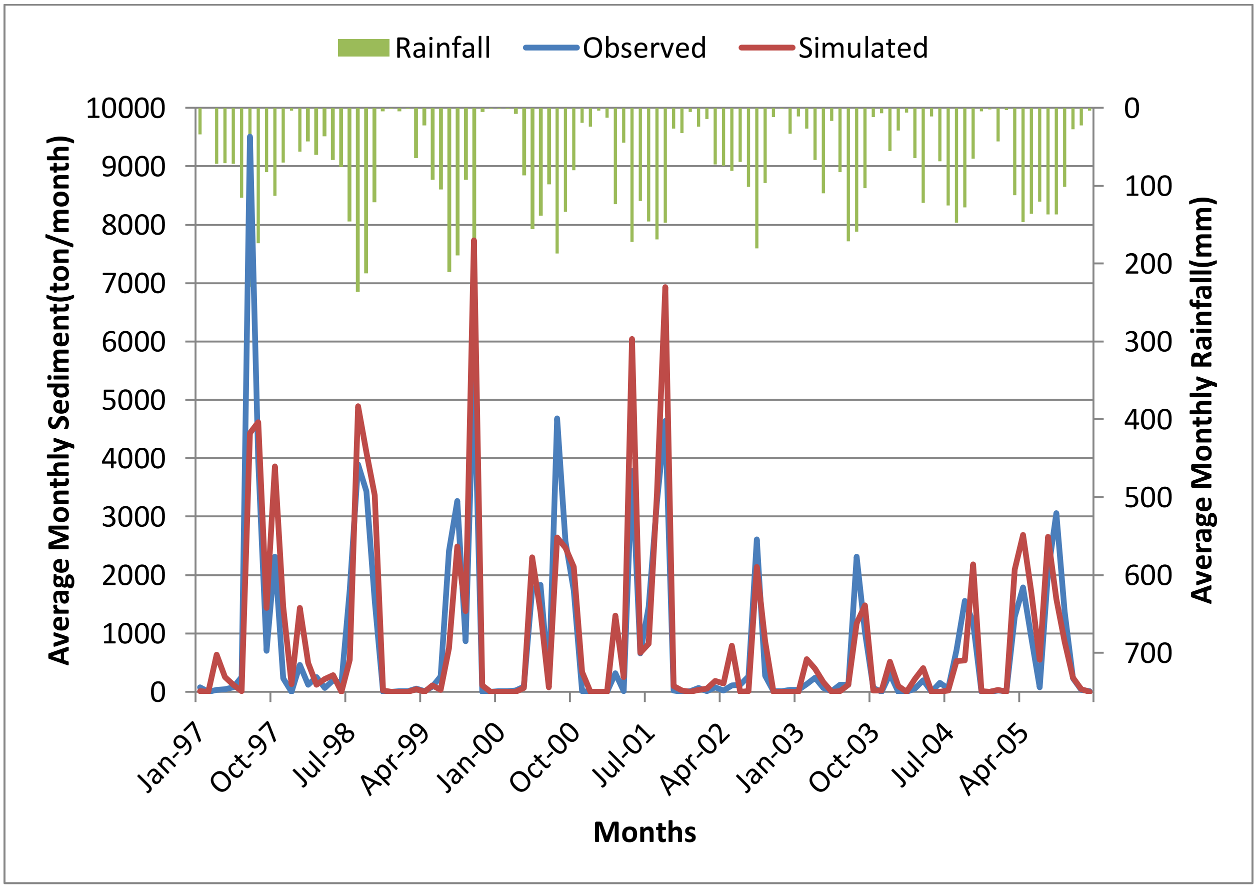

Figure 6.6:-Monthly average simulated and observed sediment yield for the calibration periods.

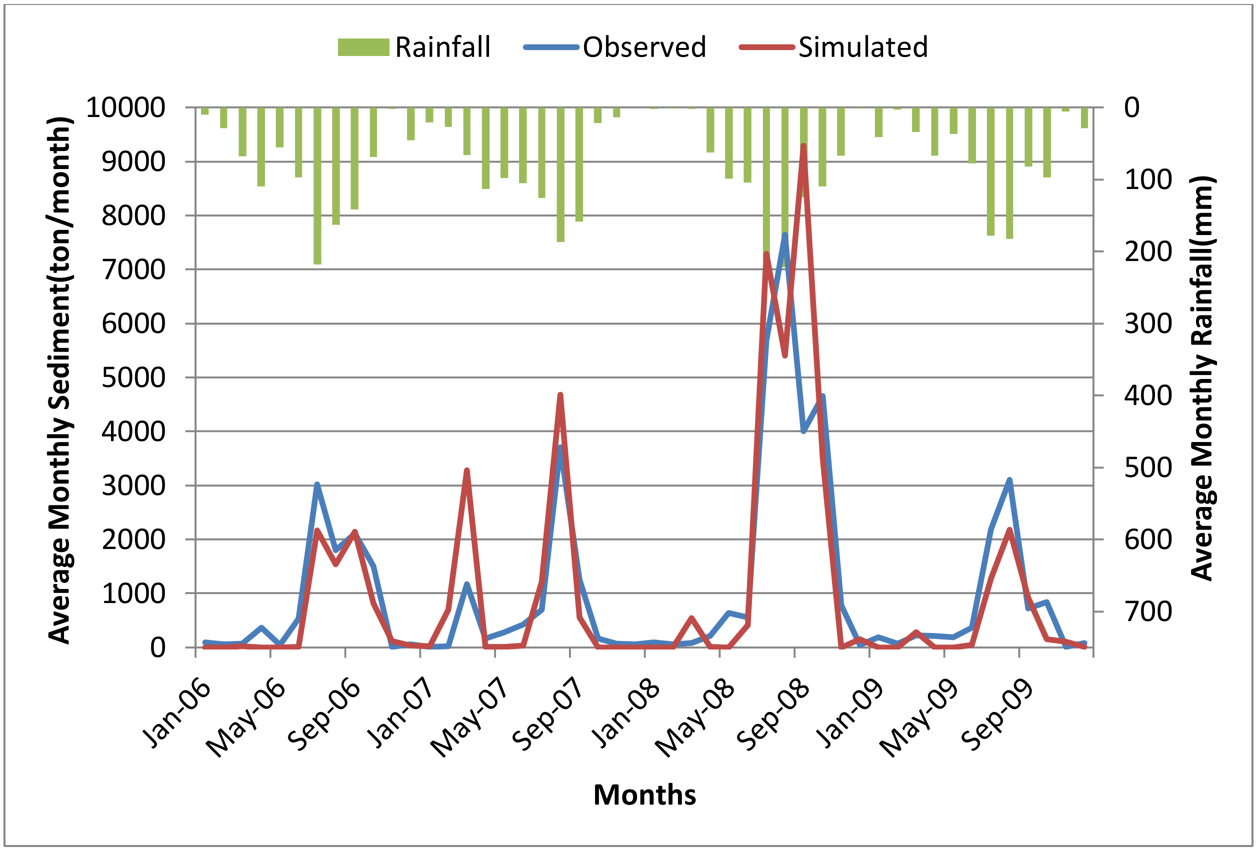

Figure 6.7:-Monthly average simulated and observed sediment yield for the validation periods.

6.4 Impact of Land use Land cover on Runoff and Sediment yield

A comparison of the land uses of 1986 and 2005 in the Keleta watershed revealed some noteworthy changes in the area. The impacts of land-use change were assessed by running the calibrated and validated models for the period from 1986 to 2005. SWAT was run using the two land cover maps (1986 and 2005 maps) and keeping the DEM and soil maps constant while changing only the land use. It was found that the greatest impact was observed on the amount of surface runoff and sediment yield. Table 6.6 shows that in 1986 the watershed was contributed the total annual runoff 1424.24mm and sediment yield 54.98t/ha, whereas in 2005 watershed contributed the total annual runoff 1557.33mm and sediment yield 73.11t/ha was recorded, thus, showing an increase by 133.09mm runoff and 18.13t/ha during the two period. This is because of the expansion of cultivation land over forest, shrubs land and grassland that results in the increase of surface runoff and sediment yield following rainfall events. We can explain this in terms of the crop soil moisture demands. Crops need less soil moisture than forests; therefore the rainfall satisfies the soil moisture deficit in cultivation lands more quickly than in forests there by generating more surface runoff where the area under cultivation land is extensive. The results demonstrate also that the land use and land cover change have a significant effects on infiltration rates, on the runoff production, and on the water retention capacity of the soil. From this we can conclude that change in the land use/ land cover does haves an impact on the runoff and sediment yield behaviour of the watershed. The result well agrees with other local level studies (Zeleke and Hurni, (2001), Bewket, (2003), Legessa et al, (2003), Amsalu et al, (2007), Kassa, (2009), (Geremew, 2013) and Gebremicael et al, (2013)). These local studies reported the dramatic changes of the natural vegetation cover into the agricultural crop land.

Table 6.6:-Average monthly runoff and sediment yield for the year 1986 and 2005

Month	Runoff(mm)			Sediment(t/ha)		
	LULC 1986	LULC 2005	Net difference	LULC 1986	LULC 2005	Net difference
January	23.73	24.74	1.01	1.79	2.22	0.43
February	16.11	17.27	1.16	1.29	1.55	0.26
March	103.73	118.63	14.9	6.46	8.53	2.07
April	84.07	98.94	14.87	5.26	7	1.74
May	137.69	157	19.31	7.31	9.65	2.34
June	83.15	94.35	11.2	2.66	3.44	0.78
July	226.61	255.74	29.13	5.22	6.87	1.65
August	357.06	381.25	24.19	9.94	13.47	3.53
September	203.23	210.55	7.32	5.83	7.99	2.16
October	141.85	150.5	8.65	6.12	8.42	2.3
November	32.05	33.3	1.25	2.75	3.5	0.75
December	14.96	15.06	0.1	0.35	0.47	0.12
Total	**1424.24**	**1557.33**	**133.09**	**54.98**	**73.11**	**18.13**

The Figure 6.8 and 6.9 shows again the increase in annual and runoff depth and sediment yield in 2005 compared to the values in 1986.

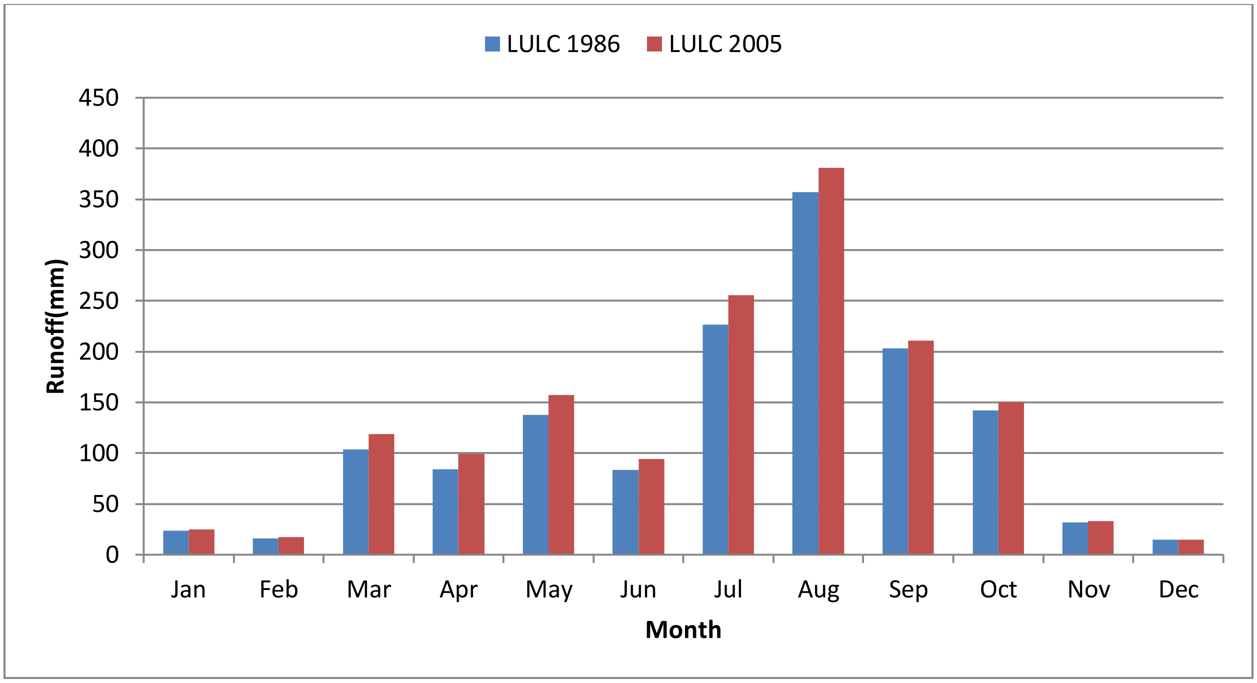

Figure 6.8:-Impact of land use/ land cover on runoff for the year 1986 and 2005

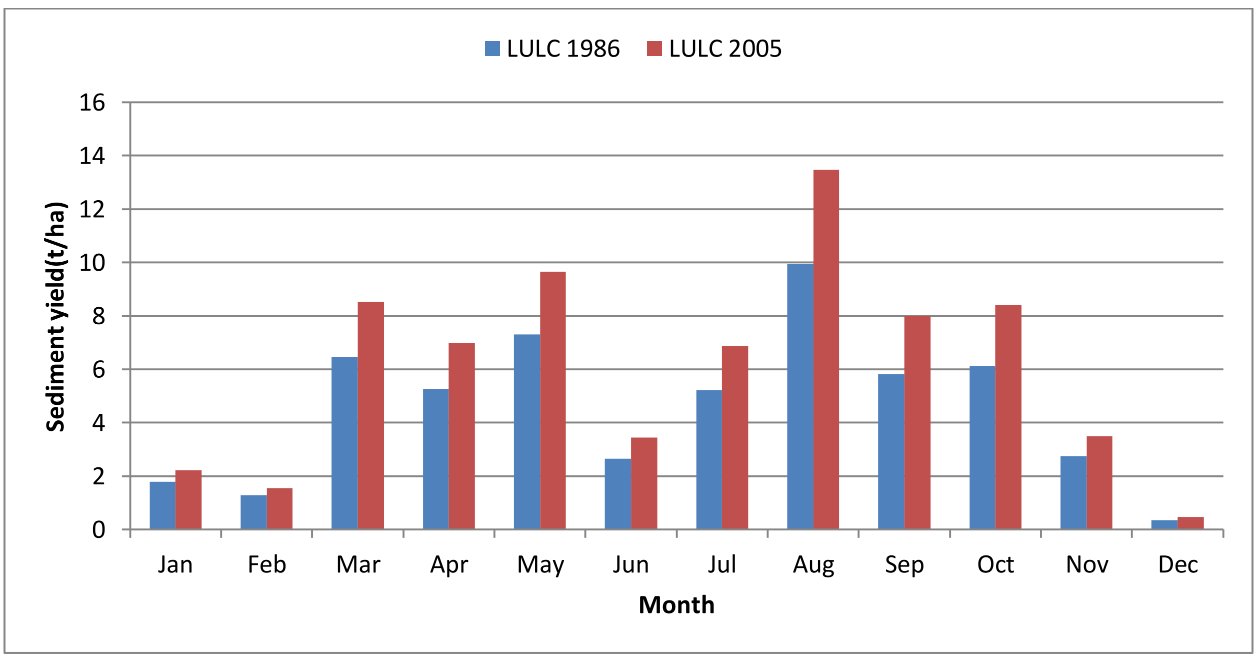

Figure 6.9:-Impact of land use/ land cover on sediment yield for the year 1986 and 2005

6.5 Spatial variability of sediment yields

The delineation of sub-basins in SWAT is based on an automatic procedure using DEM data. This tool carries out advanced GIS functions to aid in segmenting the watershed into several hydrologically connected sub-watersheds for use in modeling with SWAT. From this, average monthly runoff and sediment yield were calculated for 35 sub-watersheds in the Keleta watershed. In both model runs, the modeled precipitation for each year was kept constant; the average annual precipitation was the same for both LULC 1986 and LULC 2005. Table 6.7 documents the runoff and sediment yield by sub-watershed. As show in (Table 6.8) the contribution of average annual sediment yield in each sub-watershed range from 0.06 to 13.83$tha^{-1}y^{-1}$ in 1986, whereas in 2005 the sub-watershed contributed from 0.26 to 17.86$tha^{-1}y^{-1}$ of the sediment yield. Similarly the average annual runoff observed in each sub-watershed ranged from 45.19mm to 249.48mm in the year 1986 and 42.04mm to 285.82mm during the year 2005. The spatial variability of sediment yield were identified and represented for 1986 and 2005 in Figure 6.10 and Figure 6.11 respectively.

Hurni, (1983) has conducted a research to estimate the rates of soil formation for Ethiopia. The range of the tolerable soil loss level for the various agro-ecological zones of Ethiopia was found from 2 to 18$tha^{-1}y^{-1}$ (Hurni, 1985). The actual annual sediment yield in the study more 90% of area between under recommended tolerable soil loss rate and the left area less than recommended i.e sub-watershed 1,2,6,8,10 and 34 in 1986 and sub-watershed 1,8 and 10 in 2005.

The average annual sediment yields vary considerably between the 35 sub-watersheds of the Keleta watershed (Figure 6.12). In 1986, the highest sediment yields were calculated for the eastern and along the middle part of the watershed (sub-watersheds 5, 21 and 22). The lowest sediment yields were estimated for the sub-watershed along the western and upper part of the watershed. In 2005, increasing the sediment yield overall sub-watershed, especially in middle and eastern part of the watershed the sediment yield is strongly increasing (sub-watersheds 5, 18,21,22,23,25,26,27 and 30). The increasing sediment yield predicted in these sub-watershed may be due to increasing under cultivation, steep sloping areas, high population pressure, cultivating of the steep-lands, and other environmental problems. These sub-watersheds were, hence, assigned as the top priorities and were recommended to be considered for the future conservation plans.

Table 6.7:-Average annual runoff and sediment yields from the sub-watershed

Sub-watershed	Area(ha)	% Area	Rainfall(mm)	Runoff(mm)		Sediment yield($tha^{-1}y^{-1}$)	
				LULC1986	LULC2005	LULC1986	LULC2005
1	6.04	0.01	830.16	52.29	107.82	0.06	0.26
2	2282.69	1.98	915.51	178.42	211.79	1.42	5.67
3	1507.42	1.31	829.68	151.06	179.02	2.33	5.17
4	2894.98	2.52	915.51	199.28	226.66	2.91	5.94
5	8082.14	7.03	915.22	221.28	233.88	13.83	17.86
6	1673.00	1.45	915.51	168.75	186.57	1.70	4.42
7	585.55	0.51	915.51	248.55	260.01	3.77	9.08
8	3745.28	3.26	858.23	46.78	42.04	1.01	1.35
9	2692.32	2.34	915.51	218.44	233.80	7.90	9.91
10	87.96	0.08	858.43	45.19	42.82	0.46	0.57
11	3617.64	3.15	857.20	124.32	117.27	2.85	3.82
12	1241.81	1.08	858.43	185.73	189.88	4.45	6.42
13	391.52	0.34	858.43	178.30	178.37	3.25	3.44
14	185.41	0.16	858.43	178.60	178.77	6.18	8.22
15	3420.16	2.97	858.43	140.15	138.08	3.13	3.25
16	445.85	0.39	858.43	179.74	180.16	9.13	9.18
17	4248.04	3.69	858.43	158.40	155.96	2.60	2.65
18	2422.40	2.11	858.43	133.75	150.38	9.85	13.09
19	362.20	0.31	858.43	182.10	185.26	9.92	11.76
20	5694.23	4.95	858.43	153.87	173.47	8.15	9.21
21	5269.95	4.58	1151.89	237.57	277.03	12.57	14.30
22	7262.02	6.31	1151.75	249.48	285.82	12.47	14.07
23	103.48	0.09	858.43	197.99	192.30	7.82	13.38
24	1086.59	0.94	858.43	198.26	190.52	7.49	10.57
25	5472.60	4.76	858.43	148.90	174.49	10.02	12.24
26	3391.70	2.95	858.43	155.93	179.87	11.39	14.27
27	5983.13	5.20	858.43	155.72	175.68	11.60	13.56
28	321.66	0.28	858.43	191.95	191.51	11.16	11.75

29	2752.69	2.39	800.90	143.67	148.38	3.23	3.69
30	2754.41	2.40	858.43	167.17	189.56	11.23	13.24
31	8785.83	7.64	858.34	161.69	168.35	5.59	7.69
32	4180.77	3.64	858.43	87.38	123.54	3.45	7.32
33	4081.60	3.55	800.90	121.65	148.84	3.28	4.17
34	9238.58	8.03	858.43	77.65	101.01	1.41	3.77
35	8729.78	7.59	858.43	98.72	137.36	6.12	9.09

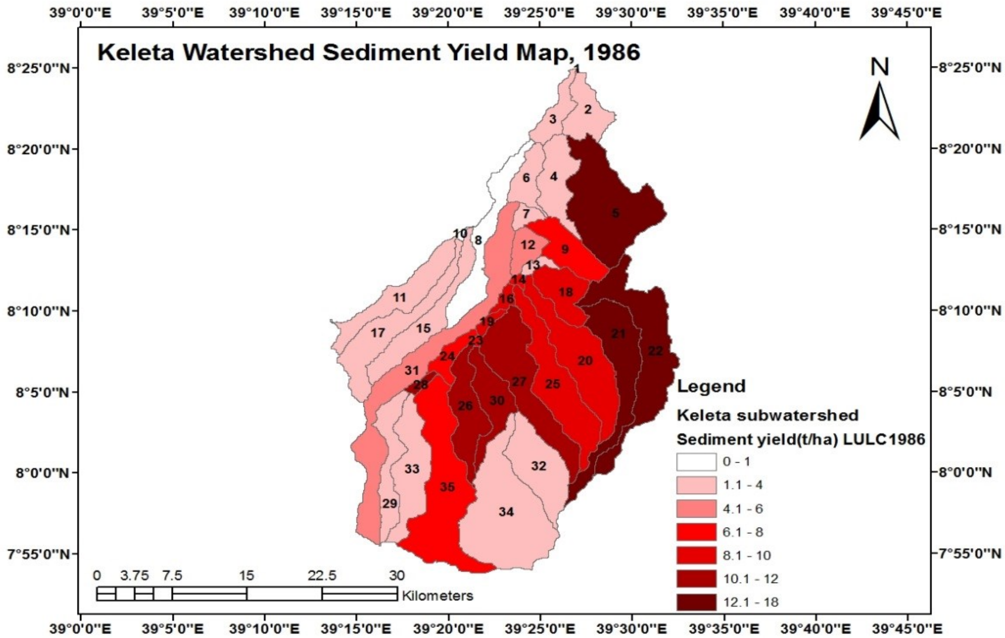

Figure 6.10:-Spatial variability annual sediment yield for LULC1986

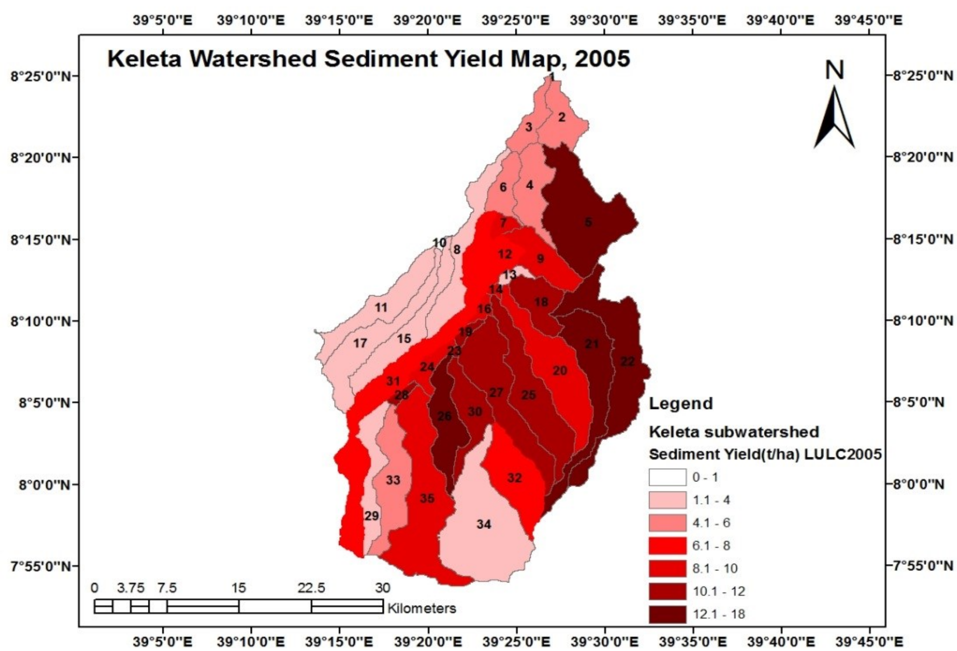

Figure 6.11:- Spatial variability annual sediment yield for LULC2005.

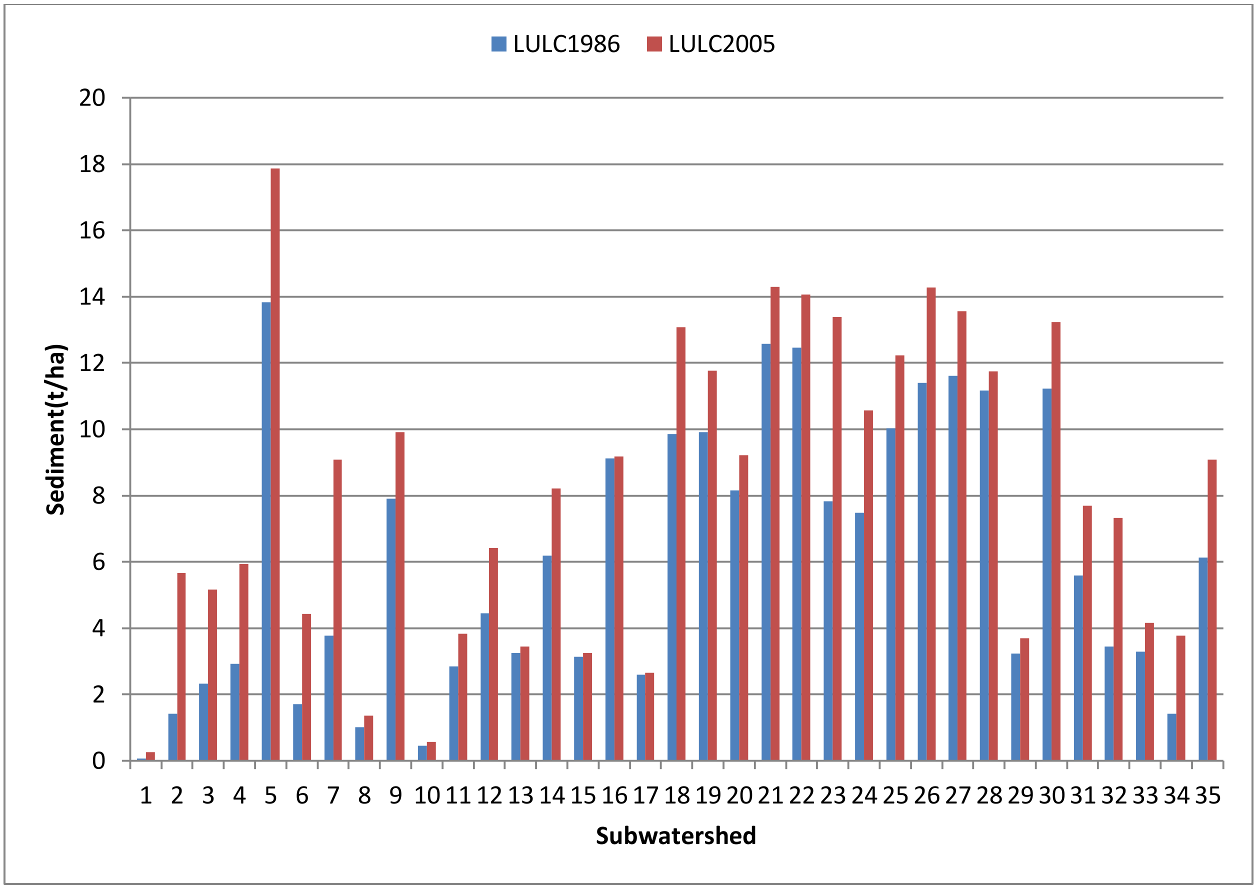

Figure 6.12:-Spatial variability of sediment yield in subwatershed during two periods

As result shown in figure above sub-watershed 8, 10,13,15,16 and 17 were very small increasing the sediment yield during the period of 2005 as compare to 1986. This is due to gentle slope and slightly change land cover. In other sub-watershed were very increasing the sediment yield variability during 2005. This is due to increasing under cultivation, steep sloping areas, high population pressure, cultivating of the steep-lands.

CHAPTER SEVEN

7 CONCLUSIONS AND RECOMMENDATIONS

7.1 Conclusions

In this study, satellite data and GIS were integrated with a hydrological model to estimate the impacts of land use and land cover change in the Keleta watershed. Use of GIS and remotely sensed data were found to be helpful tools to detect and analyse spatiotemporal land cover dynamics. These techniques were applied to assess the land use/cover dynamic effects on the hydrology and sediment yield of the watershed. The impacts of the land cover change on runoff and sediment yield was analysed using the hydrological model, SWAT. The land use and land cover changes in Keleta watershed from 1986 to 2005 were identified from TM and ETM+ satellite images, respectively. A SWAT model was calibrated for the Keleta watershed and validated for runoff and sediment yield analysis.

Land use/ land cover maps were prepared from these satellite data using Maximum Likelihood classifier of supervised classification technique. The digital images were classified into six main categories i.e Afro-alpine, Forest, Shrubs land, Grassland, Cultivation land and Built up. The results of remote sensing assessment on the land cover of the watershed revealed that a considerable reduction of forests, grasslands, afro-alpine and shrubs land and increase cultivation land and built up over the two decade period.

After preparing all the thematic maps and database as per the format of SWAT2005 model, simulation was performed for monthly values of runoff and sediment yield. The sensitivity analysis using SWAT model was carried out. Eight and two most important parameters that control the runoff and sediment yield of the studied watershed were identified respectively. On the other hand, model calibration and validation have showed that the SWAT model simulated the flow quit satisfactorily. The values of the model performance efficiency indicators, viz. Coefficient of determination (R^2), Nash-Sutcliffe model efficiency (NSE), Root mean square error standard deviation ratio (RSR) and percent bias (PBIAS) are found to be 0.82, 0.81, 0.44 and -9.29% in calibration and 0.83, 0.76, 0.49 and -7.92% for the validation period. Similarly, sediment model efficiency indicators R^2, NSE, RSR and PBIAS 0.73, 0.69, 0.55 and -10.65% for calibration and 0.74, 0.62, 0.61 and 2.81% for validation period. This shows that, the SWAT model simulated well both for runoff and sediment yield in the Keleta watershed.

The impact of land use/ land cover on runoff and sediment yield was also studied based on the monthly simulated and observed values of 1986 and 2005. The results of the model for both periods of land use and land cover (1986 and 2005) indicated, that the average annual runoff 1424.24mm for 1986 and 1557.33mm for 2005. Similarly average annual sediment yield 54.98tha^{-1} for 1986 and 73.11tha^{-1} for 2005. The average annual spatial variability of sediment yield in each sub-watershed range from 0.06 to 13.83tha^{-1}y^{-1} in 1986, whereas in 2005 the sub-watershed contribution ranged from 0.26 to 17.86tha^{-1}y^{-1} of the sediment yield. From the analysis of these results we can conclude that the continuation of the land use/ land cover change is become a serious threat to the Keleta watershed.

7.2 Recommendations

Watershed management and conservation practices are recommended to be applied for these severe parts of the watershed area; several practices can be suggested comprising land contouring, terracing in the hilly regions, and planting certain kinds of trees. The study revealed that the model, with its corresponding optimum set of parameters, is able to predict water flow and sediment yield values, which might be beneficial for future planning and management. The built SWAT model can be utilized to simulate different scenarios to examine the effect of different types of management practices and land use land cover in mitigating the problems of soil erosion and sedimentation.

The study found out that land use changes witnessed in the Keleta watershed, have impacted the hydrological response of the watershed in terms of increased surface runoff and sediment yield. However, further studies to include other hydrological models, Landsat TM before 1986 and high resolution satellite images after ETM and of recent time is recommended.

This study does not consider the influence of long-term climatic cycles that could be important on the interpretation of the trend results. Therefore, it is recommended to further investigate the effect of the regional climate at different time spans and assess its impact on the runoff and sediment yield of the Keleta watershed.

Reference

Abebe, S. (2005). Land-Use and Land-Cover change in headstream of Abbay watershed, Blue Nile Basin, Ethiopia. Addis Ababa University.

Amsalu, A.L., Stroosnijder, L., de Graaf, J.,. (2007). Long-term dynamics in land resource use and the driving forces in the Beressa watershed, highlands of Ethiopia. J. Environ. Manage. 83 (4), 448–459.

Arnold, J. G., Kiniry, J. R., Srinivasan, R., Williams, J. R., & Neitsch, S. L. (2011). Soil and water assessment tool: Input/output file documentation version 2009. Texas Water Resources Institute Technical Report No. 365. Texas A&M University System College Station, Texas 77843-2118.

Arnold, J.G., Allen, P.M., Bernhardt, G. (1993). A comprehensive surface groundwater flow model. Journal of Hydrology 142: 47-69.

Arnold, J.G., R. Sirinivasan, R.S. Muttiah, and J.R. Williams. (1998). Large Area Hydrologic Modeling and Assessment – Part I: Model Development. Journal of the American Water Resources Association (JAWRA) 34(1): 73-89.

Arnold, J.G., Williams, J.R., Maidment, D.R. (1995). Continuous-time water and sediment routing model for large basins. Journal of Hydraulic Engineering 121(2): 171-183.

Atasoy, M., Biyik, C., Ayaz, H., Karsli, F., Demir, O., Baskent, E. Z. (2006). Monitoring land use changes and determinating the suitability of land for different uses with digital Photogrammetry. Remote Sensing and Photogrammetry, Cairo, Egypt.

Bagnold, R. (1977). Bedload transport in natural rivers. Water Resources Research 13(2): 303-312.

Bakker M., G. Govers, A. Doorn, F. Quetier, D. Chouvardas and Rounsevell. (2008). The response of soil erosion and sediment export to land-use change in four areas of Europe: The importance of landscape pattern. Geomorphology Vol. 98, pp.213-226.

Bärlund, I., Kirkkala, T., Malve, O., Kämäri, J. (2007). Assessing SWAT model performance in the evaluation of management actions for the implementation of the Water Framework Directive in a Finnish catchment. Environmental Modelling & Software 22, 719–724.

Belay, T. (2002). Land cover/use changes in the Derekolli catchment of the South Welo Zone of Amhara Region, Ethiopia. Eastern Africa Social Science Research Review 18(1): 1-20.

Bergström, S. (1995). The HBV model. In: Sing, V.P. (Ed), Computer models of watershed hydrology. Water Resources Publications, Colorado, 443-476.

Beven, K. (2000). Changing Ideas in Hydrology: The Case of Physically- Based Models.Journal of Hydrology 105:157-172. Catchments, Tanzania. Proceedings of the 3rd International SWAT conference, Zurich, 2005. .

Bewket, W. (2003). Towards integrated watershed management in highland ethiopia: the Chemoga watershed case study, PhD thesis, Wageningen University and Research Centre, ISBN 90-5808-870-7.

Bewket, W., Sterk, G. (2005). Dynamics in land cover and its effect on stream flow in the Chemoga watershed, Blue Nile basin, Ethiopia. Hydrological Processes, 19, pp. 445-458.

Bronstert, A., D. Niehoff and G. Burger. (2002). Effects of Climate and LULC Change on Storm Runoff Generation: Present Knowledge and Modeling Capabilities Hydrol. Process., 16, 509–529.

Brooks K.N., Ffolliott, P. F., Gregersen, H.M.and Thames, J. L.,. (1991). Hydrology and the management of watersheds. Ames, Iowa: Iowa State University Press.

Bruijnzeel, L. (1990). Hydrology of moist tropical forests and effects of conversion: A stateof-knowledge review. Paris: UNESCO International Hydrological Programme.

Bruijnzeel, L. A. and Bremmer, C. N. (1989). Highland-lowland interactions in the GangesBrahniaputra river basin: A review of published literature. ICIMOD Occasional Paper, No. 11.

Calder I.R. (1998). Water-resource and land use issues. SWIM Paper 3. Colombo: IIMI. .

Calder, I. (1995). The impact of land use change on water resources in sub-Saharan Africa: a modeling study of Lake Malawi. J. Hydrology, 170, 123-131.

Calder, I. (2002). Forests and hydrological services: reconciling public and science perceptions. Land Use and Water Resouerces Research 2, 2.1-2.12(www.luwrr.com).

Cantón Y., A. Sole- Benet, J. de Vente, C. Boix-Fayos, A. Calvo-Cases, C. Asensio and J. Pui gdefabregas . (2011). A review of runoff generation and soil erosion across scales in semiarid southeastern Spain. J ournal of Arid Environment Vol. 75, pp.1254-1261 .

Chang, M., and Lee R. (1974). Objective double-mass analysis. Water Resources Research, 10(6), 1123-1126.

Chekol, A. (2006). Modeling of hydrology and soil erosion of upper Awash river basin, Ethiopia. Pub. PhD Thesis. University of Bonn, Germany.

Chow, V.T., Maidment, D.R., Mays, L.W. (1988). Applied Hydrology. McGraw-Hill Book Company, New York.

Croke, B.F.W., W.S. Merritt and A.J. Jakeman. (2004). A dynamic model for predicting hydrologic response to land covers changes in gauged and ungauged catchments. J.Hydrology, 291, 115-131.

DeBie C.A., J.A.V. Leeuwen and P.A. Zuidema. (1996). The Land Use Database: Knowledge-based Software Program for Structured Storage and Retrieval of User-defined.

Denboba, M. (2005). Forest conversion-soil degradation-farmers' perception nexus: Implications for sustainable land use in the southwest of Ethiopia. Ecology and Development Series No. 26, 2005.

Easton, Z.M., Fuka, D.R., White, E.D., Collick, A.S., Biruk Asharge B., McCartney, M., Awulachew, S.B., Ahmed, A.A., Steenhuis, T.S. (2010). A multi basin SWAT model analysis of runoff and sedimentation in the Blue Nile, Ethiopia. Hydrology and Earth System Sciences Discussions, 7, pp.3837-3878.

FAO. (2002). Land-Water Linkages in Rural Watersheds Case Study Series. Food and Agriculture Organization of the United Nations, Rome, Italy.

Foody, G. (2001). Monitoring the magnitude of land-cover change around the southern limits of the Sahara. Photogramm. Eng. Remote Sensing 2001, 67, 841–847.

Garedew, E. (2010). Land-Use and Land-Cover dynamics and rural livelihood perspectives, in the semiarid areas of the central Rift Valley of Ethiopia, PhD thesis, Swedish University of Agricultural Sciences. .

Gassman, P. W., Reyes, M. R., Green, C. H., & Arnold, J. G. (2007). The Soil and Water Assessment Tool: Historical development, applications, and future research direction. American Society of Agricultural and Biological Engineers, 50(4), 1211-1250. ISSN 0001-2351. .

Gebrehiwet, K. (2004). Land use and land cover changes in the central highlands of Ethiopia: The case of Yerer mountain and its surroundings. M.Sc Thesis, Addis Ababa University, Environmental Science.

George F. Pinder and John F. Jones. (1968). Determination of the Groundwater Component of Peak Discharge from the Chemistry of total runoff Journals of Water resource Research 3(2). 438-445.

Geremew, A. (2013). Assessing the impacts of land use and land cover change on hydrology of watershed: A Case study on Gilgel–Abbay Watershed, Lake Tana Basin, Ethiopia.

Goetz A.F.H., P.J. Mckintosh, and L.R. Leslak . (1999). Multiyear calibration of Landsat TM for studies of land use and land use change in the high plains. In: Proceedings 13th

International Conference Applied Geologic Remote Sensing, 1-3 March 1999. Ann Arbor, MI: ERIM, II, pp.183.

Green WH and Ampt GA. (1911). Studies on soil physics, 1. The flow of air and water through soils. Journal of Agricultural Sciences1911; 4: 11-24 .

Gupta, H.V. S. Sorooshian, and P.O. Yapo. (1999). Status of automatic calibration for hydrologic models: Comparison with multilevel expert calibration. Jounral of Hydrologic Engineering 4 (2): 135-143. DOI: 10.1061/(ASCE)1084-0699(1999)4:2(135).

Haan, C. T., Barfield, B. J. and Hayes, J. C. (1994). Design Hydrology and Sedimentology for Small Catchments.handbook." Section 3 Sedimentation.

Hadgu, K. (2008). Temporal and spatial changes in land use patterns and biodiversity in relation to farm productivity at multiple scales in Tigray, Ethiopia. PhD Thesis Wageningen University, Wageningen, the Netherlands.

Hargreaves, G.L., Hargreaves, G.H., Riley, J.P. (1985). Agricultural benefits for Senegal River basin. Journal of irrigation and Drainage Engineering 111(2): 113-124.

Hashiba H., K. Kameda, S. Uesugi and S. Tanaka. (2000). Land use change analysis of Tama River Basin with different spatial resolution sensor data by Landsat/MSS and TM. Adv. Space Res. 26, 1069.

Herold, M. (2003). The spatiotemporal form of urban growth: Measurement, analysis and modeling. Remote Sens. Environ. 6,286.

Hooghoudt, S. (1940). Bijdrage tot de kennis van enige natuurkundige grootheden van de ground. Versl. Landbouwkd. Onderz. 46: 515-707.

Hubbard, K. (1994). Spatial variability of daily weather variables in the high plains of the USA. Agric. Forest Meteorol. 68, 29 + - 41.

Huisman, S., Ann van Griensven, Raghavan Srinivasan, Lutz Breuer,. (2004). European SWAT School, Advanced Course, 112 (Intitute for Landscape Ecology and Resouce Management, University of Giessen, Hienrich-Buff-Ring 26, 35392 giessen, Germany) .

Hurni H. (1983). "Soil Formation Rates in Ethiopia" Ethiopian High lands Reclamation Study, December 1983.

Hurni H. (1985). Soil conservation manual for Ethiopía. Ministry of Agriculture. Addis Abeba, Ethiopia.

Hurni H., K. Herweg, B. Portner and H. Liniger. (2008). Soil Erosion and Conservation in Global Agricultural. Springer Science+Business Media B.V. .

Hurni, H. (1983). “Soil Formation Rates in Ethiopia” Ethiopian High lands Reclamation Study, December 1983.

Hurni, H. (1993). In: Pimentel, D. (Ed.), Land Degradation, Famine, and Land Resource Scenarios in Ethiopia: World Soil Erosion and Conservation. Cambridge University Press, Cambridge, UK.

Kassa Tadele M. (2009). Watershed Hydrological Responses to Changes in LandUse and Land Cover, and Management Practices at Hare Watershed, Ethiopia Phd Thesis 37.

Kassa, G. (2003). GIS based analysis of land use and land cover, land degradation and population changes: A study of Boru Metero area of south Wello, Amhara Region, MA Thesis, Department of Geology, Addis Ababa University. 110pp.

Kidanu, S. (2004). Using Eucalyptus for soil and water conservation on the highland Vertisols of Ethiopia, PhD Thesis, Wageningen University, The Netherlands.

Lal, R. (2001). Soil degradation by erosion. Land Degradation and Development Vol. 12, pp. 519-539.

Lambin E.F., H.J. Geist and E. Lepers. (2003). Dynamics of land use and land cover change in tropical regions. Annu. Rev. Environ. Resour.2003.28:205-241.

Legesse D., C. Vallet-Coulomb and F. Gasse. (2003). Hydrological response of a catchment to climate and land use changes in Tropical Africa: case study South Central Ethiopia. Journal of Hydrology 275: 67-85.

Lemlem, A. (2007). Assessing the Impact of Land Use and Land Cover Change on Groundwater Recharge Using Remote Sensing and GIS: A Case of Awassa Catchment, Southern Ethiopia. M.Sc. Thesis. Addis Ababa University, Ethiopia.

Lenhart, T., Eckhardt, K., Fohrer, N., Frede, H.G. . (2002). Comparison of two different approaches of sensitivity analysis. Physics and Chemistry of the Earth 27 (2002), Elsevier Science Ltd., 645–654.

Lu, D.; Mausel, P.; Brondízio, E.; Moran, E. (2004). Change detection techniques. Int. J. Remote Sens. 25, 2365–2401.

Meyer W.B and Turner B.L. (1994). Changes in land use and land cover: A Global Perspective. Combridge: Combridge University Press. New York.

Meyer, W. (1995). Past and Present Land-Use and Land-Cover in the USA. Consequences, pp.24-33. New York.

Monteith, J. (1965). Eavaporation and the environment. P. 205-234. In The state and movement of water in living organisims, XIXth Symposium. Soc. For Exp. Biol.Swansea, Cambridge University Press.

Morgan, R. (2005). Soil Erosion and Conservation. 3rd edition. Longman Group Unlimited. London, UK.

Moriasi, D.N., Arnold, J.G., Van Liew, M.W., Binger, R.L., Harmel, R.D., Veith, T. (2007). Model evaluation guidelines for systematic quantification of accuracy in watershed simulations.Transactions of the American Society of Agricultural and Biological Engineers 50(3): 885-900.

Nash JE and Sutcliffe JV. (1970). River flow forecasting through conceptual models. Part I –A discussion of principles. Journal of Hydrology 10: 282–290.

Nearing M.A., F.F. Pruski and M.R. O'Neal. (2004). Expected climate change impacts on soil erosion rates: a review. Journal of Soil and Water Conservation Vol. 59, pp. 43-50.

Neitsch, S.L., Arnold, J.G., Kiniry, J.R., and Williams, J.R. (2005). Soil and Water Assessment Tool, Theoretical documentation: Version 2005. Temple, TX. USDA Agricultural Research Service and Texas A & M Black land Research Centre.

Nejadhashemi, A.P., Wardynski, J., Munoz, J.D. (2011). Evaluating the impacts of land use changes on hydrological responses in the agricultural regions of Michigan and Wisconsin. Hydrology and Earth System Sciences Discussions, 8, pp. 3421-3468.

NMSA. (2001). Initial National Communication of Ethiopia to the UNFCCC. Addis Ababa, Ethiopia.

OWWDSE. (2013). Soil survey of the Upper Awash Sub basin final draft report.

Pandey A., V.M. Chowdary and B.C. Mal. (2007). Identification of critical erosion prone in the small agricultural watershed using USLE, GIS and remote sensing. Water Resources Management Vol. 21, pp. 729-746.

Pender, J., Gebremedhin, B., Benin, S., and Ehui, S. . (2001). Strategies for sustainable agricultural development in the Ethiopian highlands. EPTD discussion paper No. 77. Environment and Production Technology Division.Washington, USA.

Priestley, C.H.B. and R.J. Taylor. (1972). On the Assessment of Surface Heat Flux and Evaporation Using Large Scale Parameters. Mon. Weath. Rev. 100:8192. Project: A comparison on USDA-ARS experimental watersheds.

Prol-Ledesma R.M., E.M. Uribe-Alcantara and O. Diaz-Molina. (2002). Use of cartographic data and Landsat TM images to determine land use change in the vicinity of Mexico City. Int.J. Remote Sens. 23, 1927.

Saltelli, A., Chan, K. and Scott, E.M. (2000). Sensitivity Analysis, John Wiley & Sons, Chichester. .

Saveniji, H. (1995). New definition for moisture recycling and the relation with land-use changes in the Sahal. J. Hydrology, 167, 57-78.

Setegn S.G., R. Srinivasan, B. Dargahi and A.M. Melessa . (2009). Spatial delineation of soil vulnerability in the Lake Tana Basin, Ethiopia. Hydrological Processes 23, 3738-3750.

Seto K.C., C.E. Woodcock, C. Song, X. Huang, Lu., R.K. Kaufmann. (2002). Monitoring Land Use Change in the Pearl River Delta Using Landsat TM. International Journal of Remote Sensing, 23(10), 1985-2004.

Sharpley, A.N. and J.R. Williams. (1990). EPIC-Erosion Productivity Impact Calculator, 1. Model documentation. U.S. Department of Agriculture, Agricultural Research Service, Tech. Bull. 1768.

Singh, A. (1989). Review Article Digital change detection techniquesusing remotely-sensed data. Int. J. Remote Sens. 1989, 10, 989–1003.

Stefanov, W. (2001). Monitoring urban land cover change: An expect system approach to land cover classification of semiarid to arid urban centers.

T.G. Gebremicael, Y.A. Mohamed, G.D. Betrie, P. van der Zaag and E. Teferi,. (2013). Trend analysis of runoff and sediment fluxes in the Upper Blue Nile basin: A combined analysis of statistical tests, physically-based models and landuse maps.

Tekle, K. and Hedlund, L. (2000). Land Cover Changes between 1958 and 1986 in Kalu District, Southern Wello, Ethiopia. Mountain Research and Development, 20(1): 42 - 51.

Tesfahunegn, G.B., Vlek, P.L.G., Tamene, L.,. (2012). Management strategies for reducing soil degradation through modeling in a GIS environment in northern Ethiopia catchment. Nutrient Cycling in Agroecosystems, 92, pp.255-272.

Tibebe, D. and Bewket W. (n.d.). Surface runoff and soil erosion estimation using the SWAT model in the Keleta Watershed, Ethiopia. Land Degradation and Development. http://dx.doi.org/10.1002/1dr.1034.

Tronci, N., Molteni, F., Bozzini, M. (1986). A comparison of local approximation methods for the analysis of meteorological data. Arch. Meteorol., Geophys. Bioclimatol. 36, 189±211.

USDA Soil Conservation Service (SCS). (1972). National Engineering Handbook Section 4 Hydrology, Chapters 4-10.

Van Grienseven A., T. MeixenerS. Grunwald, and R. Srinivasan. (2005). Evaluation of models using SWAT-2005. SWAT 2005 3rd international conference zurich Switzerland.

vanGriensven, A., Ndomba, P., Yalew, S., & Kilonzo, F. (2012). Critical review of SWAT applications in the Upper Nile Basin countries. Hydrology and Earth System Sciences, 16, 3371-3381. http://dx.doi.org/10.5194/hess-16-3371-2012.

Veith, T.L., and Ghebremichael, L.T. (2009). How to: applying and interpreting the SWAT autocalibration tools. In: Proceedings of the Soil and Water Assessment Tool International Conference, Boulder, Colorado, 26-33. .

Wang G., G. Gertner, V. Singh, S. Shinkareva, P. Parysow and A. Anderson. (2003). Spatial and temporal prediction and uncertainty of soil loss using the revised universal soil loss equation: a case study of rainfall-runoff erosivity R factor. Ecological Modelling Vol. 153, pp. 143-155.

Williams J.R. (1969). Flood routing with variable travel time or variable storage coefficient. Transactions of the ASAE 12(1): 100-103.

Williams J.R. (1975). Sediment-yield prediction with universal equation using runoff energy factor. p. 244-252. In Present and prospective technology for predicting sediment yield and sources: Proceedings of the sediment yield workshop, November 28-30, 1972. , 1975).

Williams JR. (1995). Chapter 25: The EPIC model. P. 909-1000. In V.P. Singh (ed). Computer models of watershed hydrology. Water resources Publications, Highlands Ranch, CO.

Williams, J. (1969). Flood routing with variable travel time or variable storage coefficient. Transactions of the ASAE 12(1): 100-103.

Williams, J. (1980). SPNM, a model for predicting sediment, phosphorous, and nitrogen from agricultural basins. Water Resour. Bull. 16 (5), 843–848.

Williams, J.R. and R.W. Hann. . (1973). HYMO: Problem-oriented language for hydrologic modeling-User’s manual. USDA, ARS-S-9.

Wischmeier, W.H. and D.D. Smith. (1978). Predicting rainfall erosion losses: A guide to conservation planning. Agriculture Handbook No. 537, US Dept. of Agric., Washington, DC.

Xu, Z.X., Pang, J.P., Liu, C.M., Li, J.Y. (2009). Assessment of runoff and sediment yield in the Miyun Reservoir catchment by using SWAT model. Hydrological Processes 23, 3619–3630.

Zeleke, G and Hurni, H. (2001). Implications of Land use and land cover dynamics for mountain resource degradation in the northwestern Ethiopia highlands. Mountain Research and Development 21: 184-191.

Zhang Y., J. De Groote, C. Wolter and R. Sugumaran. (2009). Integration of Modified Universal Soil Loss Equation (MUSLE) into a GIS Framework to assess Soil Erosion Risk. Land Degradation and Development Vol. 20, pp. 84-91.

Appendix

Appendix 1:-Weather Generator Statistic and Probability Value

Variable name	Description
TMPMX(mon)	Average or mean daily maximum air temperature for month (ºC).
TMPMN(mon)	Average or mean daily minimum air temperature for month (ºC).
TMPSTDMX(mon)	Standard deviation for daily maximum air temperature in month (ºC).
TMPSTDMN(mon)	Standard deviation for daily minimum air temperature in month (ºC).
PCPMM(mon)	Average or mean total monthly precipitation (mm H2O).
PCPSTD(mon)	Standard deviation for daily precipitation in month (mm H2O/day).
PCPSKW(mon)	Skew coefficient for daily precipitation in month.
PR_W(1,mon)	Probability of a wet day following a dry day in the month.
PR_W(2,mon)	Probability of a wet day following a wet day in the month.
PCPD(mon)	Average number of days of precipitation in month.
RAINHHMX(mon)	Maximum 0.5 hour rainfall in entire period of record for month (mm H2O).
SOLARAV(mon)	Average daily solar radiation for month (MJ/m2/day).
DEWPT(mon)	Average daily dew point temperature in month (ºC).
WNDAV(mon)	Average daily wind speed in month (m/s).

Appendix 2:-Flow sensitivity output using ArcSWAT sensitivity tool including Parameters definition

Name	Description	Min	Max	Process
ALPHA_BF	Baseflow alpha factor (days)	0	1	Groundwater
BIOMIX	Biological mixing efficiency	0	1	Soil
BLAI	Leave area index for crops	0	1	Crops
CANMX	Maximum canopystorage (mm)	0	10	Runoff
CH_K2	Hydraulic conductivity in main channel(mm/hrs)	0	150	Channel
CH_N2	Manning coefficient for main channel	0	1	Channel
CN2	SCS runoff CN for moisture condition II	35	98	Runoff
EPCO	Plant evaporation conpensation factor	0	1	HRU
ESCO	Soil evaporation compensation factor	0	1	Evaporation

GW_DELAY	Groundwater delay (days)	0	50	Groundwater
GW_REVAP	Groundwater 'revap' coefficient	0.2	0.02	Groundwater
GWQMN	Threshold depth of water in the shallow aquifer required for return flow to occur (mm)	0	5000	Groundwater
REVAPMN	Threshold depth of water in the shallow aquifer for 'revap' to occur (mm)	0	500	Groundwater
SOL_ALB	Soil albedo	0	0.25	Soil
SOL_AWC	Available soil water capacity	0	1	Soil
SOL_K	Soil conductivity	0	100	Soil
SOL_Z	Soil depth	0	3000	Soil
SLSUBBSN	Average slope lenght	10	150	Geomophology
SLOPE	Average slope steepness	0	1	Geomophology
SURLAG	Surface runoff lag coefficient	0	10	Runoff
SFTMP	Snow freezing base temperature	0	5	Snow
SMTMP	Snow melt base temperature	0	5	Snow
SMFMN	Minimum melt rate for snow during the year	0	10	Snow
SMFMX	Maximum melt rate for snow	0	10	Snow
TIMP	Snow pack temperature lag factor	0	1	Snow
TLAPS	Temperature laps rate	0	50	Geomophology

Appendix 3:-Sediment sensitivity output using ArcSWAT sensitivity tool including parameters definition

Name	Description	Min	Max	Process
CH_COV	Channel cover factor	0	1	channel
CH_EROD	Channel erodibility factor	0	1	channel
SPCON	Linear parameter for calculating the maximum amount of sediment that can be reentrained during channel sediment routing	0.0001	0.01	channel
SPEXP	Exponent parameter for calculating sediment reentrained in channel sediment routing	1	2	channel
USLE_C	Minimum value of USLE C factor for land cover/plant	0	1	Crops
USLE_P	USLE equation support practice factor	0	1	Runoff

Appendix 4:-Soil parameter values used for SWAT Model

SNAM	CMPPCT	NLAYERS	HYDGRP	SOL_ZMX	CL	SOL_CRK	TEXTURE	SOL_Z	SOL_BD	SOL_AWC	SOL_K	SOL_CBN	CLAY	SILT	SAND	ROCK	SOL_ALB	USLE_K
ANvi	1	3	B	1800	0.5	0	L	300	1.43	0.14	15.49	9.94	20	40	40	3.5	0.05	0.28
							L	1100	1.47	0.12	19.83	9.7	18	32	50	3.5	0.05	0.28
							L	1800	1.53	0.12	19.74	9.97	16	34	50	3.5	0.05	0.31
VRpe	1	4	D	2000	0.5	0.1	C	300	1.25	0.1	1.32	9.97	64	21	15	1.5	0.05	0.21
							C	1000	1.23	0.11	1.24	9.97	66	21	13	0	0.05	0.21
							C	1450	1.24	0.11	0.97	9.97	64	21	15	0	0.05	0.24
							C	2000	1.22	0.12	0.84	9.97	68	19	13	0	0.05	0.24
LPum	1	1	B	450	0.5	0	L	450	1.39	0.13	16.54	9.97	22	33	45	3.5	0.05	0.28
CMeu	1	4	D	2000	0.5	0	CL	200	1.26	0.15	9.77	9.97	33	42	25	0	0.05	0.12
							CL	600	1.37	0.15	7.82	9.97	29	42	29	0	0.05	0.12
							CL	1400	1.41	0.14	2.99	9.97	37	32	31	0	0.05	0.14
							C	2000	1.4	0.13	1.26	7.45	43	32	25	0	0.05	0.14
VRcm	1	4	D	1700	0.5	0	CL	200	1.35	0.14	4.56	9.79	37	34	29	0	0.05	0.21
							C	600	1.39	0.13	1.59	9.07	43	26	31	0	0.05	0.24
							C	1100	1.35	0.12	0.59	6.4	51	22	27	3.5	0.05	0.24
							C	1700	1.43	0.13	1.14	6.74	43	24	33	7	0.05	0.24
NTha	1	3	C	1200	0.5	0	L	350	1.53	0.15	11.35	5.11	18	47	35	3.5	0.05	0.3
							SiC	600	1.34	0.14	3.09	8.49	40	41	19	3.5	0.05	0.28

							C	1200	1.39	0.14	1.62	5.7	42	37	21	3.5	0.05	0.24
CMvr	1	3	D	1800	0.5	0.5	C	450	1.27	0.12	0.77	6.79	56	27	17	3.5	0.05	0.24
							C	750	1.31	0.13	0.84	5.94	52	29	19	3.5	0.05	0.24
							C	1800	1.39	0.14	1.19	5.99	44	33	23	3.5	0.05	0.24
LVcm	1	3	D	1800	0.5	0	C	300	1.29	0.13	3.58	9.97	44	33	23	3.5	0.05	0.24
							C	800	1.3	0.12	1.39	9.97	52	25	23	3.5	0.05	0.24
							C	1800	1.22	0.11	1.51	9.97	72	17	11	0	0.05	0.24

Appendix 5:-SWAT Model soil parameters legend used

Variable name	Description
NLAYERS	Number of layers in the soil(min 1 max 10)
HYDGRP	Soil hydrographic group(A,B,C,D)
SOL_ZMX	Maximum root depth of the soil profile
ANION_EXCEL	Fraction of porosity from which an ions are exchanged
SOL_CRK	Crack volume potential of soil
TEXTURE	Texture of the layer
SOIL_Z	Minimum depth from soil surface to bottom of layer
SOL_BD	Moist bulk density
SOL_AWC	Available water capacity of surface to bottom of the layer
SOL_K	Saturated hydraulic conductivity
SOL_CBN	Organic carbon content
CLAY	Clay content
SILT	Silt content
SAND	Sand content
ROCK	Rock fragmented content
SOL_ALB	Moist soil albedo
USLE_K	Soil erodibility factor (K)

Appendix 6:-SWAT model result during the simulation

Table 1. SWAT model subbasin result description

Variable name	Definition
SUB	Subbasin number.
GIS	GIS code reprinted from watershed configuration file (.fig). See explanation of subbasin command.
MON	Daily time step: the julian date, Monthly time step: the month (1-12), Annual time step: 4-digit year, Average annual summary lines: number of years averaged together
AREA	Area of the subbasin (km2).
PRECIP	Total amount of precipitation falling on the subbasin during time step (mm H2O).
SURQ	Surface runoff contribution to streamflow during time step (mm H2O).
GW_Q	Groundwater contribution to streamflow (mm). Water from the shallow aquifer that returns to the reach during the time step.
WYLD	Water yield (mm H2O). The net amount of water that leaves the subbasin and contributes to streamflow in the reach during the time step. (WYLD = SURQ + LATQ + GWQ – TLOSS – pond abstractions)
SYLD	Sediment yield (metric tons/ha). Sediment from the subbasin that is transported into the reach during the time step.

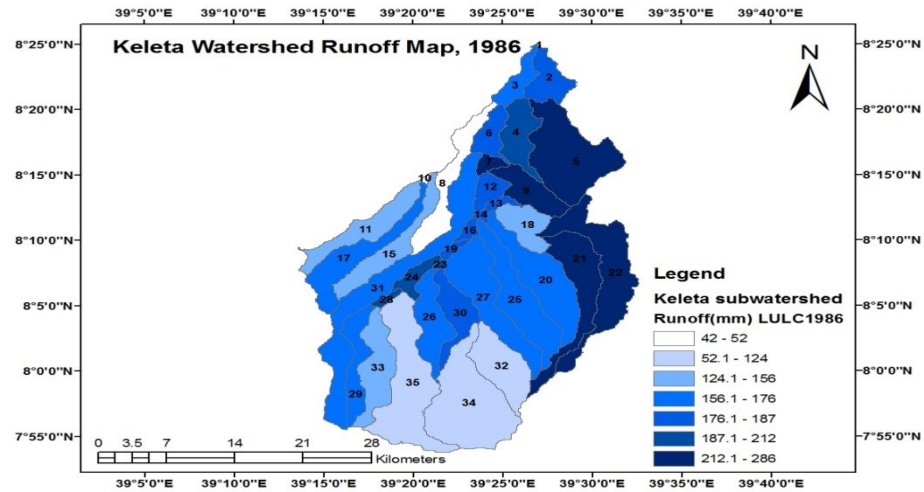

Figure 1. A spatial variability map of the watershed showing SWAT simulated annual runoff for LULC1986

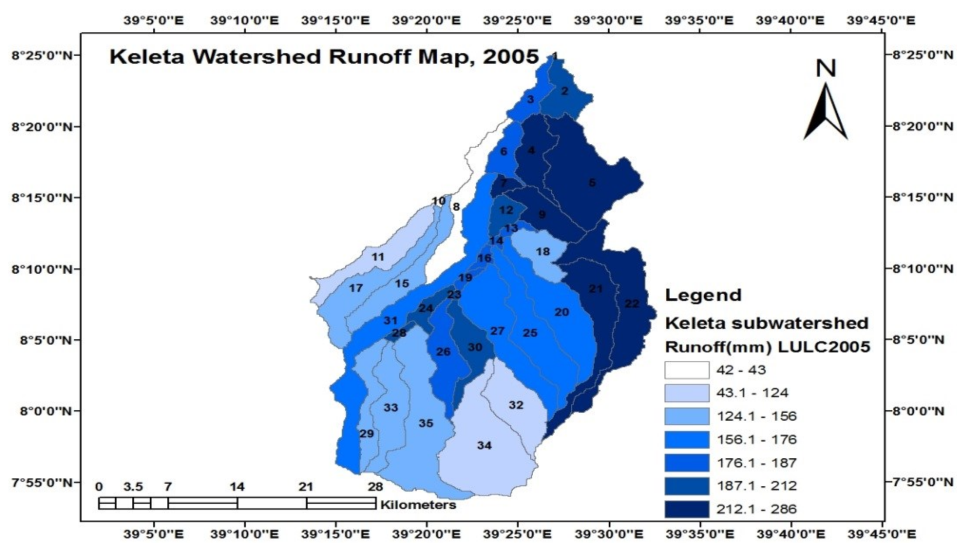

Figure 2. A spatial variability map of the watershed showing SWAT simulated annual runoff for LULC1986